POLITECNICO DI TORINO

Master of Science in Mechanical Engineering

Master's Degree Thesis

Simulation-driven optimization of a HPDI Argon-Hydrogen engine

Supervisor

Daniela Misul

Supervisor at Scania

Amirali Kerachian

Supervisor at KTH

Jens Fridh

Candidate

Giuseppe Penza

A.Y. 2024-2025

Simulation-Driven Optimization of a HPDI Argon-Hydrogen Engine

Student: Giuseppe Penza
Supervisor: Assoc. Prof. Jens Fridh, Full Prof. Daniela Misul

Master of Science Thesis
Politecnico di Torino - Fluid Machinery
KTH Industrial Engineering and Management
Mechanical Engineering

Abstract

This thesis presents a simulation-driven study on the optimization of a High-Pressure Direct Injection Argon-Hydrogen internal combustion engine operating in a closed-loop configuration. The objective is to explore the potential of hydrogen as a carbon-free fuel, combined with argon as a thermodynamically advantageous inert working fluid. A detailed 1D model is developed in GT-POWER, starting from a conventional six-cylinder diesel engine architecture and progressively modified to implement turbocharging, charge-air cooling, and turbo-matching strategies.

The work begins with baseline simulations to assess convergence behavior and the inherent efficiency of the closed-loop base architecture. A fixed-geometry turbocharger is then introduced to recover exhaust energy, revealing the need for improved thermal management due to increased intake temperatures. A charge-air cooler is subsequently added, successfully restoring thermal stability and improving Brake Thermal Efficiency. Parametric studies on argon content, initial pressure, and air-fuel equivalence ratio (λ) demonstrate that argon dilution and system pressure are critical to achieving optimal efficiency.

Finally, a compressor and turbine matching analysis is carried out by tuning mass and efficiency multipliers, resulting in a peak BTE of 57% and a reduction in Brake Specific Fuel Consumption by 2%. The final model confirms that turbo-matching is essential to unlock the full potential of a closed-loop hydrogen ICE. From an environmental standpoint, the proposed system eliminates carbon emissions, making it a promising solution for the future of sustainable heavy-duty transportation.

Future work will involve extending this model with variable geometry and electric turbochargers and conducting real engine validation in test cells, as a means to implement it in commercial vehicles.

FORWARD

I would like to express my sincere gratitude to my academic supervisors at KTH Royal Institute of Technology, Associate Professors Jens Fridh and Andreas Cronhjort, for their continuous guidance, insightful feedback, and support throughout the course of this thesis.

I am equally grateful to my academic supervisor at Politecnico di Torino, Full Professor Daniela Misul, for her support during my earlier academic development and for the collaborative framework that made this international thesis possible.

Special thanks are extended to my team at Scania CV AB for their invaluable contribution to this work. In particular, I would like to thank my supervisor Amirali Kerachian, and my manager Björn Lindgren, for their technical mentorship and for the respect they treated me with since the first day. The opportunity to be involved in such an innovative and expiring project within the Scania family has been both an honor and an exceptional learning experience.

A volte, soprattutto nel mio caso, i ringraziamenti più sinceri si nascondono dietro poche parole.

A tutte le persone che mi hanno accompagnato in questo percorso, i miei amici in Italia e in Svezia, grazie.

Ai miei nonni speciali, zii e cugini fantastici, grazie.

Alla mia famiglia, mamma, papà, Vi, Checco, Maia, questa è per voi.

Giuseppe Penza

Stockholm, June 2025

NOMENCLATURE

Notations

Symbol	Description
CO_2	Carbon Dioxide
NO_x	Nitrogen Oxides
γ	Specific heat ratio
η	Specific heat ratio
λ	Air-to-fuel ratio
f	Degrees of freedom
$C_{v,m}$	Molar heat capacities at constant volume
$C_{p,m}$	Molar heat capacities at constant pressure
W_{out}	Work output
Q_{in}	Energy input
…	…

Abbreviations

ICE	Internal Combustion Engine
HPDI	High Pressure Direct Injection
CFD	Computational Fluid Dynamics
APC	Argon Power Cycle
BTE	Brake Thermal Efficiency
FGT	Fixed Geometry turbocharger
PFI	Port Fuel Injection
CR	Compression Ratio
BSFC	Brake Specific Fuel Consumption
PMEP	Pumping Mean Effective Pressure
CAC	Charge-Air Cooler
DOE	Design Of Experiments
…	…

TABLE OF CONTENTS

List of Figures

1 INTRODUCTION

1.1 Background

The global transition towards sustainable energy solutions is driving the development and optimization of innovative power generation technologies. Among these, hydrogen stands out as a promising alternative for reducing carbon emissions, particularly when used in Internal Combustion Engines (ICE). Its potential to contribute to zero-emission solutions aligns closely with the growing demand for environmentally friendly transportation systems.

Historically, ICE technology has been widely used in the transportation and industrial sectors, especially in heavy-duty applications such as trucks, buses, and construction equipment. These engines, relying predominantly on fossil fuels, have been the backbone of global logistics and infrastructure development for more than a century. However, their extensive use has contributed significantly to greenhouse gas emissions, particularly CO_2, making decarbonization of this sector a pressing priority.

In the context of heavy duty transport, the implementation of hydrogen as a fuel in ICEs represents a promising pathway to achieve substantial emission reductions. Hydrogen-powered internal combustion engines offer the advantage of utilizing a well-established technology while eliminating almost 100 % of carbon emissions during operation. In addition, their adaptability to existing manufacturing and service infrastructure makes them a practical solution to accelerate the transition to sustainable transportation.

An advanced concept that further enhances the efficiency of hydrogen ICEs is the Argon Power Cycle. By leveraging argon's unique properties, such as its inert nature and superior thermal characteristics, this cycle improves the thermal efficiency of the engine. The combination of hydrogen as a clean fuel and argon as a working fluid provides an opportunity to achieve high-efficiency, zero-emission engines. This integration is particularly impactful for heavy duty vehicles, where efficiency gains and carbon emission reductions can have a significant global effect due to their extensive usage.

This thesis is conducted in collaboration with Scania CV, a leader company in sustainable transportation solutions. By exploring the potential of a high-pressure direct injection (HPDI) Argon-Hydrogen engine, this research contributes to Scania's efforts to advance innovative propulsion technologies and support society's transition to a sustainable future.

1.2 Purpose

The purpose of this thesis is to investigate the optimization of Hydrogen High-Pressure Direct Injection systems integrated with the Argon Power Cycle, using advanced one-dimensional simulation techniques. Combining argon chemical properties as an inert gas and a sustainable fuel ICE, a clear focus of this project involves reaching greater efficiency and zero-emission performance.

A key objective is to identify optimal systemic configurations and operational parameters that maximize engine performance and minimize losses. Particular emphasis will be placed on evaluating the implementation of a turbocharger in the engine, playing a critical role in ensuring the engine's reliability and behavior under high-pressure operating conditions.

Furthermore, this study will contribute to the refinement of combustion models, with the goal

of accurately predicting and optimizing hydrogen combustion behavior in an argon-rich environment. Starting from a baseline diesel engine model for Scania trucks, this thesis aims to progessively develop an HPDI argon-hydrogen configuration in GT-SUITE, suitable for engine testing in the future, following the current pre-development phase.

Ultimately, this research seeks to provide valuable information and practical solutions to advance the development of sustainable propulsion systems, supporting Scania's commitment to environmental innovation in the transportation sector.

1.3 Limitations

This analysis is limited to 1D simulations in GT-SUITE, based on a finite number of convergence criteria, later explained in the methodology chapter. This involves a certain number of limitations and constraints.

Being part of a pre-development program in Scania, there will be no real-engine testing during the thesis period, or any hardware prototyping included, although considerations about technical and logical requirements will be conducted and discussed in chapter 6.

Furthermore, the base engine architecture is referred to a six-cylinder diesel layout, commonly used in the majority of current Scania trucks and tuned for diesel applications; the turbocharging components, containing compressor and turbine maps validated through CFD analysis, are also optimized for diesel engines.

Simulations are conducted at steady-state conditions, since in this development phase, transient analysis are not considered as a priority.

1.4 Methodology

This thesis follows a simulation-driven approach focused on optimizing the thermodynamic performance of the engine. The process begins with the development of a 1D GT-SUITE model based on an existing diesel engine architecture. This model, initially configured for open-loop hydrogen operation, is adapted to a closed-loop Argon Power Cycle. Following this, turbocharging strategies are progressively introduced to enhance the overall engine performance under a wide range of initial conditions.

At each stage, the updated model is evaluated through a series of steady-state simulations, quantifying the impact of the implemented variables on brake thermal efficiency, turbocharger performance, and overall thermal behavior. Comparisons are drawn after each major hardware modification to assess gains or trade-offs. While this section outlines the general workflow, specific simulation settings, calibration methods, and sweep parameters are described in detail in chapter 3.

The results of the simulations and analyzes will be used to validate the proposed solutions.

1.5 Research questions

This research aims to explore the feasibility and optimization of a closed-loop Argon Power Cycle applied to a hydrogen-fueled internal combustion engine, evaluating its potential to enhance efficiency while maintaining practical implementation constraints. A fundamental aspect

of this study is the comparison between closed-loop and open-loop architectures of the same technology, assessing their respective advantages and limitations in terms of thermal efficiency, emissions, and overall system performance.

The first key research question is: what are the thermodynamic and operational advantages of the closed-loop cycle, analyzing the argon as a working fluid on combustion dynamics, heat transfer as well as exhaust gas recirculation?

One of the key advantages of a closed-loop configuration is the greater number of degrees of freedom which, although increasing system complexity, allow exploring unconventional thermodynamic states that deviate significantly from those typically encountered in conventional engine architectures. How does this complexity influence the current study?

A second fundamental aspect examines the role of turbocharging in such an unconventional cycle. How does a fixed-geometry turbocharger impact on boosting efficiency and mitigating pumping losses? What are the advantages of turbo-matching strategies in optimizing the system response and enhancing engine flexibility?

A critical research question concerns the cooling phase, focusing on the optimization and integration of existing heat exchanger solutions provided by Scania suppliers in the closed-loop engine model; how can water vapor be extracted from the engine to re-establish stable conditions in the loop? Which is the best composition of the working fluid (argon–oxygen mixture) to enhance the cooling performance, critical for restoring optimal thermal conditions at the start of each engine cycle?

Moreover, the role of the initial charging pressure of the working fluid is investigated; does a direct correlation between flow pressure and engine efficiency exist, considering the potential increase in mechanical stress within the engine?

By addressing these research questions, this study aims to establish a deeper understanding of turbocharging, thermal management, and combustion performance in hydrogen-powered closed-loop ICE systems.

2 THEORETICAL BACKGROUND

2.1 Argon Hydrogen Internal Combustion Engine

Internal combustion engines have been the dominant power source for transportation and industrial applications for over a century, relying primarily on fossil fuels such as gasoline and diesel. The basic principle of an ICE is the conversion of chemical energy stored in fuel into mechanical work through a combustion process. The earliest practical internal combustion engine was developed in the 19th century, with figures such as Étienne Lenoir and Nikolaus Otto playing crucial roles in its evolution. Lenoir's engine, introduced in the 1860s, was one of the first to use a fuel-air mixture ignited by an electric spark, while Otto's development of the four-stroke cycle in 1876 set the foundation for modern gasoline engines. Compression-ignition engines, later introduced by Rudolf Diesel in 1892, further revolutionized the field by offering higher thermal efficiency and better fuel economy compared to their spark-ignition counterparts. Throughout the 20th century, several advancements in materials, fuel injection, and turbocharging continuously improved the efficiency and power output of ICEs, making them the backbone of global mobility. However, despite these technological developments, the reliance on fossil fuels still leads to growing concerns about environmental sustainability, greenhouse gas emissions, and air pollution. These concerns have driven extensive research into alternative fuels that can maintain the practicality of ICEs while reducing their environmental impact.

Hydrogen has emerged as one of the most promising alternatives to conventional fossil fuels due to its clean combustion properties, energy density and potential for high efficiency. Interest in hydrogen as a fuel dates back to the early days of combustion research, with notable experiments conducted by Étienne Lenoir, who reportedly ran his early engine prototypes on a hydrogen-air mixture. In the 20th century, NASA and aerospace engineers extensively used hydrogen in rocket propulsion, proving its high energy content and viability as a fuel. The first serious attempts to integrate hydrogen into conventional ICEs for transportation began in the mid-to-late 20th century, with experimental vehicles tested by manufacturers such as BMW, Ford, and Mazda. Unlike hydrocarbons, hydrogen combustion does not produce carbon dioxide (CO_2), making it particularly attractive in the quest for low-emission propulsion technologies. In addition to its zero-carbon combustion, hydrogen offers a wide flammability range, which allows for ultra-lean burn strategies that can further enhance engine efficiency [1]. Its high flame speed enables rapid combustion, potentially improving power output compared to conventional fuels. However, its low ignition energy increases the risk of pre-ignition and knock, which necessitates careful engine calibration to ensure stable and controlled combustion. One of the primary technical challenges of using hydrogen in ICEs is its low volumetric energy density, which requires high-pressure storage systems or cryogenic tanks to provide adequate vehicle range. Despite these challenges, hydrogen ICE technology has received renewed interest in recent years, particularly in applications where battery-electric solutions may not be feasible, such as heavy-duty transportation and off-road machinery. Automakers and research institutions continue to refine hydrogen ICE designs, exploring advanced fuel injection techniques, optimized combustion chamber geometries, and hybrid powertrain integrations to maximize performance while minimizing emissions.

A possible development for hydrogen ICEs relays in closed-loop engines, characterized by the substitution of air with another suitable fluid. Due to its unique thermophysical properties as an inert noble gas, argon is a valid alternative for the implementation of closed-loop cycles, resulting in Argon-Hydrogen Internal Combustion Engine (Ar-H_2 ICE).

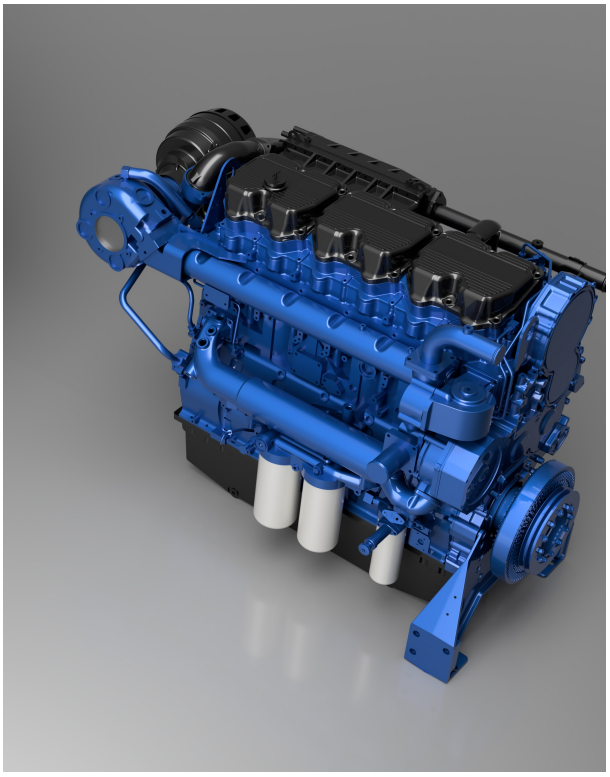

Figure 1. Model of a closed-loop engine

Unlike nitrogen, which is the predominant component of atmospheric air, argon does not participate in combustion reactions, preventing the formation of nitrogen oxides (NO_x). This characteristic alone presents a significant advantage in hydrogen-fueled engines, where high flame temperatures often lead to increased NO_x emissions. Additionally, argon's higher molar heat capacity compared to diatomic gases like nitrogen allows for better retention of thermal energy within the working fluid, leading to improved thermodynamic efficiency. By replacing nitrogen with argon in the intake charge, the heat generated during combustion remains more effectively confined to the system, reducing energy losses and increasing the proportion of heat converted into useful work [2].

The key to fully exploiting argon lies in the implementation of a closed-loop thermodynamic cycle, where the working fluid is continuously recirculated instead of being expelled after combustion. In this system, a mixture of argon and hydrogen is introduced into the combustion chamber, ignited, and expanded to perform work before being cooled and recompressed for reuse. Since argon does not undergo chemical reactions within the engine, it effectively acts as an energy carrier, transferring heat from combustion to mechanical work without being consumed or altered. This closed-loop configuration not only enhances efficiency but also enables precise control over pressure and temperature conditions, optimizing the engine's overall performance. Furthermore, the higher thermal conductivity of argon, relative to nitrogen, contributes to more uniform temperature distribution within the combustion chamber, reducing the likelihood of local overheating and pre-ignition issues commonly associated with hydrogen combustion.

Thermal efficiency improvements in an Argon-Hydrogen ICE stem from both the thermodynamic advantages of argon and the ability to operate at higher expansion ratios without the constraints imposed by atmospheric intake. Traditional internal combustion engines lose a significant portion of their energy through heat transfer to the surrounding environment and the

expulsion of exhaust gases, but in a closed-loop argon-based cycle, these losses are minimized. The higher specific heat ratio (λ) of argon, compared to nitrogen, also plays a crucial role in increasing the efficiency of the engine's expansion process, allowing for greater work extraction per combustion cycle. These combined factors result in a substantial boost in efficiency compared to conventional hydrogen ICEs operating on ambient air. However, the implementation of a fully closed-loop system introduces additional engineering challenges, particularly in the design of heat exchangers, gas recirculation components, and maintaining a stable working fluid composition over extended operation. Despite these challenges, the use of argon in a hydrogen ICE represents a promising pathway toward achieving near-zero-emission internal combustion engines with competitive efficiency level.

2.2 HPDI Technology

2.2.1 Principles of HPDI Systems

High-Pressure Direct Injection technology is a fuel injection system designed to optimize combustion efficiency by introducing fuel directly into the combustion chamber at extremely high pressures. Unlike conventional port fuel injection (PFI) or low-pressure direct injection (DI) systems, HPDI operates at pressures that might exceed 250-300 bar, allowing for precise fuel metering and improved atomization [3]. By injecting fuel at high pressure, such as hydrogen in the engine model under analysis, the fuel droplets achieve finer dispersion, which enhances mixing with the working fluid and leads to a more complete and controlled combustion process. This results in increased thermal efficiency, reduced fuel consumption, and lower emissions compared to traditional injection methods.

In an HPDI system, a small pilot quantity of a highly ignitable fuel, often diesel or another liquid fuel, could be injected first to initiate combustion, followed by the main injection of the primary gaseous fuel at high pressure. In this thesis, this option is not further investigated, as the focus specifically regards the potential of zero-carbon fuels.

In hydrogen applications, HPDI technology allows the introduction of late-cycle fuel, reducing the likelihood of backfiring and abnormal combustion phenomena associated with the low ignition energy of hydrogen [3]. Additionally, HPDI systems enable engines to operate with leaner air-fuel mixtures, improving thermal efficiency and reducing NO_x emissions, as coherently demonstrated in Chapter 4.
Advanced injector designs and electronic control systems further enhance the precision of fuel delivery, optimizing performance across different engine loads and operating conditions.

2.2.2 Relevance of Argon-Hydrogen Fuel Mixtures in HPDI Engines

The use of argon-hydrogen fuel mixtures in HPDI engines presents a highly innovative approach to enhance thermal efficiency while maintaining precise combustion control. In an HPDI system, where high-pressure direct injection is crucial for optimizing fuel-air mixing and ignition timing, the presence of argon as the bulk gas enhances the thermodynamic efficiency of the process. As explained in Section 2.1, it ensures that the energy released during hydrogen combustion is efficiently converted into pressure rather than being lost to rotational or vibrational molecular excitations, maintaining a controlled and stable combustion process at high compression ratios. Moreover, by operating in a closed-loop system with argon as the primary diluent instead of nitrogen-rich atmospheric air, the formation of NO_x emissions is drastically reduced, addressing one of the key challenges associated with high-temperature hydrogen combustion.

Since HPDI relies on precise injection timing and stratification of the fuel mixture, the presence of argon helps moderate peak combustion temperatures while still enabling rapid flame propagation due to hydrogen's high reactivity. This results in a more efficient energy transfer from chemical bonds to mechanical work, maximizing the power output per unit of fuel consumed.

Moreover, the elimination of atmospheric nitrogen from the intake charge prevents any interference with ignition characteristics, ensuring that the combustion process remains predictable and repeatable under varying load conditions. The combination of HPDI technology with an argon-hydrogen fuel mixture represents a significant step forward in achieving high-efficiency, near-zero-emission internal combustion engines, making it an attractive solution for applica-

tions where conventional fuels are being phased out in favor of sustainable alternatives.

2.2.3 Selection of the noble gas for closed-loop ICE

The selection of argon as the noble gas for implementation in a closed-loop internal combustion engine is based on both engineering and economic considerations. The required volume to charge the engine cycle is approximately 0.3 m^3. The specific cost per volume of monoatomic gases is

Noble gas	Cost
Helium	6.3 USD/m^3
Neon	2.5 USD/m^3
Argon	2.7 USD/m^3
Krypton	350 USD/m^3
Xenon	3500 USD/m^3

Table 1. Cost of different noble gases.

Due to their excessive cost per unit volume, krypton and xenon are immediately excluded from practical consideration, leaving the remaining noble gases as viable candidates for the working fluid.

An essential factor to address is the potential contamination of the working gas with CO_2, which would increase the molar heat capacity of the fluid, thereby reducing thermal efficiency. This contamination would necessitate more frequent purging and refilling of the noble gas tank, adding operational complexity and costs, as well as increasing CO_2 emissions. Industrial-grade argon typically contains less than 10 ppm of carbon dioxide, making it a suitable choice in this regard.

Recent computational fluid dynamics (CFD) simulations have examined the potential formation of NO_x and N_2O during the purging and refilling process. These emissions depend on trace amounts of N_2 present in the system, as well as the frequency of purging and refilling cycles. When using argon in a closed-loop cycle, NO_x emissions are found to be around 1 mg/kWh for a conventional road vehicle, a value significantly below the regulatory limits imposed worldwide. This highlights the effectiveness of argon in achieving ultra-low emissions while maintaining high thermal efficiency in closed-loop internal combustion engines.

Moreover, fluid-dynamic simulations regarding the penetration of H_2 spray in different noble gases, at the same backpressure, show how an Argon matrix leads to low penetration and low wall heat losses, compared to Helium and Neon, due to higher molar weight and lower heat transfer coefficient. Conversely, Neon and Helium are subjected to higher H_2 penetration and wall heat losses. [4] Additionally, Argon was selected because of its relatively high availability on the market and it facilitates the creation of gas-tight seals. [5]

2.2.4 Consequences of diluting with a noble gas

The use of a noble gas such as argon as a diluent in an internal combustion engine fundamentally changes the operational dynamics compared to conventional air-based systems. In a traditional

engine running on air, there is an effectively unlimited supply of the bulk gas, as atmospheric intake continuously replenishes the working fluid with each cycle. This allows the engine to operate as an open system, where fresh air is drawn in during the intake stroke, compressed, mixed with fuel, combusted, expanded to produce work, and finally expelled along with the combustion products. The cycle is inherently dependent on a continuous exchange of gases, and since air consists largely of nitrogen, which remains chemically inert in most of the combustion process, it serves as a passive working fluid that does not need to be retained or managed beyond the exhaust phase.

In contrast, when using argon—or any noble gas such as helium or neon—the system cannot rely on an external, abundant source of the bulk gas. Argon is a finite resource within the engine and must be retained, requiring a fundamental shift from an open system to a closed-loop configuration. Instead of expelling the working fluid after each cycle, the exhaust gases must be captured, cooled, and reintroduced into the intake system to maintain a consistent charge composition. This results in an engine operating with an (almost) 100% Exhaust Gas Recirculation (EGR) strategy, where the bulk gas is continuously recycled to sustain the thermodynamic cycle. The key challenge in this approach lies in the need for efficient heat exchangers to cool the exhaust gases before reinjection, preventing excessive temperature buildup that could affect combustion stability and material integrity. Additionally, the removal of residual combustion products, such as water vapor and any minor impurities, is necessary to maintain the purity of the working fluid over extended operation. Despite these engineering challenges, the closed-loop noble gas approach offers significant advantages in thermal efficiency, reduced heat losses, and the elimination of nitrogen oxides (NO_x) emissions, making it an attractive alternative for high-efficiency, near-zero-emission internal combustion engines.

2.3 Thermodynamic Principles of Argon-Hydrogen Combustion

2.3.1 Argon power cycle

Although the theoretical advantages of using argon in thermodynamic cycles have been understood since the 19th century, practical internal combustion engines have historically relied on air due to its ubiquitous availability and its dual role as an oxidizer and working fluid. The Argon Power Cycle revisits this paradigm by employing a fully closed-loop system, effectively utilizing 100% exhaust gas recirculation. This approach allows the working fluid—argon—to be retained within the system, eliminating reliance on atmospheric air and enabling independent control of system pressure[6]. Oxygen, required for combustion, is incrementally introduced along with the fuel, permitting efficient operation across varying load conditions without the decline in efficiency seen in conventional open systems.

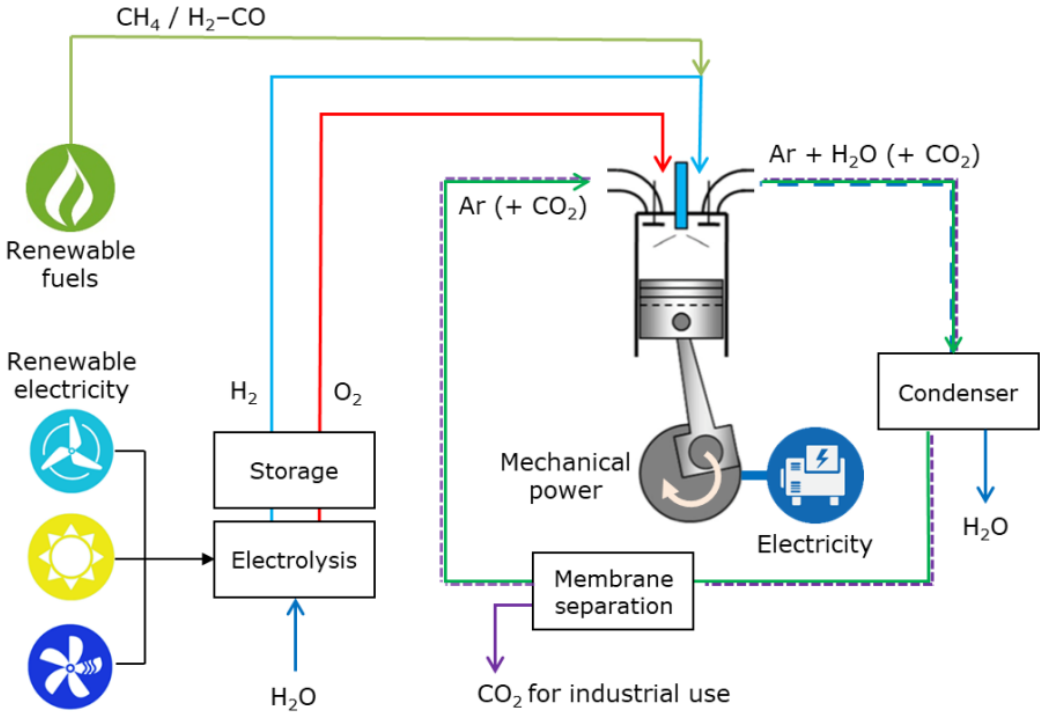

Figure 2. General schematic of an Argon Power Cycle

[2]

A notable advantage of this nitrogen-free environment is the near-elimination of nitrogen oxide (NO_x) emissions during hydrogen combustion. This creates the foundation for a clean power generation solution, especially well-suited for renewable energy integration. While hydrogen is the preferred fuel due to its clean combustion profile, the APC is also compatible with methane-based fuels such as natural gas or biogas. This multi-fuel capability allows the system to operate during hydrogen scarcity, thus enhancing its operational continuity and competitiveness with existing energy technologies.

The exhaust gases in the APC exit the combustion chamber at elevated pressures. When hydrogen is used as the primary fuel, the process concludes after condensation of the water vapor in a high-pressure condenser. In contrast, when carbon-containing fuels are utilized, the exhaust

stream passes through a membrane separation unit. This unit captures carbon dioxide (CO_2) while recycling argon back into the intake, enabled by the high partial pressure and enclosed nature of the cycle. The eventual efficiency penalty of this CO_2 separation is minimal—typically under 5%—making the process suitable for carbon capture and utilization (CCU) or long-term storage. In this thesis work the fuel does not contain carbon, therefore the engine emissions are almost null (motor oil contains carbon that leads to CO_2 contamination).

From a system perspective, the APC offers significant advantages in efficiency and cost over alternatives such as fuel cells or combined-cycle gas turbines. With efficiencies exceeding 60% and lower capital investment requirements (estimated at around 500 €/kW versus 3000 €/kW for fuel cells), the APC represents a promising solution for grid-scale energy storage and dispatch. Furthermore, its fast ramp-up capability and modular design make it well-matched to the variability of renewable energy sources.

2.3.2 Thermodynamics of an APC

One of the fundamental advantages of using argon as bulk in this engine lies in its impact on the thermal efficiency. Considering a simple Otto cycle, the theoretical efficiency is given by the expression [4]:

$$\eta = 1 - \left(\frac{1}{CR}\right)^{\gamma-1}$$

where CR is the compression ratio and γ is the specific heat ratio of the working fluid.

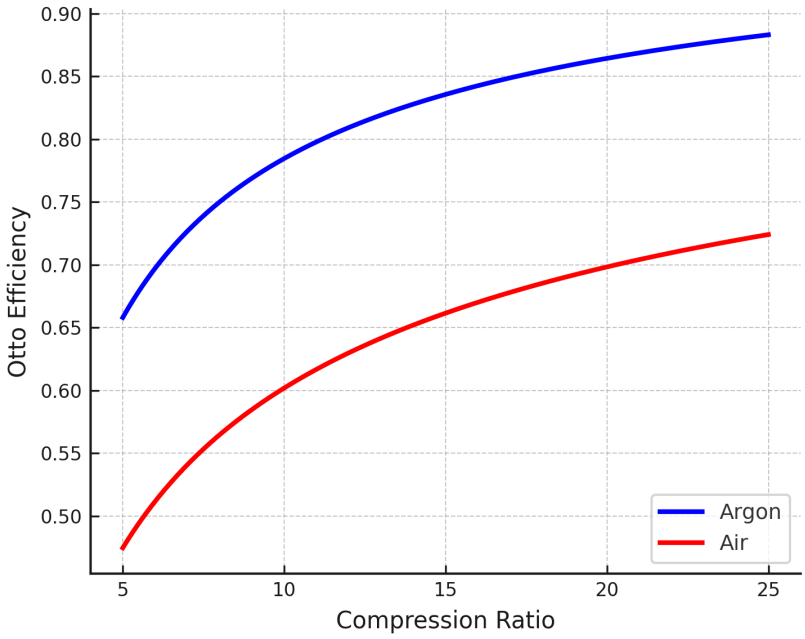

Figure 3. Otto efficiency working with Air or Argon as bulk

A higher γ value leads to a higher thermal efficiency for a given compression ratio. The specific heat ratio itself is a function of the number of degrees of freedom f of the gas, defined as:

$$\gamma = 1 + \frac{2}{f}$$

Monoatomic gases, such as argon, possess three degrees of freedom, resulting in a higher γ compared to diatomic gases such as air. For noble gases, including He, Ne, Ar, Kr, Xe, and Rn, the molar heat capacities are:

$$C_{v,m} = \frac{3}{2}R \quad \text{and} \quad C_{p,m} = \frac{5}{2}R$$

This leads to $\gamma = \frac{5}{3}$, significantly higher than the value for air (approximately 1.4), thereby improving theoretical efficiency. Figure 4 clearly illustrates this effect, showing that for the same compression ratio, engines using argon can achieve substantially higher Otto cycle efficiencies than those using air.

Moreover, a higher γ implies that the gas temperature increases more with the same heat input, enhancing thermodynamic responsiveness and potentially improving combustion kinetics.

2.3.3 Heat Transfer and Thermal Efficiency

Heat transfer and thermal efficiency are fundamental aspects in the analysis of internal combustion engines, particularly the Argon-Hydrogen HPDI engine, where the advantage obtained in energy conversion is the main purpose derived by the utilization of a monoatomic gas as bulk. Thermal efficiency (η_{th}) is defined as the ratio of the useful work output (W_{out}) to the total chemical energy input (Q_{in}) from the fuel, expressed as:

$$\eta_{th} = \frac{W_{out}}{Q_{in}}$$

This efficiency is directly influenced by the heat transfer characteristics within the combustion chamber, as any heat lost to the cylinder walls, piston, and exhaust system reduces the available energy for mechanical work. This limits the adoption of too high compression ratios that would result in critical temperature in the combustion chamber and reduced combustion efficiency.

The first law of thermodynamics governs this energy balance, stating that the total energy input is either converted into work or dissipated as heat loss. As previously shown for an Otto cyle, in the case of an argon-based closed-loop system, the specific heat ratio ($\gamma = c_p/c_v$) plays a key role in defining the ideal efficiency limits, as higher γ values lead to improved expansion work during the power stroke, enhancing overall thermal efficiency. The theoretical efficiency for an ideal Diesel cycle can be again expressed as a function of the engine's compression ratio (CR), the cut-off ratio (r_c), and the specific heat ratio (γ) of the in-cylinder gas:

$$\eta_{th} = 1 - \frac{CR^{1-\gamma}(r_c^{\gamma} - 1)}{\gamma(r_c - 1)}$$

[7]

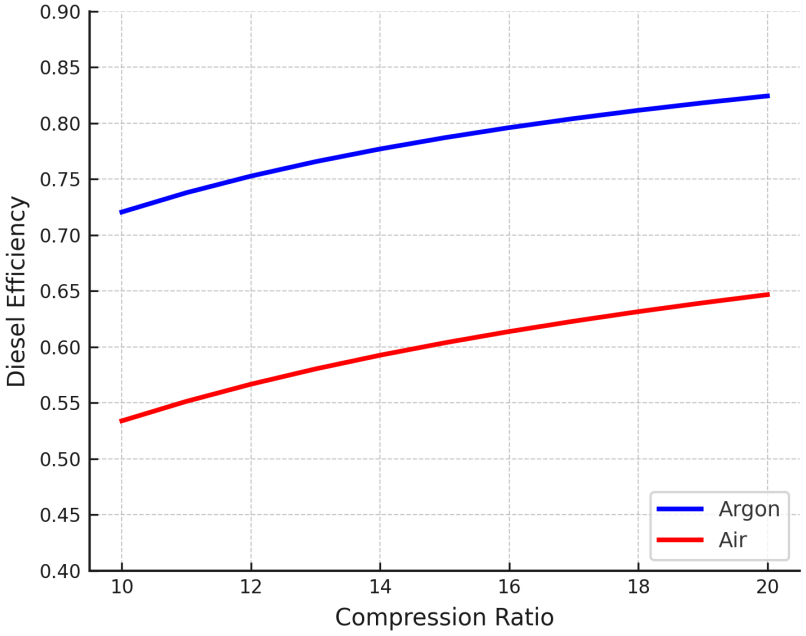

Figure 4. Diesel efficiency working with Air or Argon as bulk

This relationship once again suggests that replacing nitrogen from the air with an optimal diluent could enhance efficiency, due to a higher specific heat ratio ($\gamma = 1.67$, compared to $\gamma < 1.4$ for air).

One can compare molar heat capacity starting from C_p (specific heat at constant pressure) and γ, for both diluent and combustion products, at 1500 K (Ar is not affected by temperature):

Fluid	C_p	γ
N_2	35.149 $\frac{J}{mole \cdot K}$	1.310
H_2	32.356 $\frac{J}{mole \cdot K}$	1.346
Ar	20.730 $\frac{J}{mole \cdot K}$	1.670
H_2O	47.468 $\frac{J}{mole \cdot K}$	1.212
CO_2	57.907 $\frac{J}{mole \cdot K}$	1.168

Table 2. C_p and λ values for different bulk gases and combustion products

In a conventional air-breathing ICE, nitrogen's molecular properties contribute to increased heat losses, while argon's monatomic structure enables to reduce these energy losses, ensuring that a greater fraction of the combustion energy remains within the working fluid. This reduction in heat dissipation enhances the effective temperature rise during combustion, thereby improving thermal efficiency. The closed-loop argon cycle reduces the need for large heat rejection systems, further optimizing the energy utilization within the engine. These characteristics lead to the possibility of operating at significantly higher expansion ratios, approaching the performance of advanced power systems such as fuel cells while maintaining the high power density and reliability of internal combustion technology.

2.3.4 Chemical advantage of a monoatomic bulk gas

One of the key advantages of utilizing a monatomic bulk gas in internal combustion engines lies in its thermodynamic properties, specifically its energy storage characteristics. Unlike diatomic and polyatomic gases, which possess multiple degrees of freedom—including translational, rotational, and vibrational modes—a monatomic gas only stores energy through translational motion. In diatomic gases such as nitrogen (N_2) and oxygen (O_2), rotational degrees of freedom become active at relatively low temperatures, with nitrogen's rotational motion already fully engaged at 100 K, just above its boiling point [7]. Furthermore, vibrational modes in nitrogen start to activate at 350 K, corresponding to the beginning of the compression stroke, leading to the simultaneous functioning of all modes and to an increase of the molar heat capacity. At sufficiently high temperatures (> 3000 K), all diatomic gases approach the same molar heat capacity as all degrees of freedom become fully excited. This results in a higher heat capacity for diatomic and polyatomic gases, as a significant portion of the input energy is absorbed into rotational and vibrational excitation rather than being directly converted into translational kinetic energy, which is responsible for temperature increase. The released enthalpy of combustion from a generic fuel and its oxidant will lead to a higher pressure rise in case of monoatomic bulk gas, compared to when the same combustion products are diluted with an equivalent number of moles of a di or polyatomic gas. Consequently, the temperature increase during the compression stroke and the subsequent temperature decrease during the expansion are much more significant.

In contrast, monatomic gases like argon lack rotational and vibrational modes, meaning all the thermal energy supplied to the gas directly increases its translational kinetic energy, and thus its temperature. This property makes monatomic gases more thermodynamically efficient in processes where rapid temperature increases are desired, as less heat energy is required to achieve a given temperature rise compared to polyatomic gases. Chemical inertness allows for the prevention of unwanted side reactions that could affect combustion efficiency or lead to the formation of pollutants, maximizing efficiency and minimizing emissions.

2.4 Combustion Dynamics and Engine Performance

2.4.1 Brake Thermal Efficiency

One of the parameters that characterizes the engine performance is the Brake Thermal Efficiency, used to assess the effectiveness of an internal combustion engine in converting the chemical energy of the fuel into useful mechanical work. It is defined as the ratio of the brake power (P_b)—the actual power delivered at the crankshaft—to the total energy input from the fuel per unit time:

$$\eta_{BTE} = \frac{P_b}{\dot{m}_f \cdot LHV} \times 100$$

where:

- P_b is the brake power output [kW],
- $\dot{m}_f$ is the fuel mass flow rate [kg/s],
- LHV is the lower heating value of the fuel [kJ/kg].

The brake thermal efficiency is inherently constrained by thermodynamic losses, including heat dissipation to the cylinder walls, exhaust gas losses, and frictional losses. Compression ignition (CI) engines, such as diesel engines, typically achieve higher BTE values (30–45%) due to their high compression ratios and lean combustion characteristics, whereas conventional spark ignition (SI) engines operate at lower efficiencies (20–35%) due to throttling losses and lower compression ratios [8].

To enhance BTE, several strategies can be employed, including turbocharging, consequential turbo-matching and optimized combustion chamber design. The integration of hydrogen as a fuel in a High-Pressure Direct Injection system, combined with an Argon Power Cycle, presents a promising opportunity to improve thermal efficiency. Turbocharging increases intake pressure and temperature, thereby improving volumetric efficiency and increasing the mean effective pressure, further boosting BTE.

In Chapter 4 of this thesis, several parametric studies on variables such as argon mass, lambda, initial pressure and turbocharger multipliers, are carried out to maximize Brake Thermal Efficiency under different initial conditions. In closed-loop cycles, a straightforward cause-and-effect relationship cannot always be expected when altering a single parameter, due to the increased number of coupled interactions within the system [9].
For this reason, a larger number of simulations is required compared to open-loop cycles, in order to obtain accurate insights and develop effective strategies for improving a given model.

2.4.2 Closed-loop cycle thermodynamics

The thermodynamic behavior of closed-loop cycles differs significantly from that of conventional open-loop internal combustion engines. In a closed-loop configuration, the working fluid— such as an argon-oxygen mixture— is recirculated after combustion and recompressed, rather than being expelled into the environment [10]. This allows for tighter control over the fluid composition, pressure, and temperature, as well as reduced heat losses and exhaust energy dissipation.

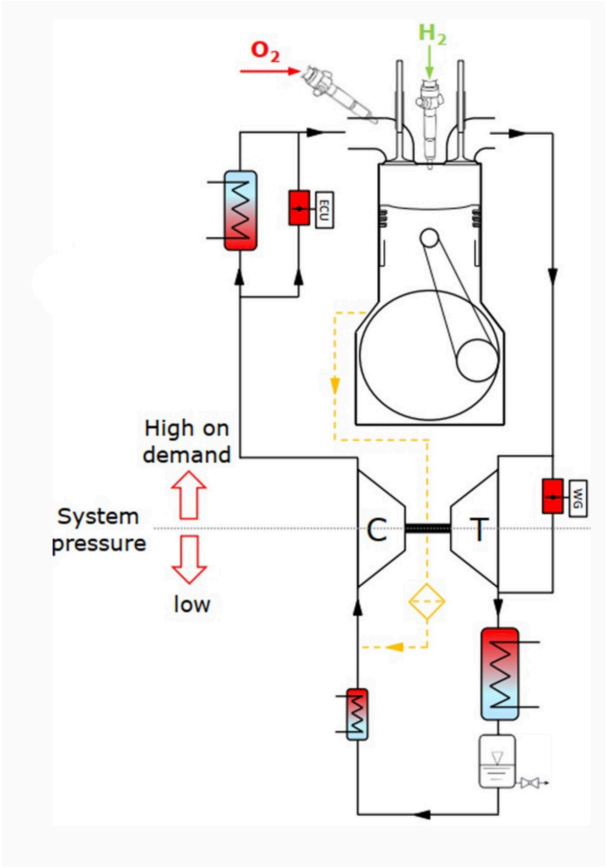

Figure 5. Closed-cycle ICE prototype

The isolation of the system from ambient conditions provides the opportunity to optimize the thermodynamic state points with different constraints, particularly with regard to intake temperature, pressure, and working fluid properties.

Compared to open-loop cycles, the working fluid can be charged up to a certain optimum pressure, as well as heated to the most convenient temperature. This process comes with the cost of a higher stress within the engine components, therefore specific fluid-mechanical studies must be carried out to ensure that required safety factors are satisfied by the solution. One can direct-inject hydrogen and port-inject argon and oxygen, as in this thesis work and in figure 5, or vice-versa, depending on the specific case. In general, exhaust gases are cooled down in order to flow back in the loop at the initial temperature and re-start the cycle under stable conditions. An heat exchanger is needed for this reason and, most importantly, to extract water vapor from the system; an additional boosting system (such as a turbocharger, a supercharger or any other boosting device) can be added to the system to exploit the high amount of heat carried by the exhaust gases [8].

In this thesis, a fixed-geometry turbocharger is implemented in a closed-loop engine model to evaluate whether recovering part of the thermal energy from the exhaust gases can effectively enhance overall engine performance and efficiency, particularly under high load conditions.

2.5 Turbocharging in Argon-Hydrogen Engines

Turbocharging is a widely implemented technology in ICE to enhance performance and efficiency by increasing the intake air (or corresponding fluid) pressure. Using the energy of exhaust gases to drive a turbine connected to a compressor, a turbocharger leads to higher power output without increasing its displacement. In this study, turbocharging enables the pressure drop to be mitigated within the closed-loop argon cycle, allowing for more efficient fuel combustion, improved thermal efficiency, and reduced emissions.

Initially, turbochargers were primarily employed in high-performance applications such as motorsport and aviation to maximize power output. However, advancements in engineering and stricter emissions regulations have led to their wide use in commercial cars, or heavy duty trucks, such as in many Scania vehicles.

A turbocharger consists mainly of a turbine and a compressor connected on the same shaft. In open-loop engines, the turbine extracts energy from the exhaust gases, converting it into mechanical work to drive the compressor. The compressor, in turn, increases the air density entering the combustion chamber, allowing for a higher mass flow rate of air and fuel, which results in increased power output [11]. The efficiency of this process is influenced by turbine and compressor design, as well as turbocharger configurations, including single-entry, twin-entry, and variable geometry turbochargers (VGTs).

By optimizing combustion conditions and enabling smaller, more efficient engine designs, turbochargers contribute to the development of cleaner and more sustainable transportation technologies. Their integration into modern internal combustion engines remains essential as the industry transitions toward alternative propulsion solutions, aligned with Scania CV values.

2.5.1 Turbocharger relevance to Argon-Hydrogen engines

The implementation of a turbocharger in a closed-loop Ar-H_2 engines presents both opportunities and challenges. Turbocharging can enhance the overall efficiency of the engine by increasing the intake pressure, allowing for a higher mass flow rate of the reactants, and consequently improving combustion efficiency. A turbocharger in this configuration could further amplify the benefits brought by argon inertness, by recovering otherwise wasted exhaust energy to boost intake pressure, thereby increasing power output without significantly affecting fuel consumption.

However, the closed-loop nature of the system introduces additional complexities. Unlike conventional air-breathing engines, an Ar-H_2 engine recirculates exhaust gases, requiring precise control of pressure ratios to maintain a stable and optimized working fluid composition. In relation to this, in this thesis work a charge-air cooler will be added after the turbocharger compressor to lower the fluid temperature and obtain a reasonable combustion efficiency. Additionally, the unique thermo-physical properties of argon may influence turbine and compressor performance, would necessitate ad-hoc turbocharger designs and specific CFD studies, as described in Section 1.3.

Despite these challenges, a well-integrated turbocharger could significantly enhance the power density and efficiency of a closed-loop Ar-H_2 engine.

2.5.2 Basic turbocharger configurations

The turbocharger model implemented in the Ar-H_2 engine under analysis is a fixed-geometry turbocharger, due to its relatively simple design and its wide utilization.

A single turbocharger configuration employs a single turbine-compressor unit to increase the intake air density, thereby improving the engine's power output and efficiency. This setup is one of the most commonly used turbocharging strategies, especially in passenger vehicles, commercial trucks, and some high-performance applications due to its balance between cost, complexity, and performance. The primary advantage of a single turbocharger lies in its simplicity and compact design, making it relatively easy to integrate into various engine architectures without excessive modifications to the intake and exhaust systems. The efficiency of this process depends on factors such as turbine size, aspect ratio (A/R), and the boost control mechanism [12].

Twin-scroll turbochargers represent an advancement over traditional single-scroll designs by enhancing engine performance and efficiency through optimized exhaust gas flow. In a single-scroll turbocharger, exhaust gases from all cylinders converge into a common manifold before entering the turbine. This configuration can lead to interference between exhaust pulses, diminishing the energy delivered to the turbine and potentially increasing back pressure, which adversely affects engine scavenging and performance, particularly at lower engine speeds.

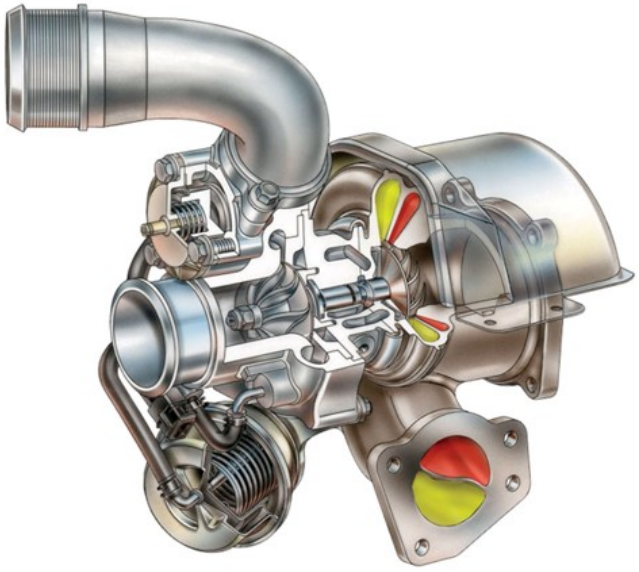

Figure 6. Twin-scroll turbocharger model.

In contrast, twin-scroll turbochargers feature a divided turbine housing that separates the exhaust channels from paired cylinders. This design ensures that exhaust pulses remain distinct as they enter the turbine, effectively reducing pulse interference and preserving exhaust gas energy. The result is improved turbine efficiency, leading to enhanced low-end torque, quicker boost response, and increased power output across a broader engine speed range. Additionally, the separation of exhaust pulses contributes to reduced engine pumping losses and improved fuel economy.

2.5.3 Advanced Turbocharger configurations

Variable Geometry Turbochargers (VGTs) are advanced turbocharging systems designed to optimize engine performance across a wide range of operating conditions, dynamically adjusting the effective AR, altering the volute's cross-sectional area to reach the optimal airflow at different engine speeds [13]. Unlike fixed-geometry systems, VGTs enable a more linear relationship between turbine pressure ratio and mass flow, enhancing performance across a broader operating range. They come with added complexity and cost due to their more intricate mechanical components. Additionally, the durability of moving parts within the turbine must be carefully considered, especially in high-temperature applications such as hydrogen combustion.

Electric turbochargers represent an advanced forced induction technology based on the integration of a high-speed electric motor directly onto the shaft of a conventional turbocharger. E-Turbos utilize electrical power to either supplement or independently drive the compressor, unlike traditional systems that rely exclusively on exhaust gas energy to spool the turbine. This results in a significant improvement in low-end torque, transient response, and turbo lag mitigation.

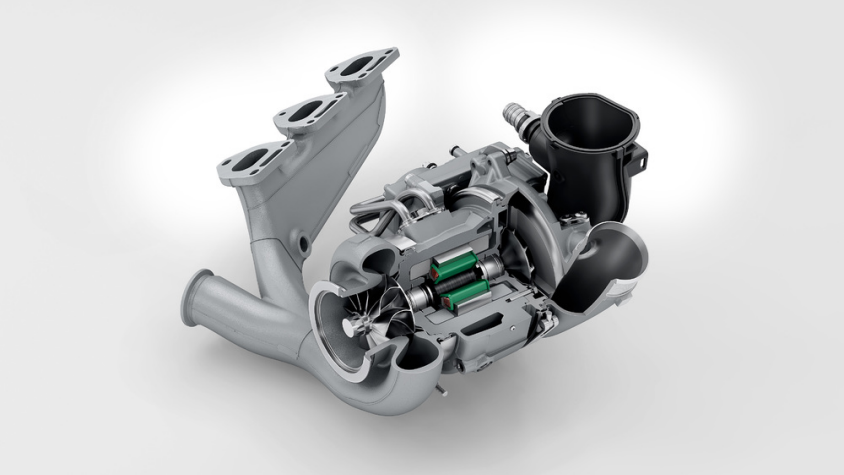

Figure 7. Electric turbocharger.

In the context of a closed-loop Argon cycle, electric turbochargers might offer distinct benefits. Since the system lacks fresh atmospheric intake and depends entirely on controlled recirculation of the working fluid, maintaining stable intake pressure across all operating conditions is critical. An electrically assisted turbocharger enables tighter control of intake-exhaust pressure differentials, allowing for consistent air–fuel ratios, minimizing misfires, and optimizing combustion phasing.

Moreover, electric turbines can recover excess exhaust energy as electrical power (turbo-compounding), potentially supporting hybrid energy storage systems or powering ancillary components.

3 METHODOLOGY

3.1 1D Modeling

3.1.1 GT-power resolution

GT-POWER can be used to predict either steady-state conditions or transient behavior of engine systems. Outputs include single-valued quantities (such as averages, maximums, minimums and so on) or crank-angle or time-resolved quantities such as:

- Engine volumetric efficiency, power, and torque;
- Flow rates and flow velocities in all passages;
- Pressure and Temperature of the gases in each component of the system;
- Temperatures of the walls of pipes, flowsplits and other components;
- DI diesel NOx and soot;
- Aftertreatment chemistry;
- Heat transfer.

The GT-POWER solver computes the performance of a generic engine by either calculating the brake torque for an imposed engine speed, in speed mode, or by solving the speed from an imposed load, according to the load mode. Speed mode is the most commonly used mode of engine simulation, especially for steady state cases, therefore the majority of the cases simulated in this thesis will be conducted under this solving method. The speed can be either imposed constant or by a dependency reference object. Speed mode typically leads to steady-state results quickly because the speed of the engine is imposed for the duration of the simulation, thus eliminating the relatively long period of transient time that is required for the crankshaft speed to reach steady-state in a loaded engine. Load mode allows the user to impose a load on the engine or to couple the engine to a vehicle model so that the speed of the engine will be calculated. The speed is calculated by taking into the account the predicted brake torque of the engine, the load torque applied to the engine, and the engine inertia. A load can be imposed as a constant or a transient function to model a load such as dynamometer, propeller, or transmission. Load mode can be used to calculate information about the engine's response to loads, but the nature of these simulations usually requires many simulation cycles to be run before the desired results will be achieved.

In this work, speed mode is the solving method used in the majority of the simulations and the brake torque is computed in each iteration in order to fulfill one of the convergence criteria, as explained more in detail in Section 3.3.2.

3.1.2 Governing equations

The simulation of unsteady, compressible flow through internal combustion engine components is based on a one-dimensional solution of the fundamental conservation laws: mass, momentum, and energy. In this work, these governing equations are applied to discrete control volumes representing the internal flow path, such as intake/exhaust runners, valves, and combustion

chambers, as part of a 1D engine modeling framework implemented in GT-SUITE. The fluid flow solution evolves over time using either explicit or implicit integration schemes depending on the application's temporal resolution requirements. The fluid domain is discretized into control volumes for scalar properties (e.g., pressure, temperature, internal energy) and boundary interfaces for vector quantities (e.g., velocity, mass flux), following a staggered-grid approach. The governing equations for each subvolume take the following differential form:

$$\frac{d(\rho V)}{dt} = \sum \dot{m}_{\text{in}} - \sum \dot{m}_{\text{out}}$$
$$\frac{d(\rho u V)}{dt} = \sum \dot{m}(h + \frac{u^2}{2}) - \dot{Q}_{\text{wall}} - \dot{Q}_{\text{loss}}$$
$$\frac{d(\rho \vec{v} V)}{dt} = -\sum A \left(p + \frac{1}{2}\rho u^2 \right) + F_{\text{fric}} + F_{\text{body}}$$

Here, ρ represents the local fluid density, V is the control volume, and $\dot{m}$ denotes the mass flow rate across the control volume boundaries. Energy conservation is governed by the change in internal energy u, including the effects of enthalpy transport, kinetic energy, and thermal losses via wall heat transfer $\dot{Q}_{\text{wall}}$. Momentum conservation accounts for pressure forces, velocity gradients, frictional resistance, and gravitational or inertial body forces. The formulation also incorporates thermodynamic closure through the equations of state, which relate ρ, u, p, and T for each species present. Time integration schemes vary in accuracy and stability; the explicit method offers high resolution of wave dynamics at the cost of smaller time steps, whereas the implicit method enables faster convergence for quasi-steady or low-speed flow conditions. For the present engine cycle analysis, the explicit solver is employed to capture transient wave dynamics and combustion-related pressure pulsations with high fidelity. The list of parameters included in the governing equations is:

- ρ — Fluid density [kg/m^3]
- V — Control volume [m^3]
- $\dot{m}$ — Mass flow rate [kg/s]
- u — Specific internal energy [J/kg]
- h — Specific enthalpy [J/kg]
- p — Static pressure [Pa]
- $\vec{v}$ — Velocity vector [m/s]
- A — Cross-sectional flow area [m^2]
- $\dot{Q}_{\text{wall}}$ — Heat loss through walls [W]
- F_{fric} — Friction force [N]
- F_{body} — Body force (gravity, acceleration) [N]

As explained in the following paragraphs, these equations are also determinants of the convergence criteria of the 1D engine model implemented on GT-SUITE. [14]

3.1.3 CFD Integration

To enhance the fidelity of the 1D engine simulation, high-resolution Computational Fluid Dynamics (CFD) data were integrated at several critical stages of the modeling process. CFD simulations were performed on key components, namely the turbine, compressor, and combustion chamber, to extract detailed flow characteristics, thermal gradients, and localized turbulence behavior that cannot be resolved in one-dimensional formulations.

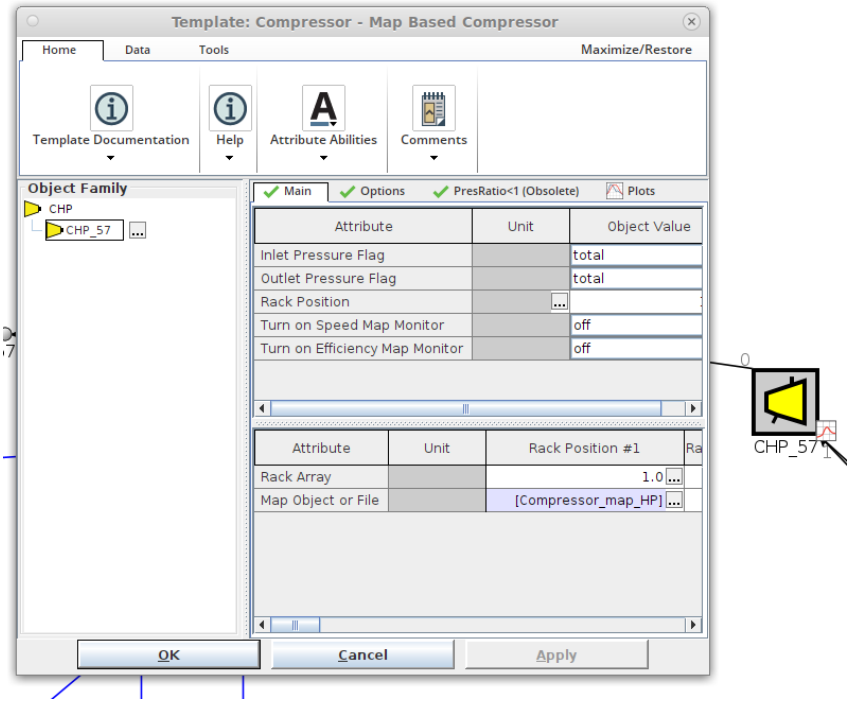

Figure 8. Compressor map obtained with CFD.

The data obtained from steady and transient CFD runs were used to refine the performance maps of both the turbine and compressor by correcting for non-ideal flow behavior, such as flow separation and heat transfer losses, under varying load and boost conditions. The integration of CFD thus ensured that the reduced-order GT-SUITE model remained physically grounded and predictive across a wide range of operating conditions.

Being this thesis work part of a bigger project co-developed with Scania CV AB and currently in the pre-development phase, every CFD simulations was conducted by other teams within the company and tuned for diesel engine components, such as cylinders, compressors and turbines. This assumption is well established and has been taken consciously, representing the best possible trade-off between time and working/economic resources. Though this might not be the most accurate assumption possible, the time required to implement CFD simulations focused on hydrogen fuel, considering also the non-homogeneous conditions that characterize a closed-loop engine, has been considered too long at this stage of the project. Several considerations and corrections are therefore taken into account throughout the 1D simulations, with regard to cylinders and turbocharger components. Since the very beginning of the study, a direct injection (DI) diesel combustion model has been implemented in the GT-SUITE coherently with the Hydrogen Direct Injection engine under analysis, while several studies on turbomatching have been conducted in order to exploit both the turbine and the compressor potential..

3.1.4 Time-domain solver

The transient simulation of the engine cycle is carried out using an explicit time integration scheme, selected via the FlowControl setup in GT-SUITE. As shown in Figure 9, the ExplicitControl object governs the time-stepping procedure, which enables fine resolution of unsteady phenomena such as pressure pulsations, combustion wave fronts, and turbocharger interactions. The explicit method integrates state variables forward in time using small time steps determined by the Courant condition, ensuring numerical stability in regions with steep gradients or high flow velocities.

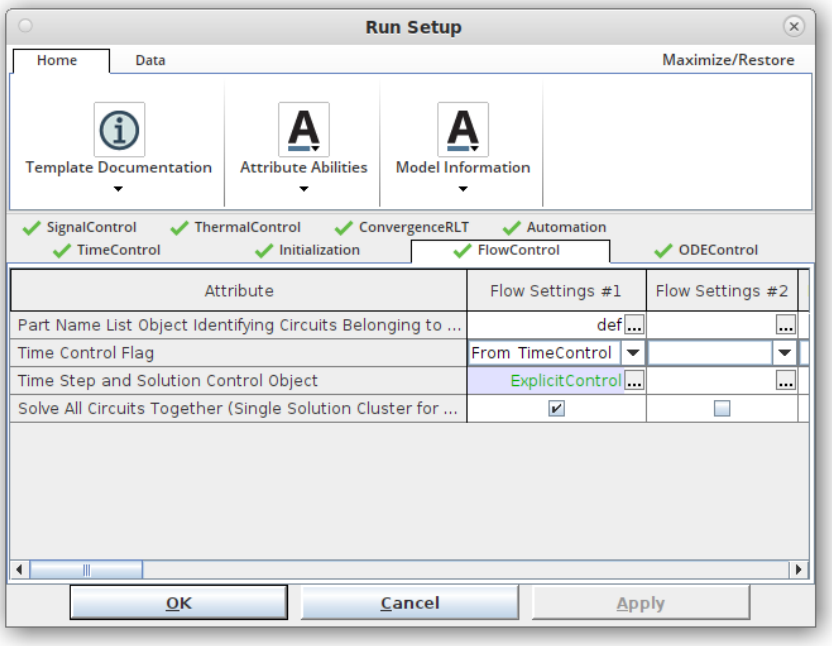

Figure 9. Explicit method time solver.

To balance accuracy with computational efficiency, the simulation is constrained to run for a user-defined range of engine cycles. For this thesis work specifically, a minimum of 40 cycles is enforced to ensure that initial transients dissipate and representative engine behavior is established, while the upper limit is capped at 600 cycles to bound simulation time and storage requirements, as shown in Figure 10. These cycle limits, along with the steady-state convergence criteria, define the temporal boundaries within which the solver attempts to reach a periodic or steady operating condition. The simulation automatically terminates once all residuals fall within predefined thresholds, and the system demonstrates consistent periodicity over consecutive cycles.

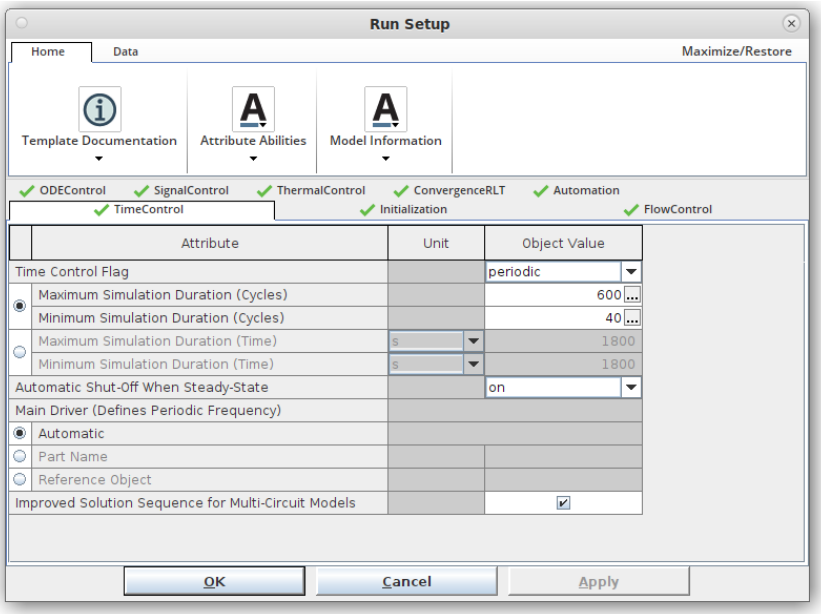

Figure 10. Number of iterations required to converge.

This relatively high number of maximum cycles reflects the difficulties generated by the simulation of a closed-loop engine, due to the oscillations of the values of the initial conditions throughout the different cycles. In general, operating with an open-loop engine implicates steadier conditions, imposed by the intake fluid (air properties can be assumed constant over a general period of time), that would lead to more predictable results from the computational point of view, therefore reducing computing time and number of iterations required to reach convergence. A closed-loop engine is much more complicated to analyze due to the high unpredictability of the flow conditions; cooling devices and/or turbocharging elements are constantly generating an impact on flow pressure, temperature and composition in between two subsequent cycles.

3.2 Base engine model

3.2.1 Initial model

The original engine architecture is related to the *CBE*1 model, present in the newest Scania trucks. A summary of its most relevant characteristics is provided in the following table.

Specification	Value / Detail
Engine type	Inline 6-cylinder, DOHC, 4 valves per cylinder
Displacement	13 L
Maximum power	560 hp
Maximum torque	2800 Nm
Bore × Stroke	130 mm × 160 mm
Fuel type	Diesel / HVO
Emissions standard	Euro 6, Twin SCR system

Table 3. Scania CBE1 engine

The initial GT-SUITE model, tuned for hydrogen applications, represents a six-cylinder internal combustion engine equipped with high-pressure direct injection functionality and is configured in a closed-loop architecture.

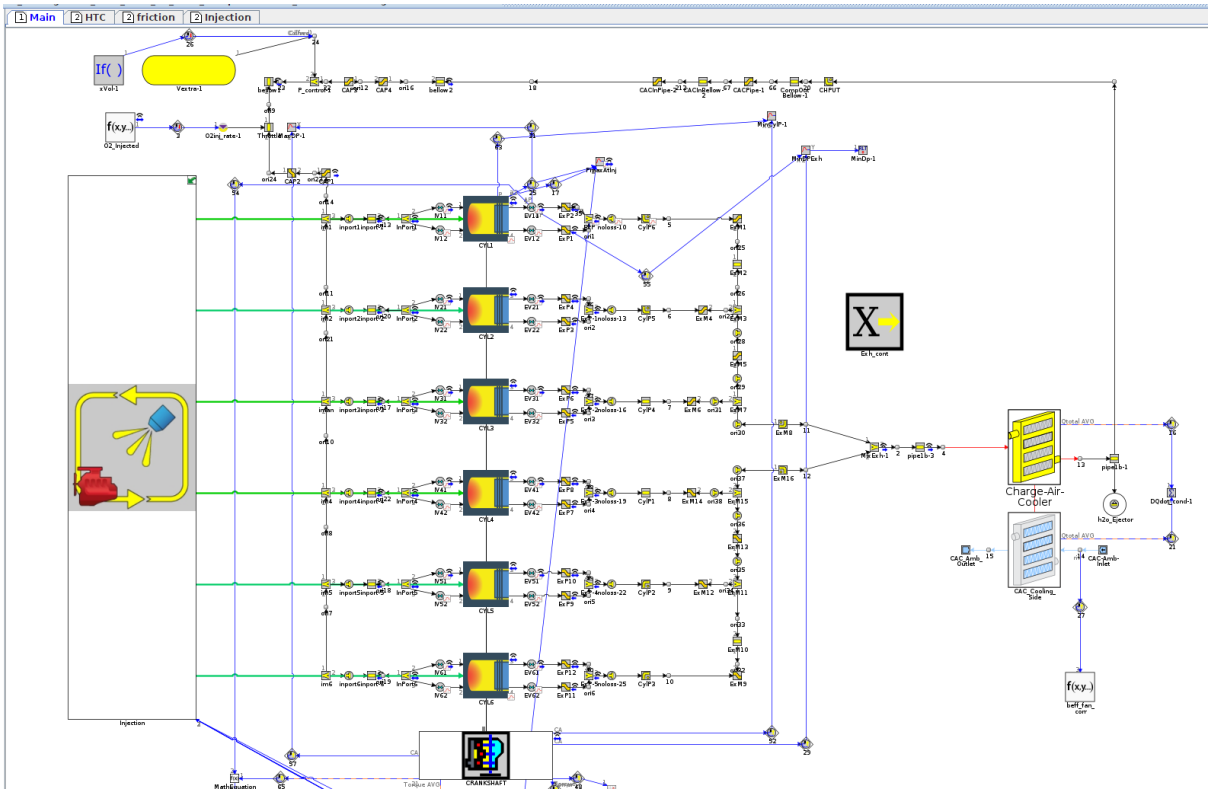

Figure 11. Initial engine 1D model implemented in GT-SUITE.

The layout shows a bank of six cylinders, each linked to an individual injector controlled via a custom injection logic block depicted in the lower-left corner. Hydrogen is therefore directly injected in the cylinders, while oxygen is port-injected.

Theoretically the opposite configuration with port-injected hydrogen and direct-injected oxygen is implementable, but it is not part of the analysis of this thesis work. The intake system comprises intake ports, throttle controls, and sensors for argon and fuel metering, with each cylinder receiving intake flow through independently modeled intake runners. At the upper left, a volume labeled "Vextra1" contains the initial amount of argon and oxygen, which will be varied and optimized throughout the simulations of the final model. It is important to underline that ideally argon recirculates within the loop, while oxygen constantly induces the combustion in the cylinders and is subsequently extracted as part of water vapor, therefore it is refilled in the following cycle to match the optimal content. Through the oxygen controller, argon and oxygen are mixed in the "Throttle" pipe object, flowing towards the intake ports in each of the six cylinders. The exhaust ports are configured with pressure sensors and valves, and the flow from all cylinders is merged and routed to a condenser cooler assembly. This component is the only one impacted by external air and therefore subject to ambient temperature; a water ejector object is part of the cooling system, managing the gas mixture composition that flows back into the cycle. The cooled charge is looped back into the intake system, establishing the recirculating architecture. The model also features a crankshaft object centrally located at the bottom, serving as the rotational reference for all engine timing and torque-power calculations.

It is important to outline that this initial model does not contain any boosting system (such as a turbocharger) and represents the benchmark for this thesis work; any additional component, starting with a turbocharger, is therefore generating a totally different model that will be compared to the base one to gather as much information as possible about the consequences of such implementation.

A schematic representation of the initial model is shown in the following figure.

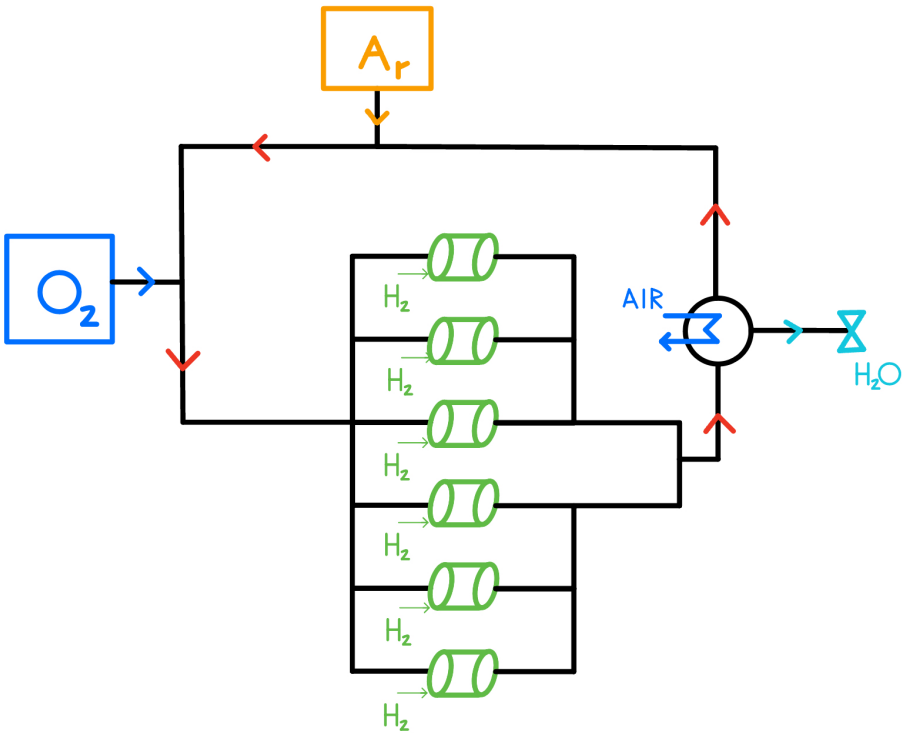

Figure 12. Simple schematic representation of the initial engine model

3.2.2 Turbocharger modeling

The first device implemented in GT-SUITE to vary the initial model described in the previous section is a turbocharger.

A fixed-geometry turbocharger is selected for this study as an initial step toward implementing boosting strategies in the closed-loop engine model. This choice was driven by its simplicity, making it an ideal baseline for integration and validation. Additionally, the unit is owned by Scania, allowing full access to validated turbine and compressor maps without confidentiality constraints. While this represents a practical starting point, it also constitutes a limitation of the current work. Future studies will explore alternative boosting architectures, including variable geometry and electrically assisted turbochargers, to further optimize system performance and flexibility.

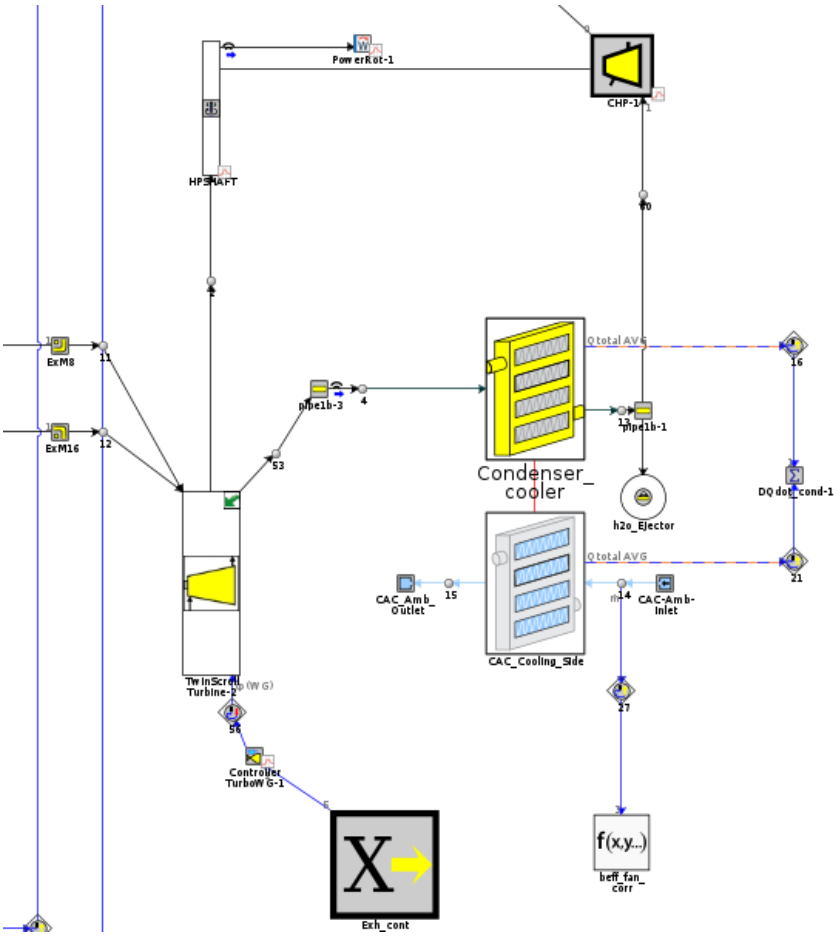

Figure 13. Turbocharger modeling

As shown in the model, the turbine is positioned downstream of the engine exhaust path and receives hot gases through a set of throttle-controlled inlets, allowing regulation of flow energy. The turbine drives the compressor, which increases the pressure and temperature of the intake flow entering the engine. [6] Unlike conventional open-loop engines, the flow exiting the compressor must respect optimal physical conditions for the engine to perform properly, therefore it has an extremely bigger impact on overall efficiency.

A schematic representation of the described model with a turbocharger is shown in the following figure.

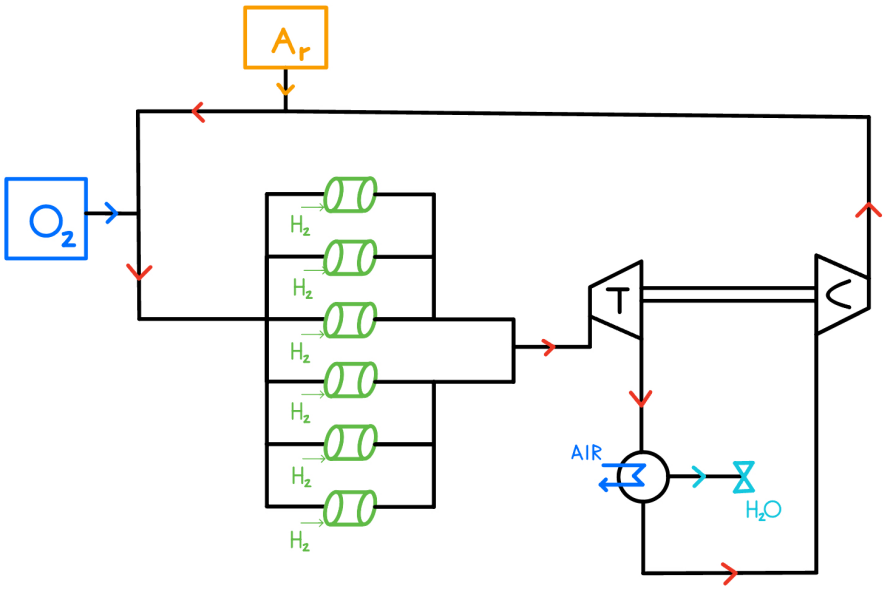

Figure 14. Simple schematic representation of the turbocharged engine model

3.2.3 Cooling modeling

To address the thermal challenges observed in earlier simulation stages (shown in the Results Section 4.2.2), a dual cooling strategy was implemented in the model.

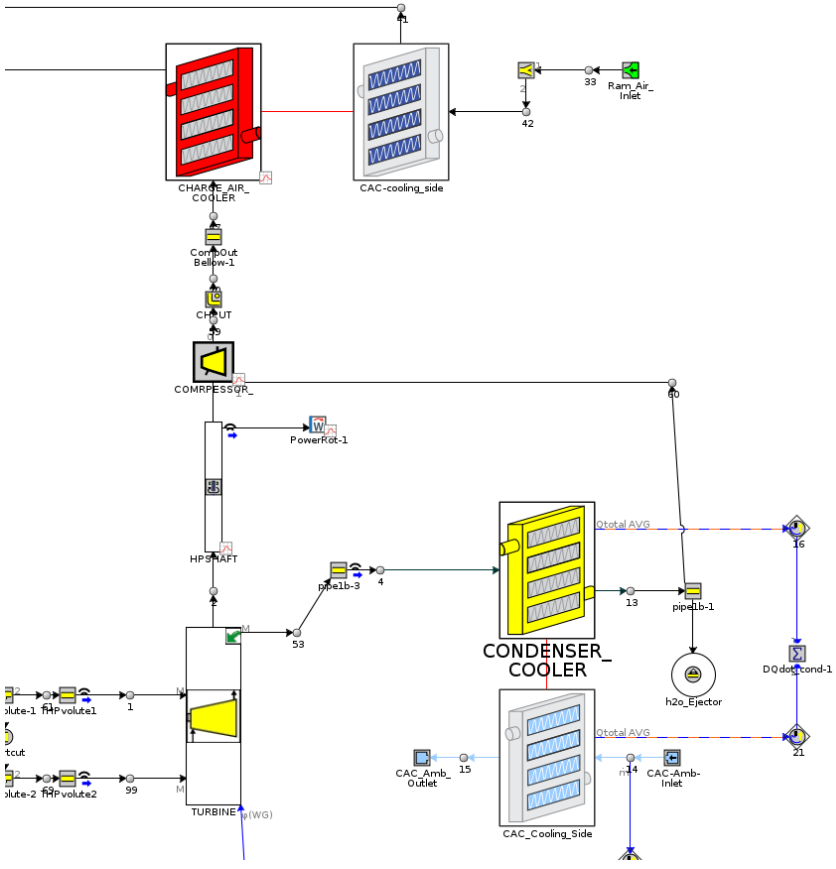

Figure 15. Cooling modeling

As shown in the figure 15, the first cooling unit is a condenser cooler positioned between the turbine and compressor. This component plays a critical role in managing the recirculated working fluid within the closed-loop system by removing residual thermal energy from the exhaust stream before it re-enters the compressor. Its placement ensures that the compressor receives fluid at a reduced temperature, thereby improving compression efficiency and mitigating thermal stress on the compressor stage.

In addition, a charge-air cooler was added downstream of the compressor to further reduce the temperature of the intake mixture before it reaches the combustion chamber. This intervention was introduced after temperature gradients across the intake path were identified as a limiting factor for combustion stability and overall system performance, as detailed in the results section. The charge-air cooler improves charge density and helps maintain consistent inlet conditions across a range of operating points.

Both cooling systems are connected to dedicated heat exchange circuits, with temperature sensors and control valves integrated to monitor and regulate flow and thermal behavior.

A schematic representation of the explained model with a Charge Air Cooler after the Turbocharger compressor is shown in the following figure.

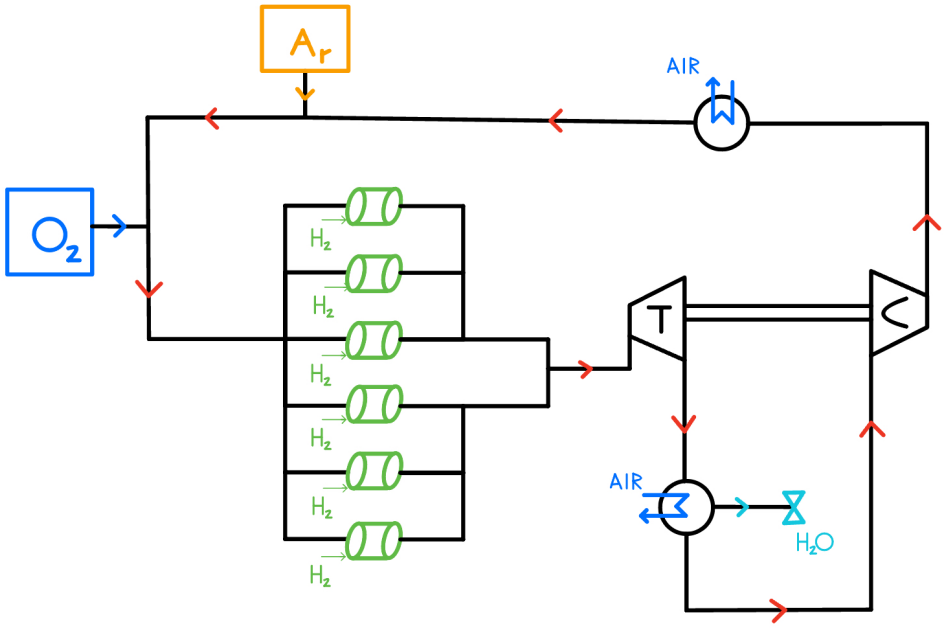

Figure 16. Simple schematic representation of the final engine model

3.2.4 Sensor modeling

This GT-SUITE model employs a comprehensive network of virtual sensors to replicate the physical measurement systems present in real engine setups. These sensors are critical for real-time monitoring, control, feedback within the simulation environment and convergence criteria. The Engine-sensors block aggregates signals such as torque, power, crank angle (CA), and rotational speed (RPM) to provide vital state variables to other components like controllers and evaluators.

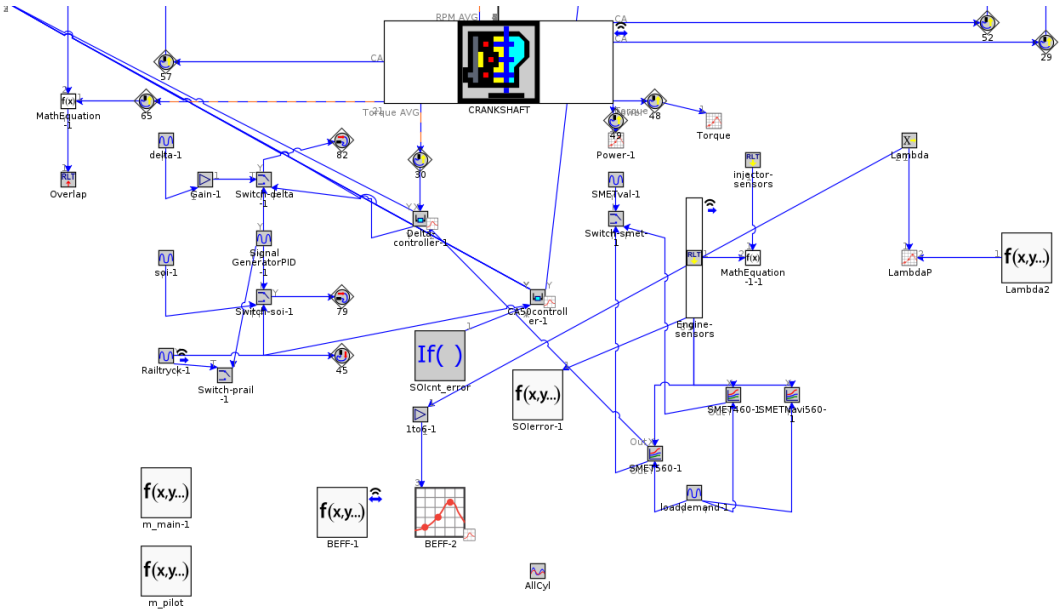

Figure 17. Sensor modeling implemented in GT-SUITE.

Injection-related parameters are monitored using blocks such as injector-sensors, which capture metrics including start of injection (SOI), injection mass, and rail pressure. These are further processed through mathematical equations and control functions to feed back into the injection controller logic. CA50controller-1 object determines the crank angle related to the 50% of the combustion in the cylinders.

Lambda sensing is modeled using the Lambda, LambdaP, and Lambda2 blocks, which quantify air-fuel mixture quality. These outputs are utilized in fuel regulation and combustion control, interfaced with feedback loops that target oxygen injection strategies to maintain optimal lambda values.

Virtual sensors also facilitate load tracking (Loaddemand-1) and effective torque calculation (BEFF-1, BEFF-2), coherently with the speed-mode that governs this simulation model, enabling precise engine performance analysis.

Overall, the sensor network forms the backbone of the model's closed-loop control systems, enabling high-accuracy simulations, despite the higher oscillations in gas compositions and thermodynamic properties between two subsequent cycles.

3.2.5 Combustion modeling

The engine cylinder model is structured to represent each combustion chamber individually, allowing precise control and analysis of localized phenomena. In the configuration shown, each cylinder (CYL1 to CYL6) is linked to a shared set of physical and thermodynamic submodels.

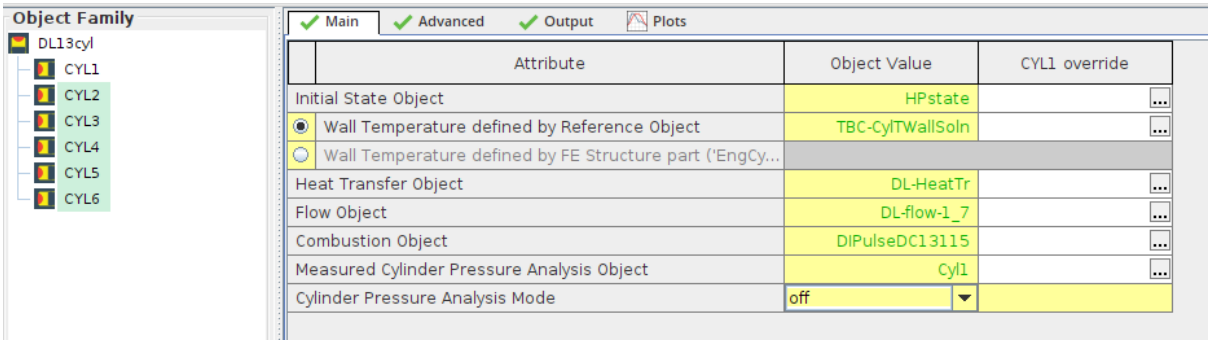

Figure 18. Combustion model in the cylinders

The initial state, defined through the object HPstate, sets the thermodynamic properties of the working fluid (Argon-oxygen mixture before the hydrogen injection) at the start of the simulation. Wall temperature distribution is mapped to represent heat transfer boundary conditions accurately.

To adapt this combustion framework to hydrogen use, several modifications were applied: for example, the air-fuel equivalence ratio and the injector pulse profiles were re-tuned to align with the combustion behavior of hydrogen, particularly under lean combustion conditions where hydrogen exhibits improved efficiency. These adaptations preserve the underlying structure of the diesel combustion model while extending its applicability to alternative fuels in high-efficiency, low-emission applications.

Such combustion model, initially tuned for Diesel applications, inevitably affects the overall accuracy of the engine model; being this thesis work part of a bigger project currently in the pre-development phase, this aspect represents one of the improvements to be made for the future. Both CFD and structural analysis are needed to optimize a general model for argon-hydrogen applications; phenomena such as combustion and components such as compressor, turbine and heat exchanger require specific tuning to reach maximum accuracy and, most importantly, to understand how to properly exploit certain physical properties.

3.3 Engine development method

3.3.1 Sequential comparison

The methodology followed in this thesis is based on a sequential and comparative evaluation of different configurations applied to the argon-hydrogen closed-loop engine. The process begins with the definition and validation of the baseline engine model shown in section 3.2.1; additional components are subsequently added to the model to analyze the impact of a turbocharger within the closed-loop configuration.

As a first step, a fixed-geomtry turbocharger is implemented to verify whether pressure boosting is beneficial compared to the initial model. These two setups are directly compared on a one-to-one basis to assess their relative impact on engine performance and thermal efficiency under the unique operating conditions of Ar-H_2 combustion.

To further refine the analysis, an additional charge-air cooler is introduced after the compressor of the turbocharger to mitigate thermal gradients, as explained in the section 3.2.3 This second phase enables an isolated comparison between the two systems with inte-rcooling, providing insights into the benefits of charge air temperature management. These sets of targeted comparisons culminate in a broader, general evaluation of all tested configurations, establishing a performance hierarchy and identifying the optimal strategy for this specific combustion concept.

The final methodological step involves turbo-matching criteria to exploit the maximum potential of the pressure boosting system. Several engine configurations will be simulated through parametric studies that involve factors such as engine speed, load, argon content, ambient temperature and initial pressure in the closed loop.

3.3.2 Convergence study

The convergence study for the engine model under analysis was governed by a multi-criteria system configured under GT-SUITE's ConvergenceRLT module, present in the Run Setup section. As shown in Figure 19, four key Real-Time Log (RLT) variables were selected to evaluate convergence based on either percentage or absolute deviation over multiple update intervals. These criteria ensure that both global and component-level parameters stabilize before the simulation is automatically terminated.

The first two criteria focus on crankshaft behavior: Criterion 1 tracks the engine brake torque (btq:CRANKSHAFT), coherently with the Speed Mode resolution method of the software, while Criterion 2 monitors the air-fuel ratio (afrat:CRANKSHAFT), which in this case refers to Oxygen-Hydrogen ratio. Both are assessed using a percentage-based tolerance of 1.0%, and the system requires their stability to persist over 5 and 3 consecutive cycles respectively. Criterion 3 targets the total mass of injected hydrogen through a specific injector (totmnozcp:INJM1) using an absolute tolerance of 0.2 g/cycle over 4 update intervals. Finally, Criterion 4 observes a boundary heat flow output (output1: DQdot_cond-1), investigating the behavior of the exhaust gases cooling system in the condenser cooler, using an absolute tolerance of 1.0 W with convergence confirmed over 2 cycles.

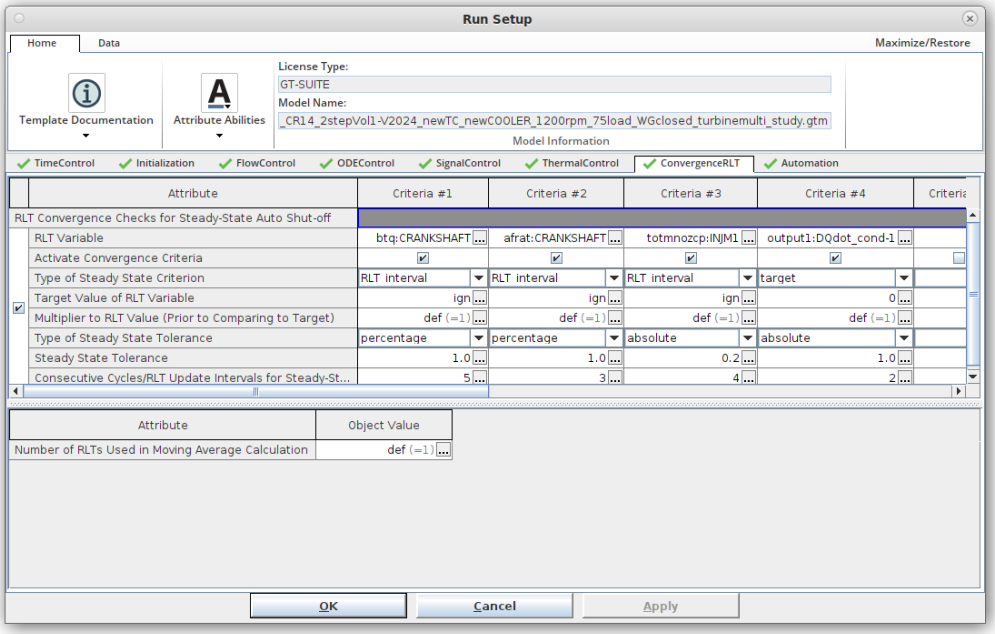

Figure 19. Convergence criteria.

Each RLT variable is evaluated at every cycle, and the convergence logic compares its variation with the specified threshold. When all active criteria have satisfied their respective tolerances for the designated number of consecutive cycles, the simulation is stopped.

3.3.3 Results evaluation and validation

Following the achievement of numerical convergence, the simulation results are subjected to a comprehensive evaluation and validation process to ensure their applicability across the full operational envelope of the engine. The GT-SUITE model is first calibrated against a range of operating conditions, including varying engine loads, rotational speeds, ambient temperatures, and altitude profiles. This parametric tuning is essential to ensure that the combustion behavior, gas exchange dynamics, and thermal interactions remain predictive outside nominal conditions.

Once the simulation model is sufficiently optimized, validation proceeds through a hierarchical testing framework. At Scania, the initial correlation phase involves engine bench testing in a controlled test cell, where measured performance metrics such as IMEP, brake torque, fuel flow, air-fuel ratio, and thermal losses are compared against their simulated counterparts. Discrepancies are analyzed and fed back into the model for refinement. Upon successful correlation at the test bench, the calibrated engine is assembled into a vehicle and subjected to on-road validation trials. These real-world tests are particularly focused on boundary conditions, including high-altitude operation, extreme ambient temperatures, and transient load scenarios. This final phase is critical to confirm that the engine can maintain performance and reliability under harsh environmental conditions, and to validate the robustness of the simulation model.

4.1 Closed-loop ICE without turbocharger

4.1.1 Convergence study

A convergence study is performed on the first model to understand how many iterations are needed to reach convergence in a closed-loop engine, according to the criterion explained in Section 3.3.2. In this first simulation the following data are used:

- Load = 75%;
- Engine speed = 1200 rpm;
- Initial pressure = 2 bar;
- Argon-Oxygen mixture = 90% Ar - 10% O_2;
- Compression ratio = 14;
- Ambient temperature is swept in the simulations.

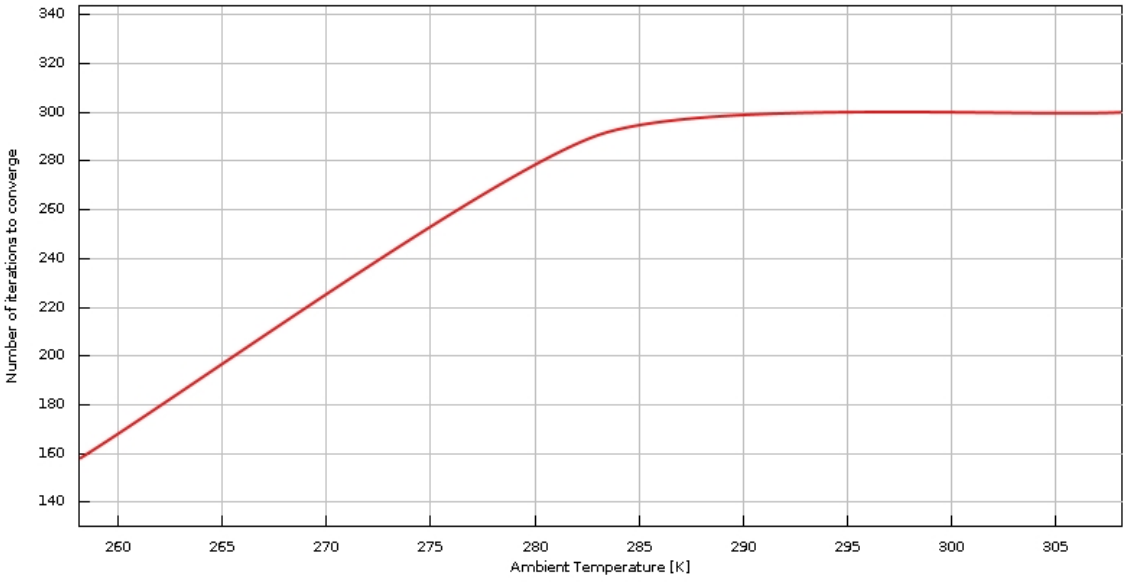

Figure 20. Convergence study on initial model sweeping on temperature

The majority of parameters are kept constant in the following simulation, but ambient temperature is fixed at 20 °C, while the DOE (Design of Experiments) is focused on a load sweep. In this thesis work, load percentage is exactly expressed in relation to torque (as a reference, 50% load is 50% of the maximum torque available). This process is needed at the beginning of a simulation process to understand the computational cost of these simulations.

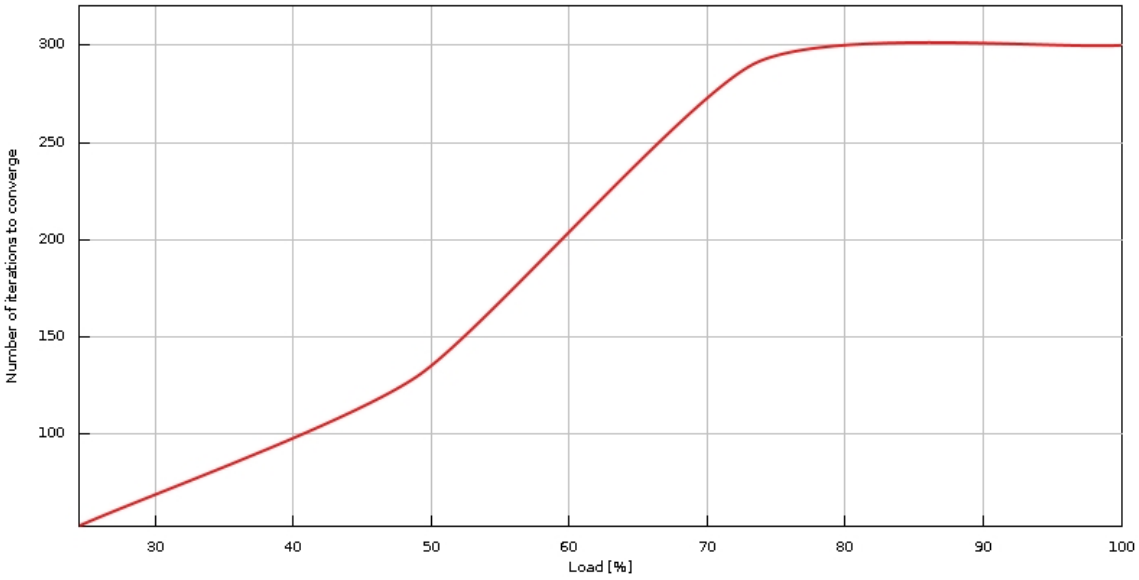

Figure 21. Convergence study on initial model sweeping on load

Convergence study results are crucial for the simulation planning over a certain number of weeks. Running 400 iterations typically takes around 90 minutes of computation time. At Scania, GT-SUITE users have access to a dedicated computing cluster with a limited number of nodes available. Therefore, simulation setups must be optimized and justified carefully to avoid excessive resource usage. Executing such simulations locally would be highly impractical due to the extended runtime and computational demands.

4.1.2 Performance of the initial model without Turbocharger

The initial model described in detail in Section 3.2.1 is simulated through a DOE to investigate its performance under stable conditions.
In particular, a first sweep on torque (and consequently load, being the engine speed constant) is studied, implementing the following conditions:

- Engine speed = 1200 rpm;
- Initial pressure = 2 bar;
- Argon-Oxygen mixture = 90% Ar - 10% O_2;
- Compression ratio = 14;
- Ambient temperature = 10 °C.

From this model onward, one can generally evaluate the impact of a device within a model through various results; particular attention is shown to parameters such as BTE (Brake Thermal Efficiency), PMEP (Pumping Mean Effective Pressure) and thermo-physical stresses in the engine components.

The following graph illustrates the variation in Indicated Efficiency across different load configurations, varying torque between 25% and 100%.

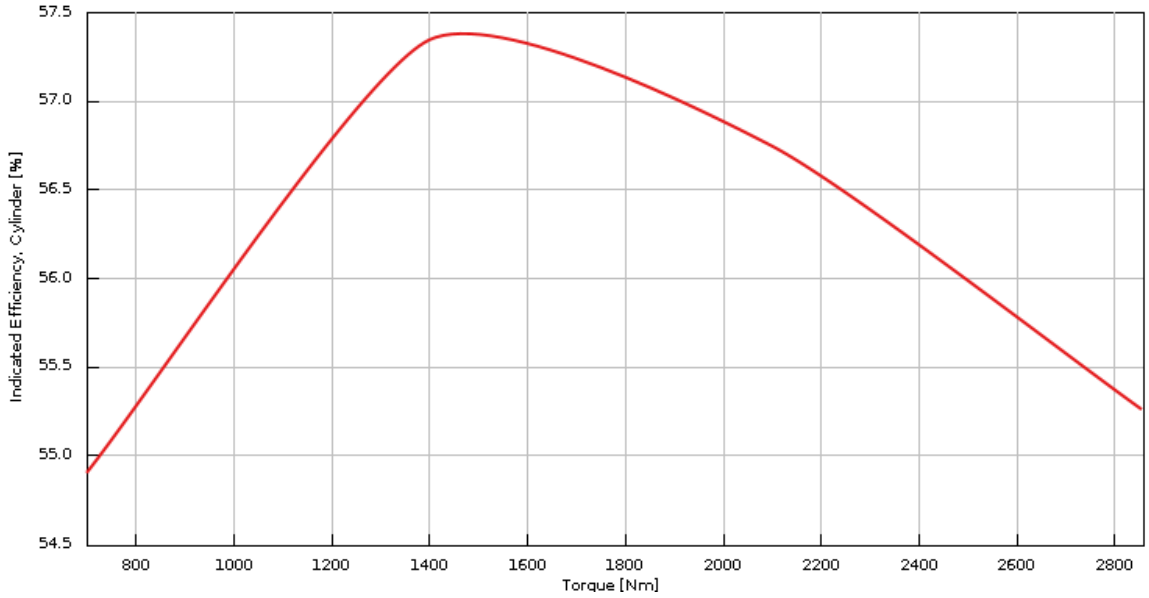

Figure 22. Torque impact on Indicated Efficiency in the initial model

Consequently, Brake Thermal Efficiency varies as follows:

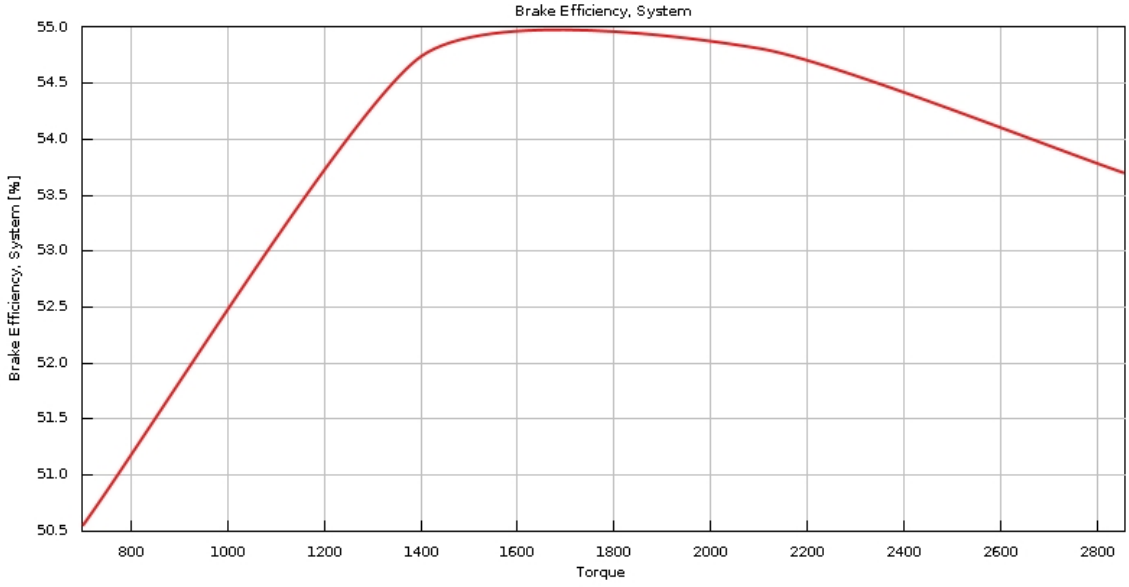

Figure 23. Torque impact on Brake Thermal Efficiency in the initial model

Pumping mean effective pressure (PMEP), defined as the average pressure gradient due to gas exchange processes during the intake and exhaust strokes of an engine, can be observed in the following plot.

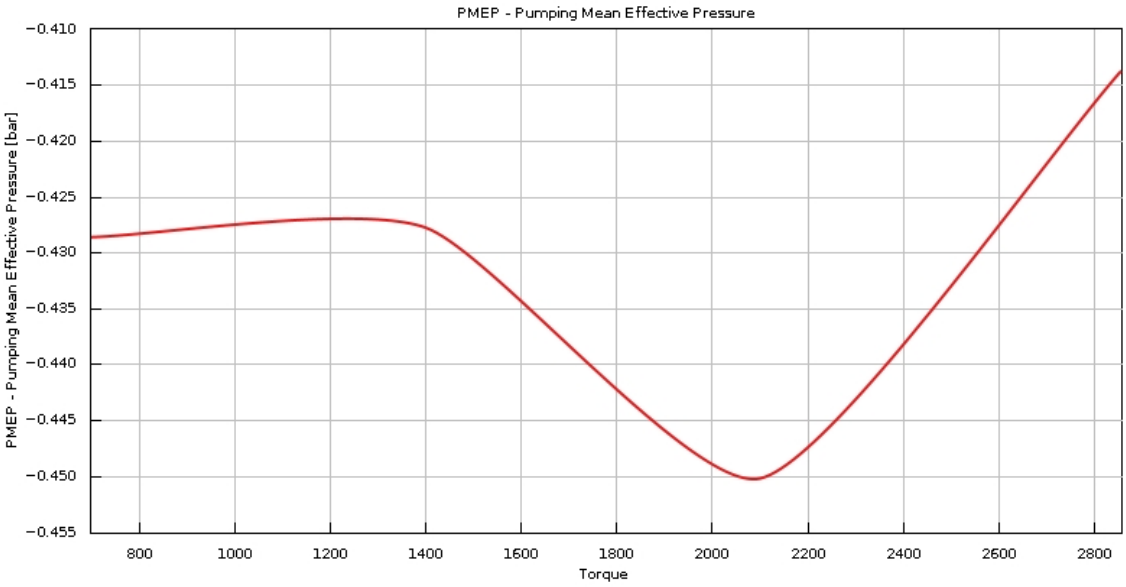

Figure 24. Torque impact on Pumping Mean Effective Pressure in the initial model

A second series of simulations is shown to investigate the relevance of ambient temperature to a closed-loop engine. Recalling that the only impact of this parameter weighs on the cooling performance of the engine, the ambient temperature is swept between -10 °C and 35 °C, keeping the other conditions constant and setting the torque at 75%.
In Figure 25, one can observe the effect of external air temperature on BTE.

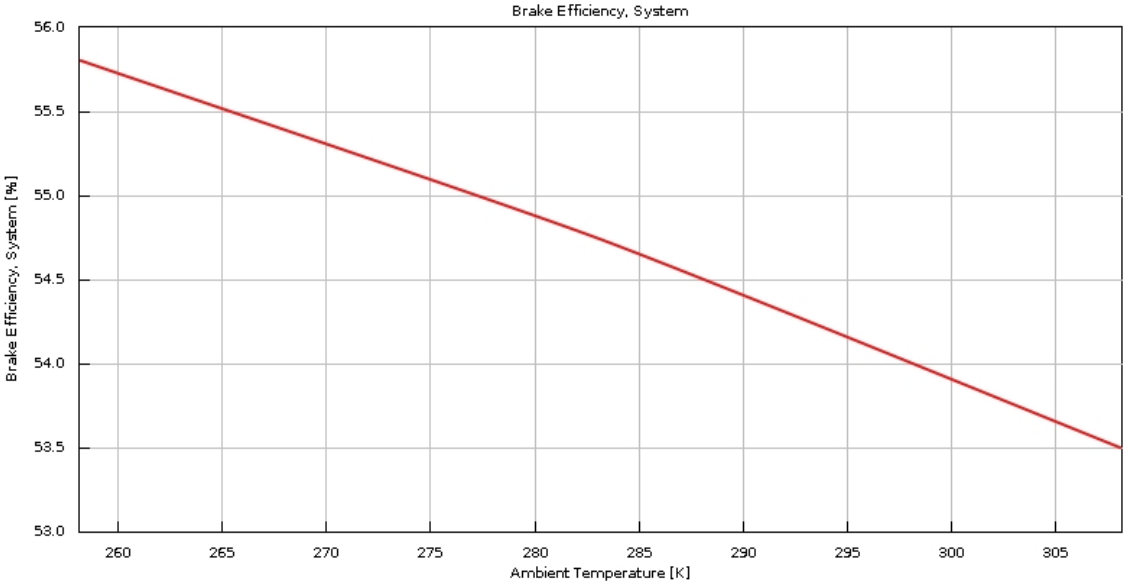

Figure 25. Ambient Temperature impact on Brake Thermal Efficiency in the initial model

Another fundamental aspect to consider when evaluating the performance of a new engine concept is Brake Specific Fuel Consumption (BSFC), defined in this case as the amount of hydrogen consumed per unit of brake power output.
In the following chart, one can visualize the impact of ambient temperature on BSFC in the described conditions.

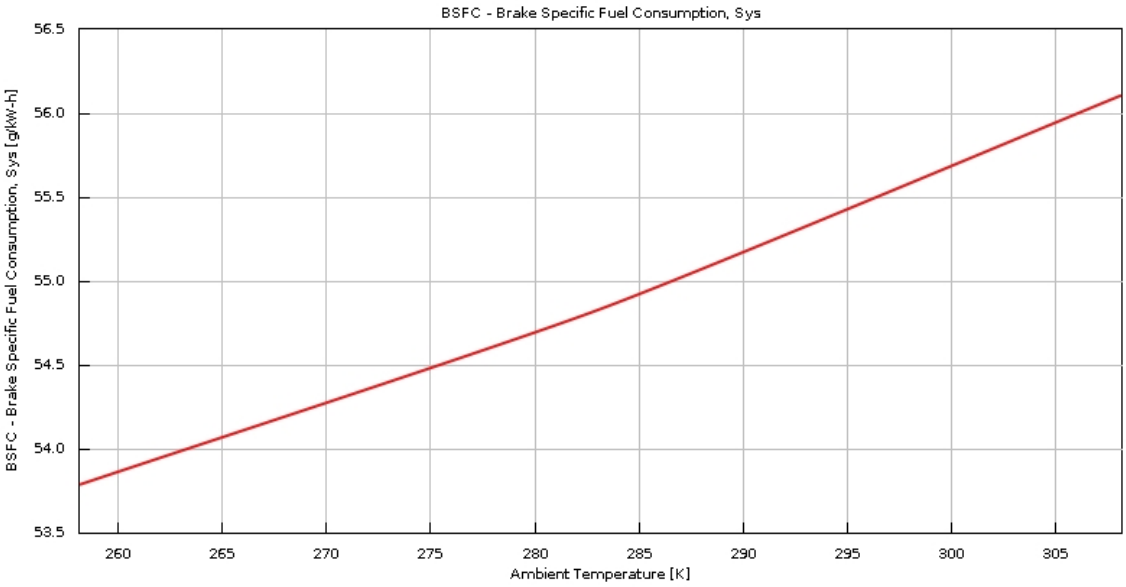

Figure 26. Ambient temperature impact on Brake Specific Fuel Consumption in the initial model

4.2 Introduction of a Turbocharger

4.2.1 Turbocharged closed-loop ICE performance

A fixed-geometry turbocharger is implemented in the engine model, as described in Section 3.2.2, to analyze the effect of a pressure-boosting system within a closed-loop machine. Several simulations were conducted to investigate diverse conditions, varying parameters such as torque, initial pressure, ambient temperature, argon content and wastegate opening. A temperature sweep parametric analysis is shown in the following pictures, operating in such conditions:

- Engine speed = 1200 rpm;
- Load = 100%;
- Initial pressure = 2 bar;
- Argon-Oxygen mixture = 87.5% Ar - 12.5% O_2;

The following figure summarizes the BTE outcomes obtained from the simulations.

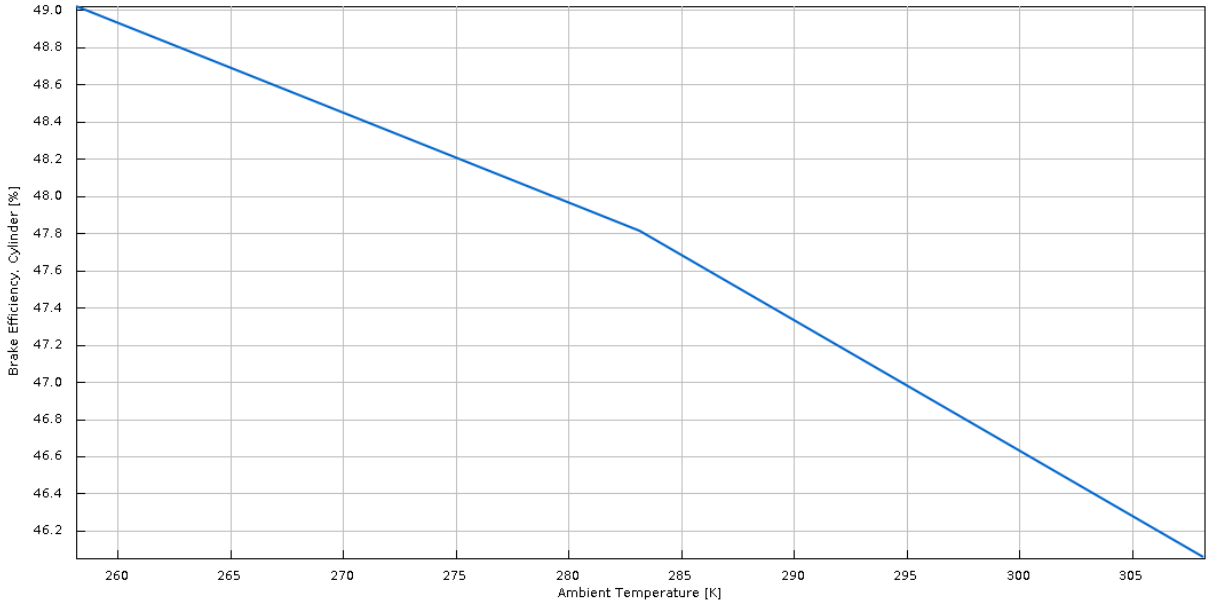

Figure 27. Ambient temperature impact on Brake Thermal Efficiency in the turbocharged model

The turbine efficiency is affected by the ambient temperature, as shown in Figure 28.

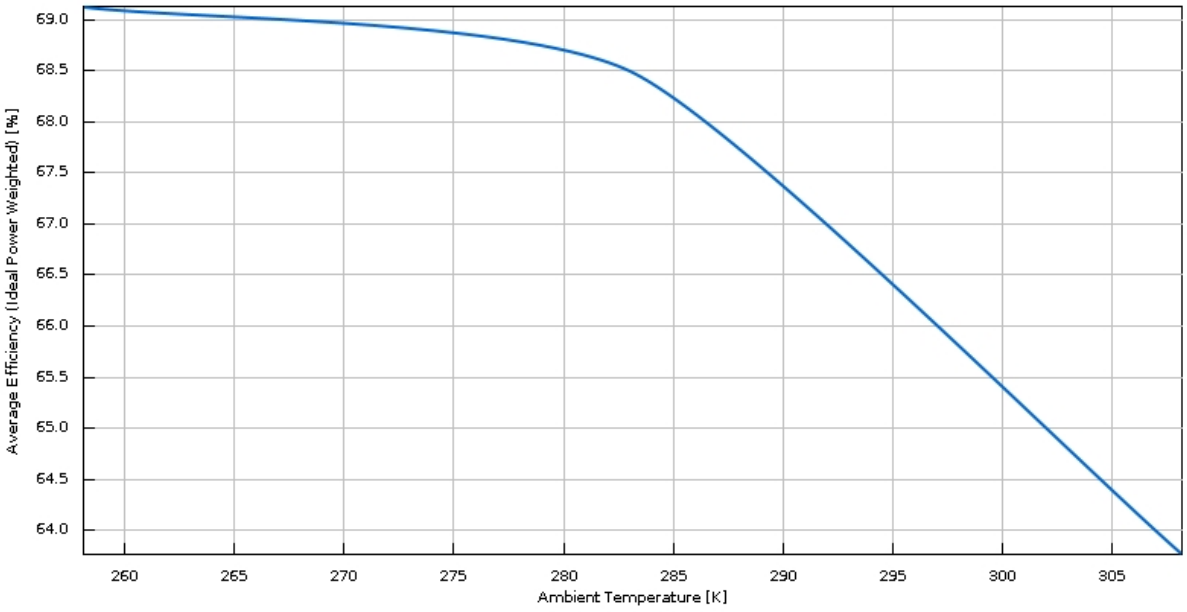

Figure 28. Ambient temperature impact on Turbine efficiency in the turbocharged model

External air temperature is also determinant for the condenser cooler performance which sets the temperature of the Ar-O_2 flow at the inlet of the compressor. Its average efficiency varies as:

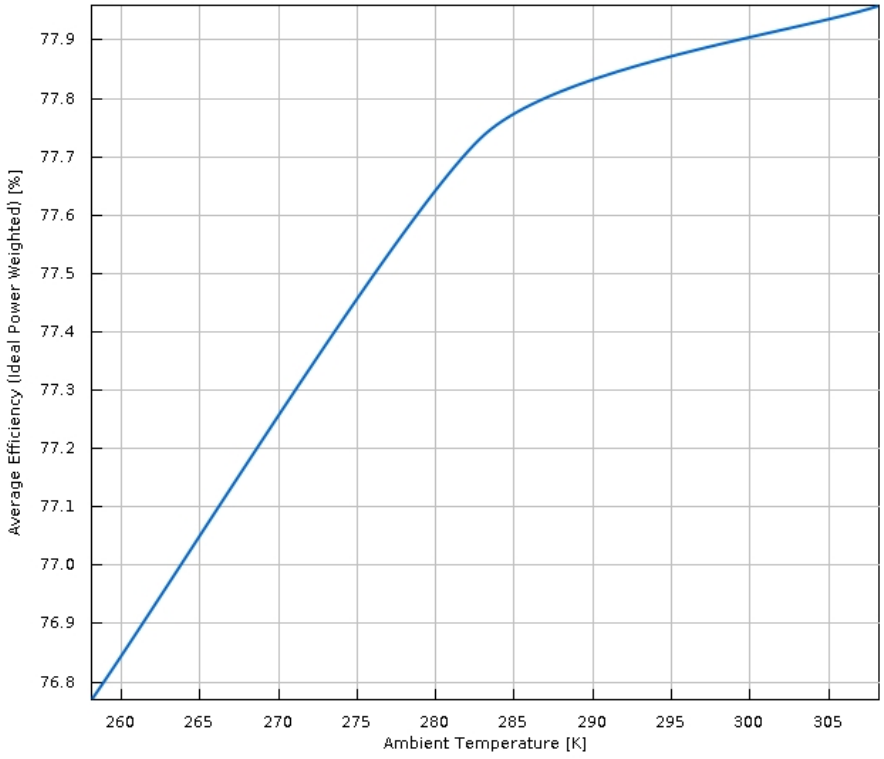

Figure 29. Ambient temperature impact on Compressor Efficiency in the turbocharged model

4.2.2 Comparison with the initial model

One can visualize a one-to-one comparison between the previous model and the boosted-model under analysis.

Similar conditions to those described in Section 4.2.1, expect from load reduced at 50%, are simulated to visualize the immediate effect of a turbocharger in the closed-loop initial model. An overview of BTE performance is provided:

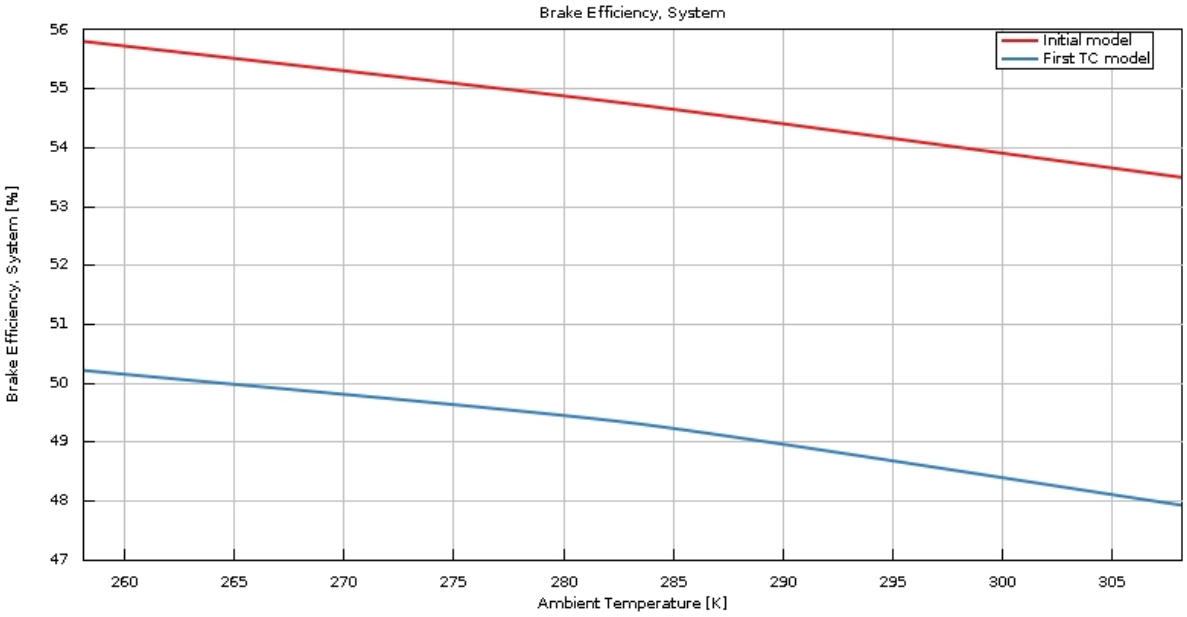

Figure 30. Ambient temperature impact on Brake Thermal Efficiency comparison

As the performance with a pressure-boosting system differs from the previously shown one, the BSFC is impacted and one can visualize it:

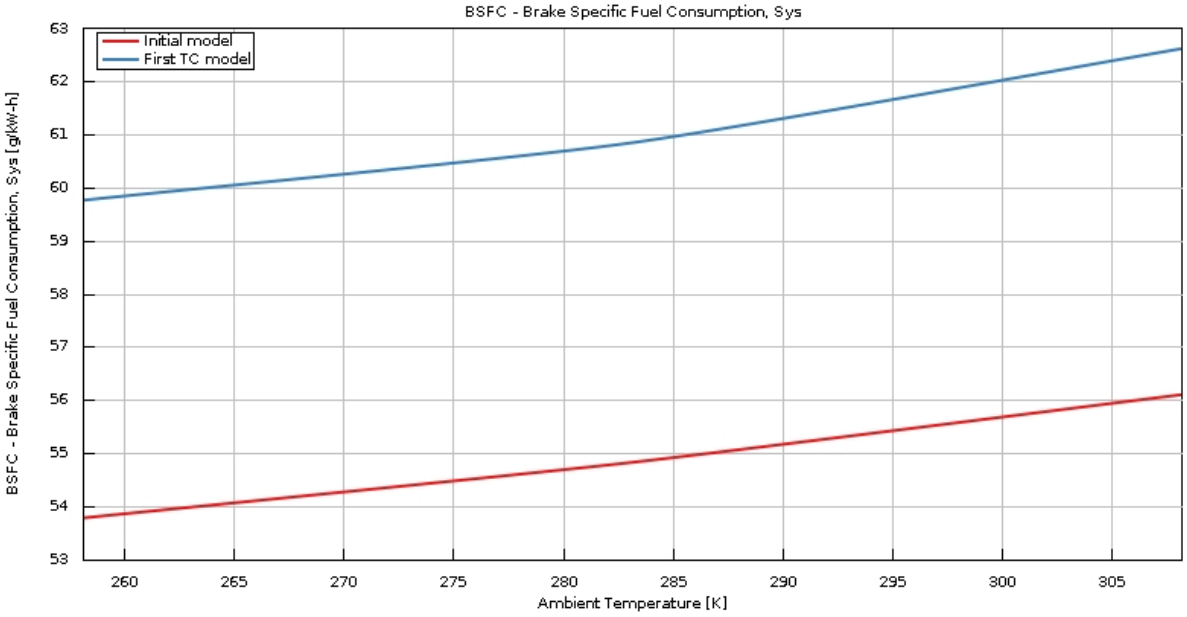

Figure 31. Ambient temperature impact on Brake Specific Fuel Consumption comparison

By analyzing the results through GT-POST, one can state that the main difference between the two models lies in the temperature at the end of the closed-loop, corresponding to the temperature after the turbocharger compressor in the latest model. One can see the temperature difference in the different models:

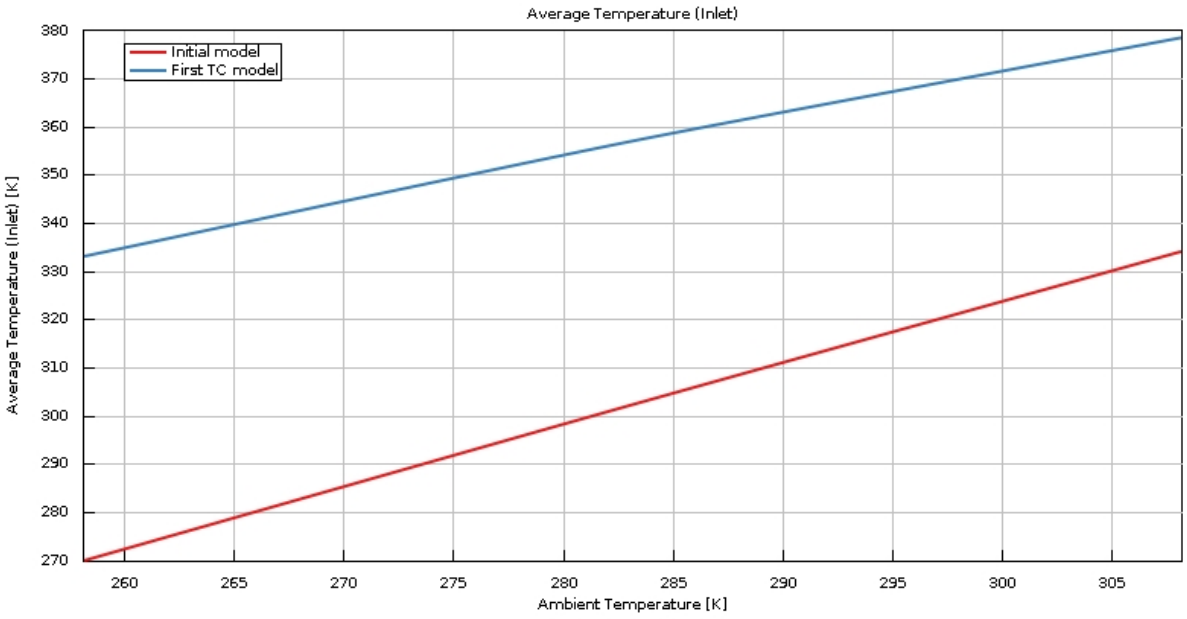

Figure 32. Ambient temperature impact on ending-cycle temperature comparison

4.3 Addition of a Charge Air Cooler

4.3.1 Implementation of a Charge Air Cooler

A Charge-Air-Cooler (CAC) device is implemented after the turbocharger compressor to re-establish optimal flow temperatures at the end of the closed-loop, as explained in detail in Section 3.2.3. The following conditions are simulated, as a first step, to visualize the direct effect of the CAC:

- Engine speed = 1200 rpm;
- Compression Ratio = 14;
- Initial pressure = 3.5 bar;
- Argon-Oxygen mixture = 85% Ar - 15% O_2;
- Ambient Temperature = 25 °C.

Load is inspected in this specific simulation, sweeping from 25 % to 100%.

Brake Thermal Efficiency varies as:

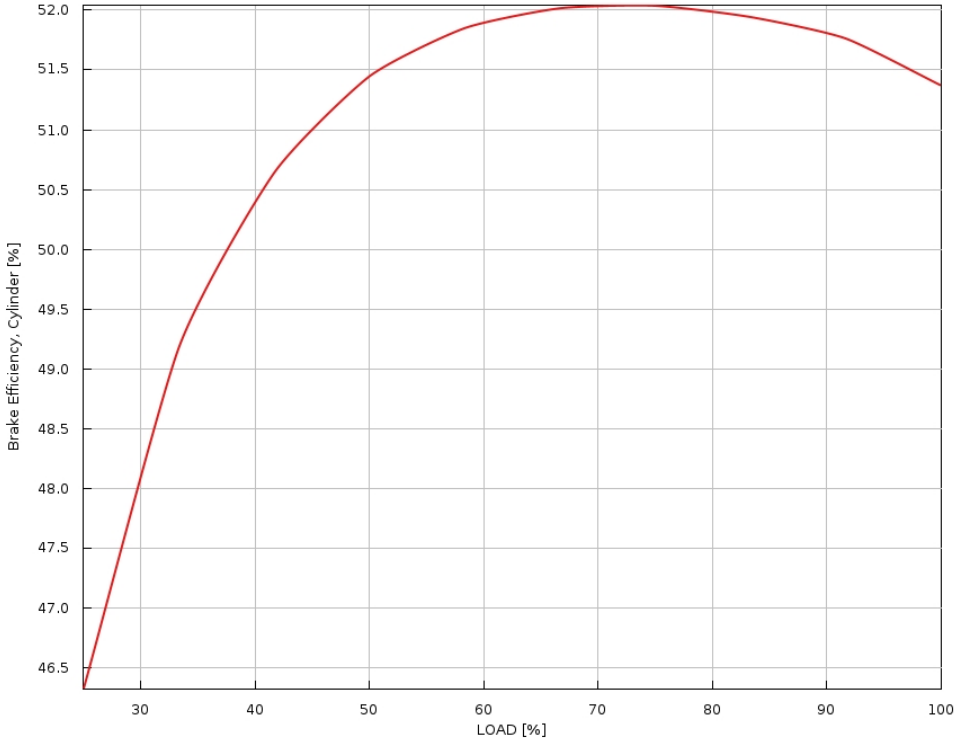

Figure 33. BTE variation over load

Once again, temperature at the end of the cycle plays a crucial role to optimize the engine, therefore one can visualize it in the next plot.

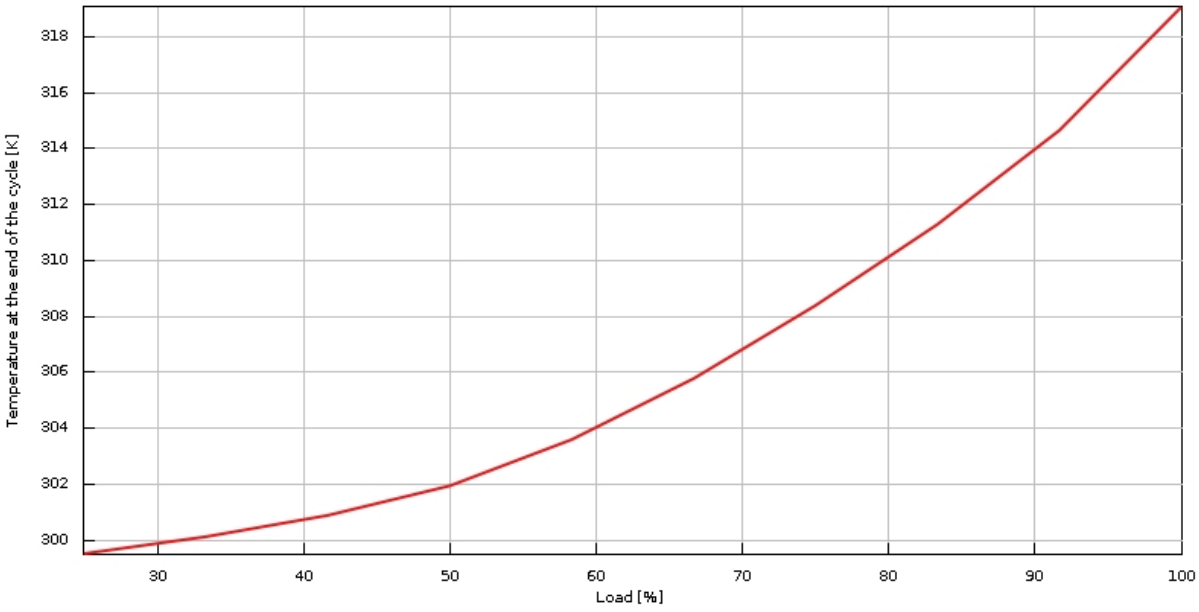

Figure 34. Average temperature at the end of the engine cycle variation over load

An overall view of the flow temperature- under 25% torque conditions- after the turbocharger, strongly impacted by the Charge-Air Cooler, is provided by GT-POST and is illustrated below:

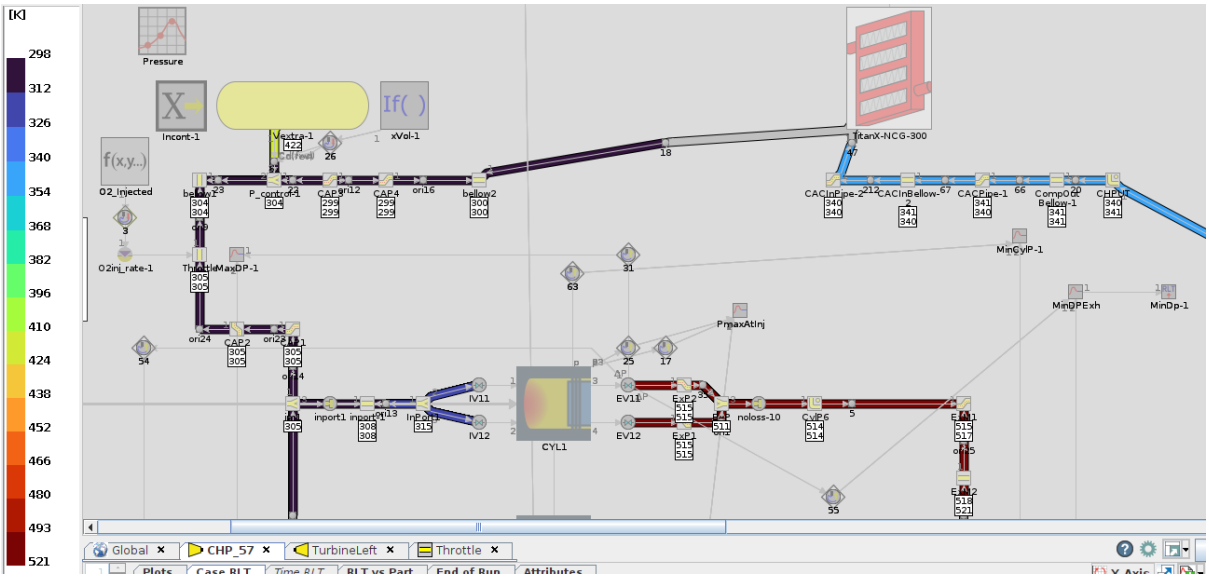

Figure 35. Temperatures inside the engine

4.3.2 Direct comparison with previous models

A direct comparison between the progressive models described in the previous sections is helpful to understand the role of the turbocharger. The initial model without boosting, the model that includes the turbocharger and the last model with anm additional Charge-Air Cooler are evaluated below, though a simulation at full load.
The comparison shows the following BTE results:

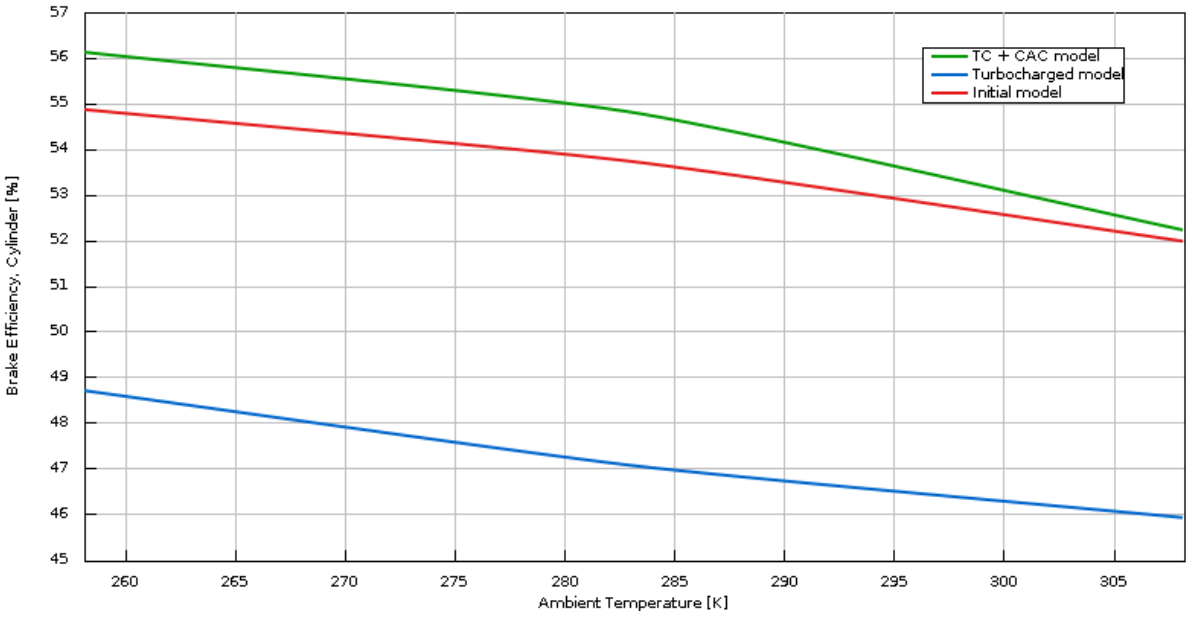

Figure 36. BTE comparison between progressive models

As the cooling capacity increases after the compressor, the engine performs better and this can be translated in fuel consumption reduction.
One can evaluate the BSFC in different configurations:

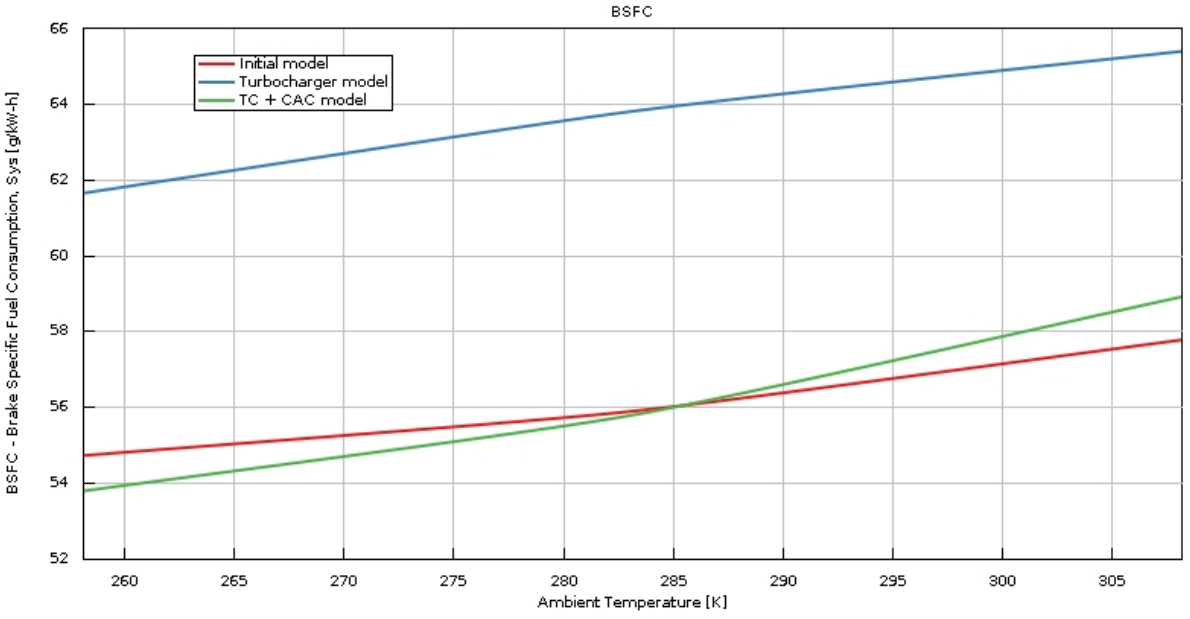

Figure 37. BSFC comparison between progressive models

4.4 Argon influence

4.4.1 Argon influence in the first turbocharged model

As explained in Section 2.3.4, Argon is a fundamental component in this hydrogen closed-loop ICE, for both chemical and environmental reasons. Argon can be varied within the engine flow in relation to oxygen content, defining the Argon-Oxygen ratio. The following model simulates how Argon content directly influences engine performance. The engine model described in Section 3.2.3, is simulated according to the following conditions:

- Engine speed = 1200 rpm;
- Lambda = 3;
- Load = 50%;
- Initial pressure = 3.5 bar;
- Ambient Temperature = 25 °C.

Brake Thermal Efficiency varies as shown in the chart below.

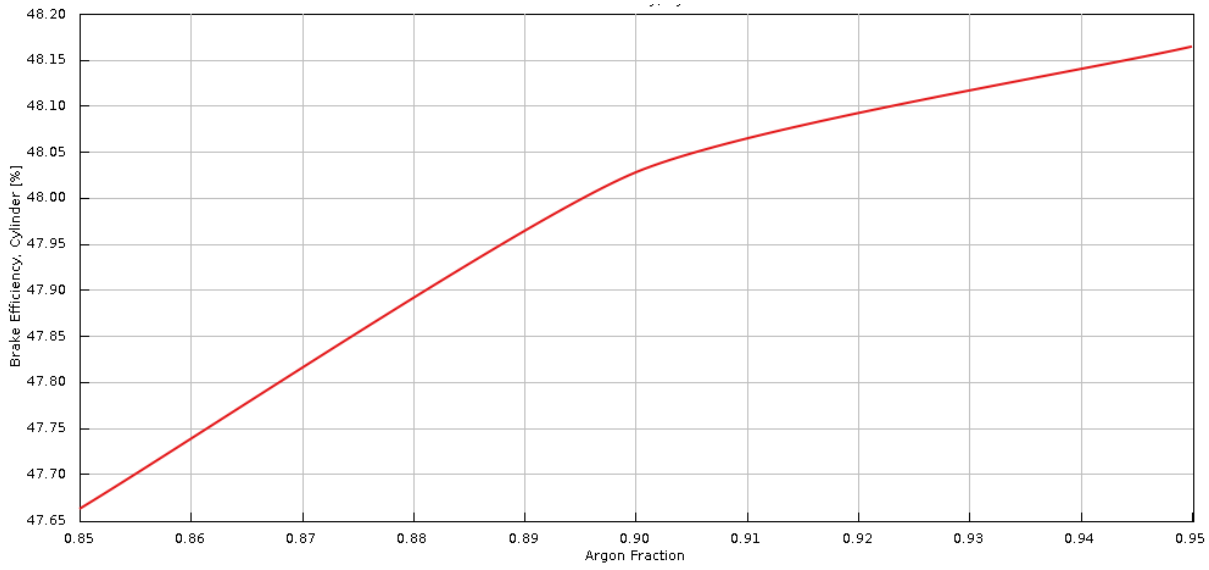

Figure 38. Argon impact on Brake Thermal Efficiency

Keeping other conditions constant, Argon strongly impacts on charge-air-cooler performance; it is possible to analyze the Argon-Oxygen flow temperature at the end of the cycle (consequently at the beginning of the following engine cycle).

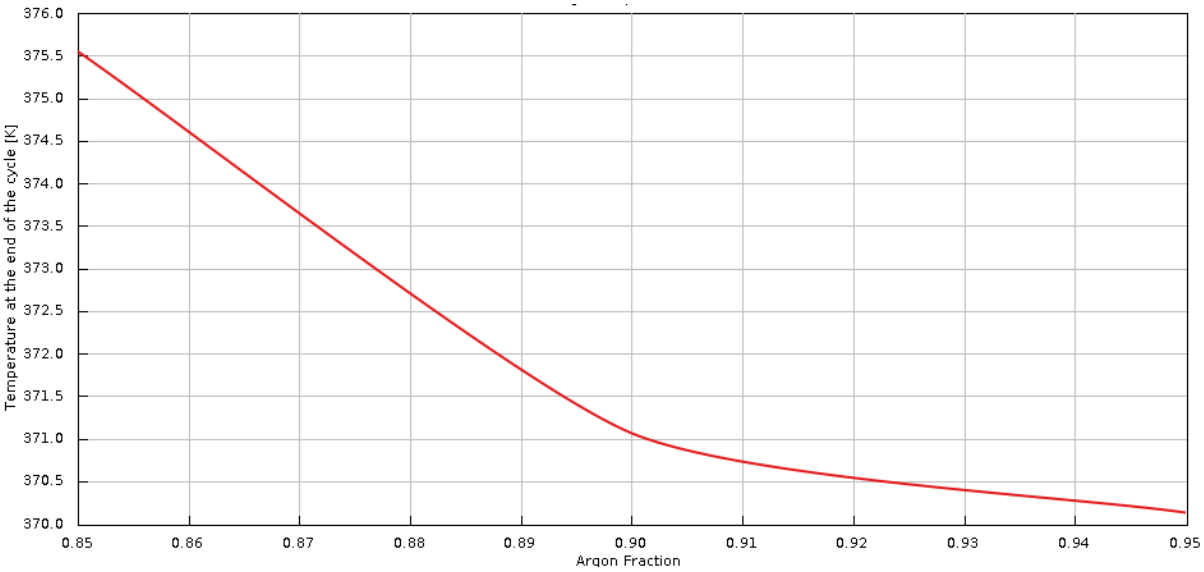

Figure 39. Argon impact on flow temperature at the end of the cycle

The working flow pressure plays a crucial role both in the combustion dynamics and in the turbocharger functioning. It is therefore interesting to verify the coupling effect of initial pressure and argon content variations in the engine model.
Brake Thermal Efficiency is once again plotted to evaluate the closed-loop performance in different cases.

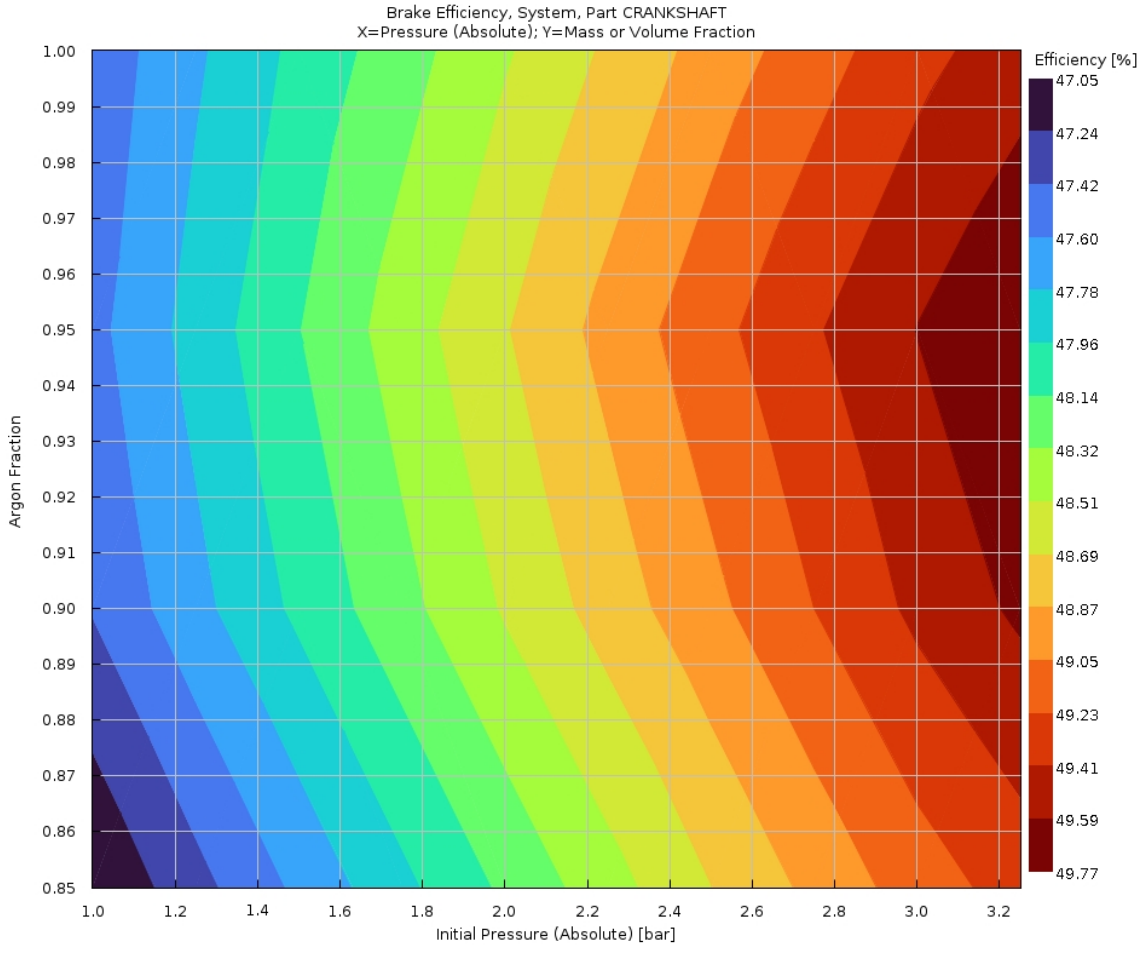

Figure 40. BTE depending on argon content and initial pressure

4.4.2 Argon influence in CAC-Turbocharger model

The same engine model in GT-SUITE is simulated in different load and initial pressure conditions, highlighted below:

- Engine speed = 1200 rpm;
- Compression Ratio = 14;
- Load = 75%;
- Initial pressure = 6 bar;
- Ambient Temperature = 25 °C.

The turbocharger works differently, due to the difference in flow compositions and physical properties, as initial pressure also determines the argon-oxygen density in both the turbine and compressor.
One can visualize the average efficiency of the turbine in figure 41.

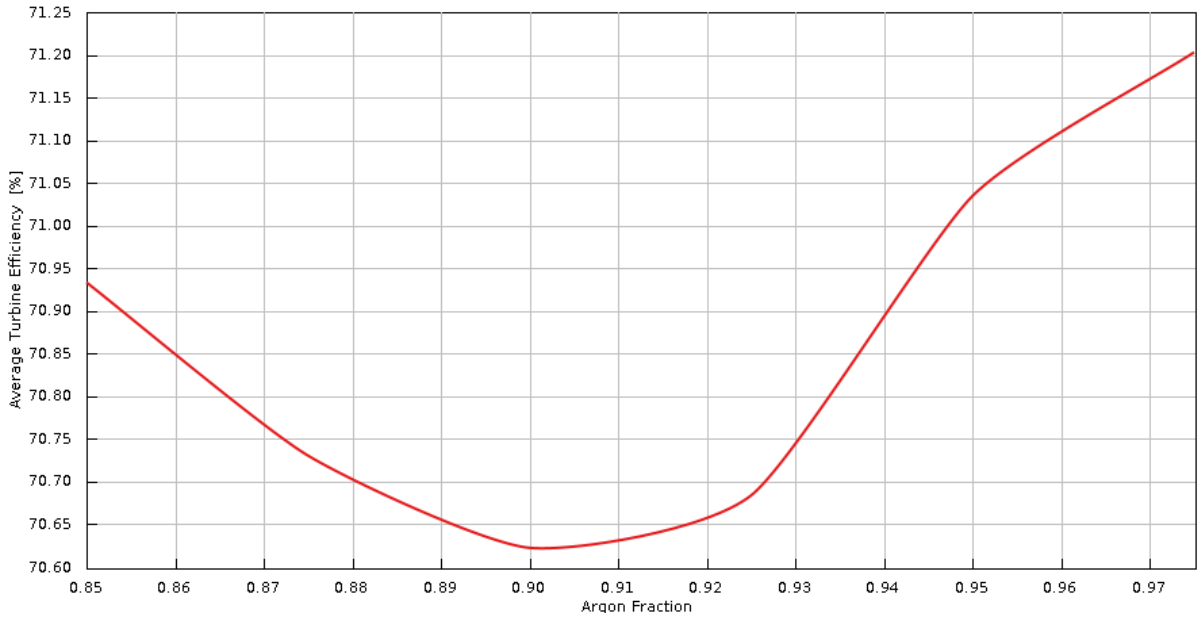

Figure 41. Argon content impact on turbine efficiency

Consequently, Brake Thermal Efficiency varies as:

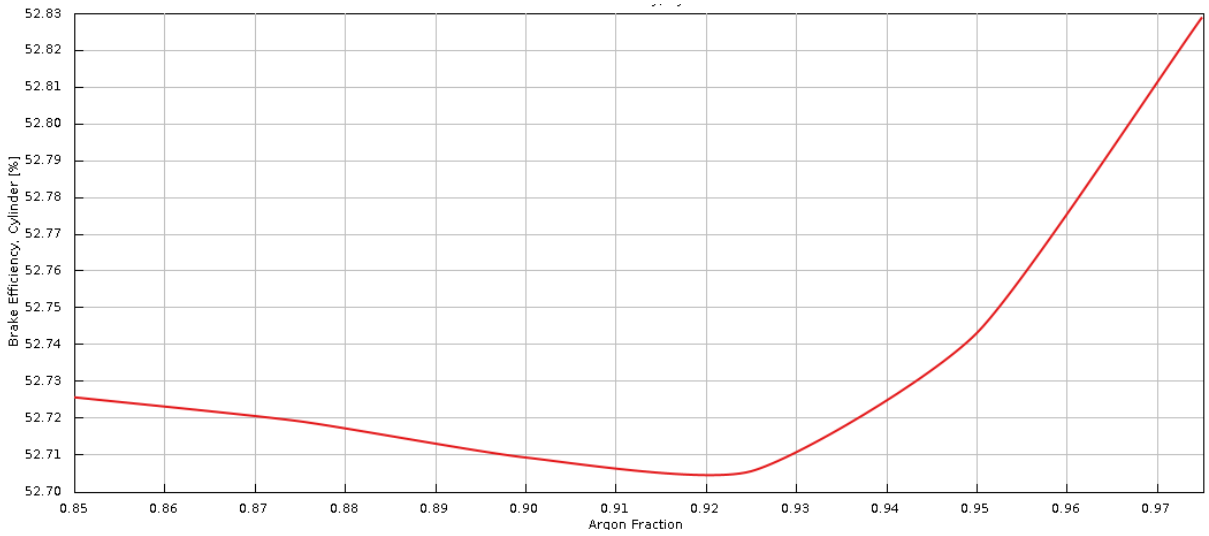

Figure 42. Argon content impact on BTE

A second study on the same engine model has been implemented to verify how the argon content variation couples a possible sweep on lambda (λ), defined as the air-fuel equivalence ratio. Indicated efficiency can be visualized in the next image.

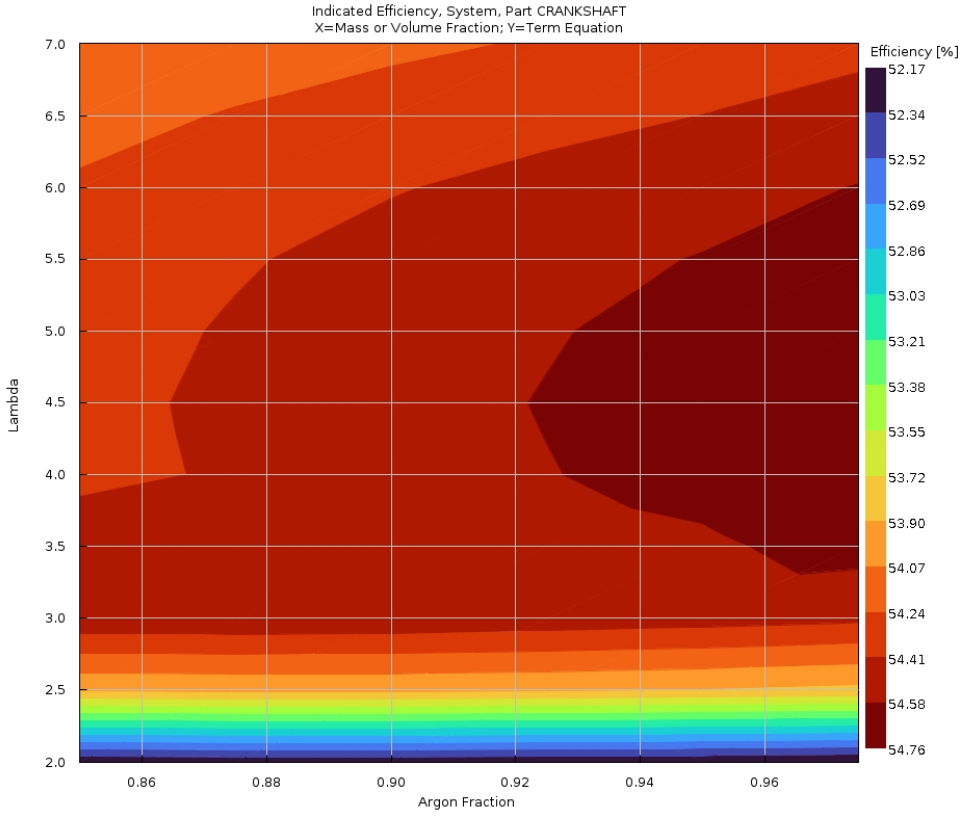

Figure 43. Indicated efficiency depending on lambda and Argon content

4.5 Initial pressure influence

4.5.1 Initial pressure impact in a closed-loop turbocharged ICE

Initial pressure, computationally defined as the initial value of pressure imposed inside the engine piping system in GT-SUITE, plays a determinant role in closed-loop engines, in which exhaust gases recirculate towards the intake without being released in the atmosphere. The engine model described in Section 3.2.3 is simulated imposing:

- Engine speed = 1500 rpm;
- Compression Ratio = 14;
- Argon-Oxygen mixture = 85% Ar - 15% O_2;
- Ambient Temperature = 25 °C;
- Load = 50%.

One can visualize the direct effect of initial pressure on Brake Thermal Efficiency in the following figure.

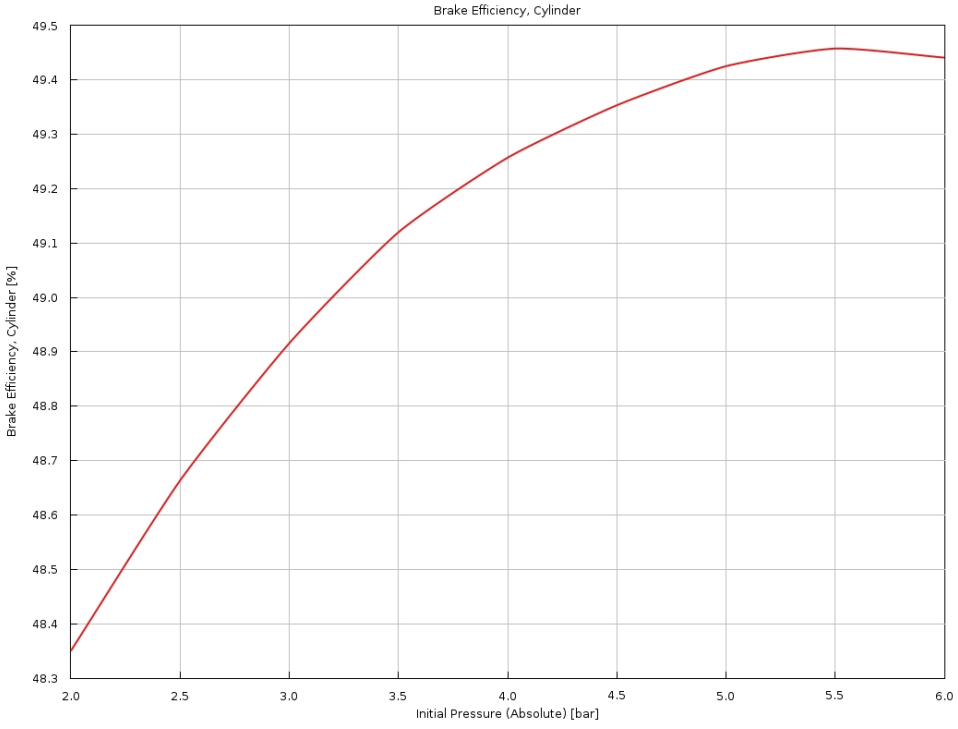

Figure 44. Initial pressure impact on BTE

Another important aspect to investigate is the turboshaft speed, limited by an upper threshold of 104500 rpm, and can be related to initial pressure as follows.

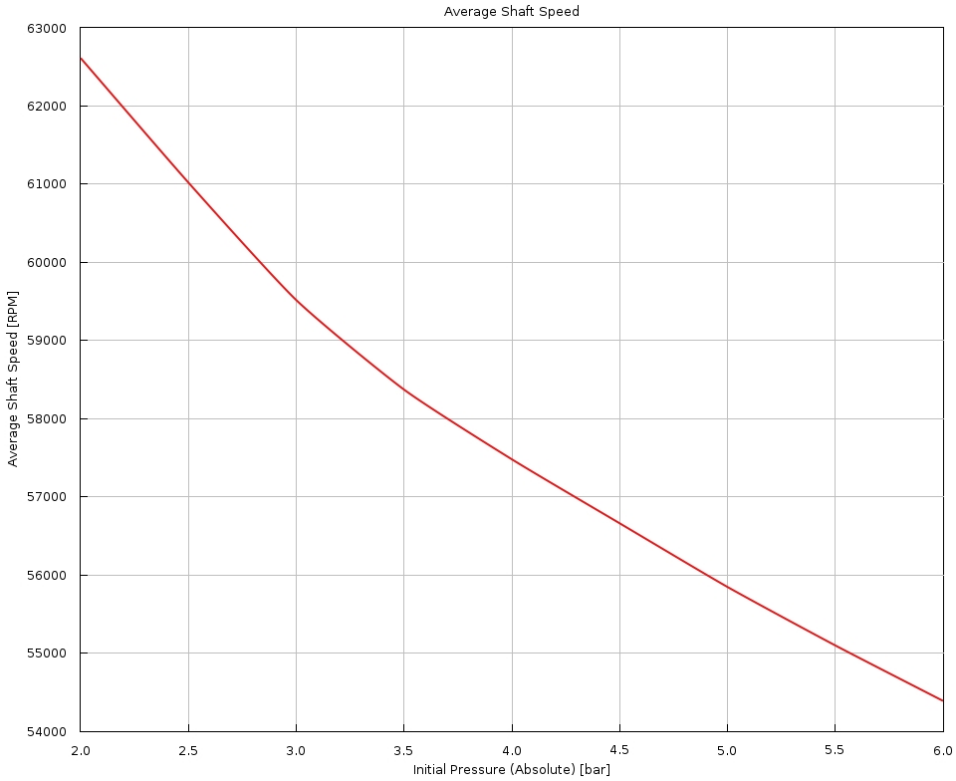

Figure 45. Initial pressure impact on turboshaft speed

On the same engine model, a double sweep has been implemented by varying load, and consequently torque, from 25% to 100%, keeping the other initial conditions constant.
The following plot investigates the combined effect of load and initial pressure on the average turbine efficiency:

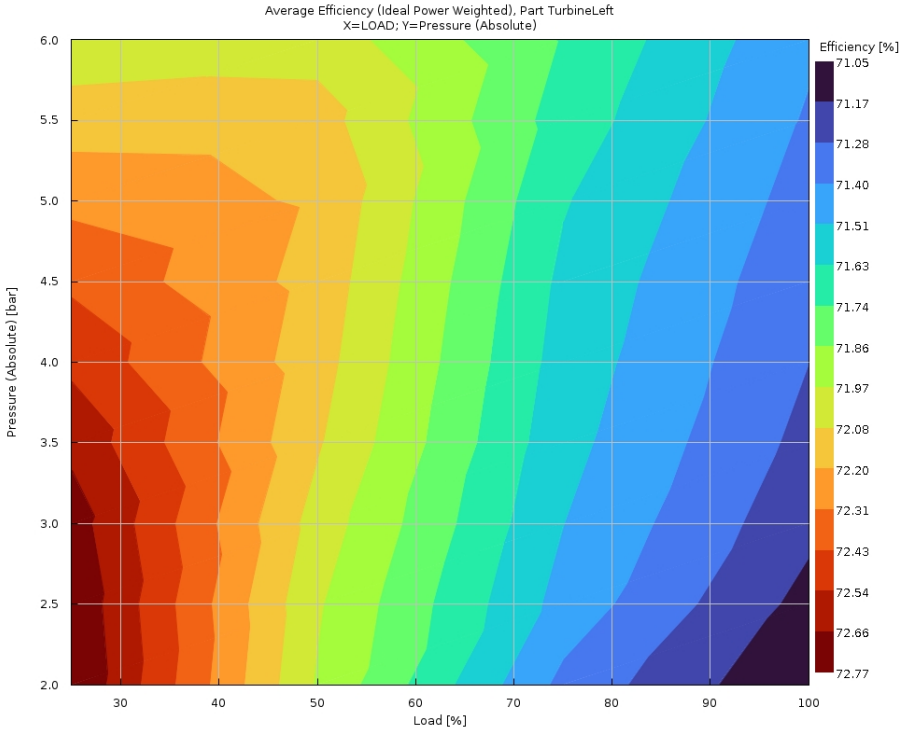

Figure 46. Load-pressure influence on turbine efficiency

Brake Specific Fuel Consumptions is strongly dependent on both torque and fluid pressure in the engine, as shown in the next plot.

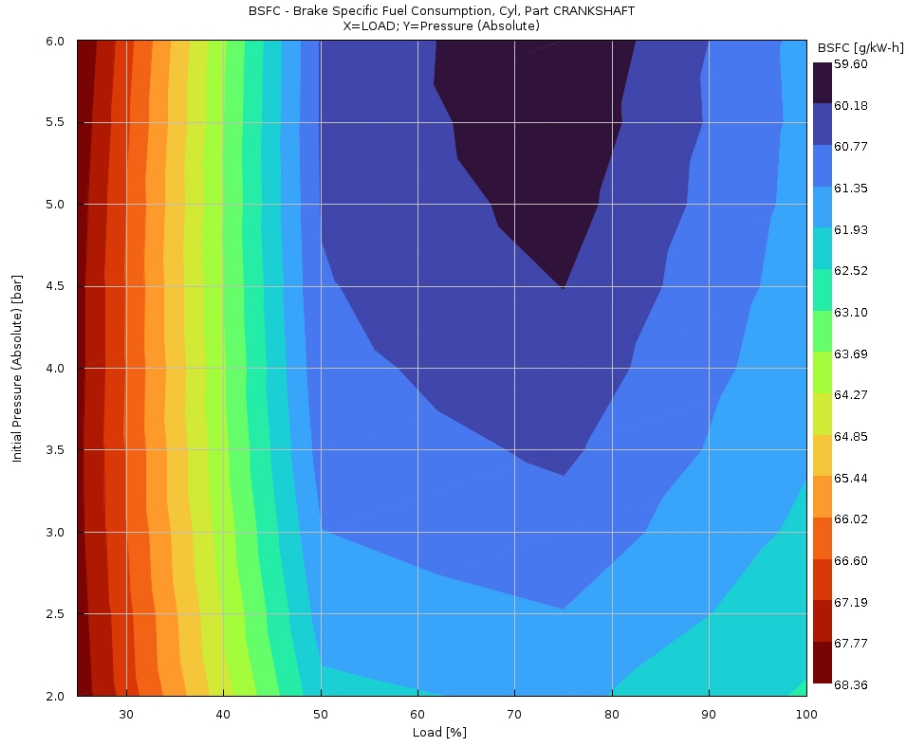

Figure 47. Load-pressure influence on BSFC

4.5.2 Initial pressure influence combined with external temperature

A similar engine model is simulated to further assess the initial pressure impact, coupled with an ambient temperature sweep. In this way the cooling capacity of the condenser cooler and charge-air cooler is varied, therefore the flow pressure inside the engine is even more determinant. The following conditions are imposed to the turbocharged model:

- Engine speed = 1200 rpm;
- Compression Ratio = 14;
- Argon-Oxygen mixture = 95% Ar - 5% O_2;
- Load = 75%.

Three different configurations are studied, varying initial pressure from 2 bar to 6 bar.

Initial pressure differs from the stationary value of flow pressure in the piping system, since the latter derives from the combination of several turbo-machines present in the engine. As a reference, the value of the flow pressure before the opening of the intake valves, identified as PL30, is shown in figure 48.

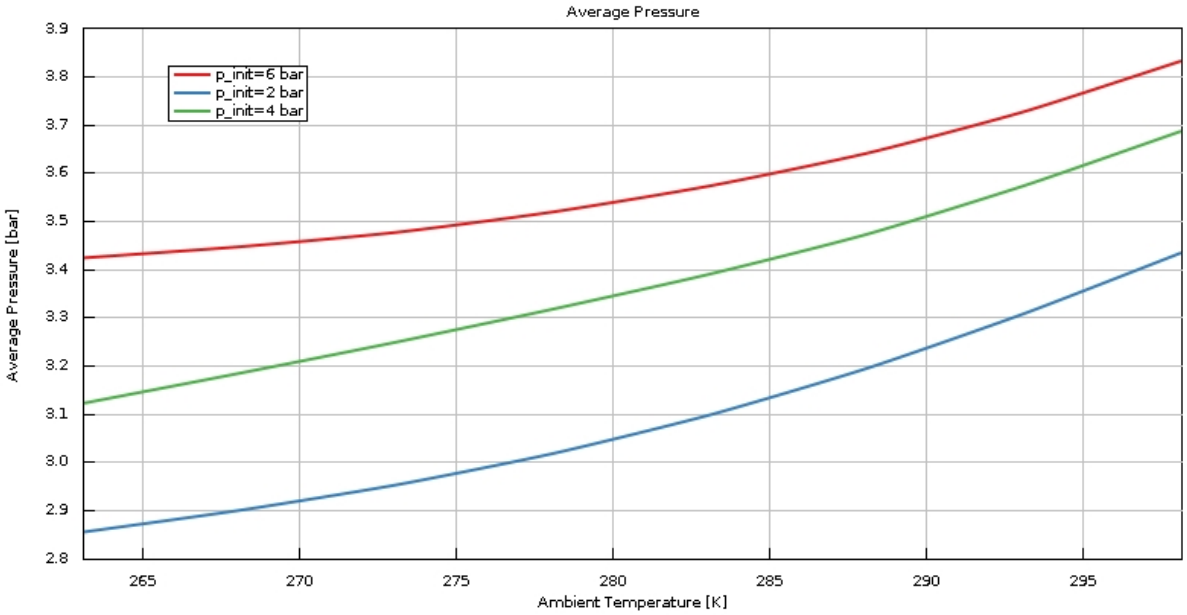

Figure 48. Intake valve opening pressure depending on initial pressure and ambient temperature

The comparison of Brake Thermal Efficiency between cases is visualized in the following chart.

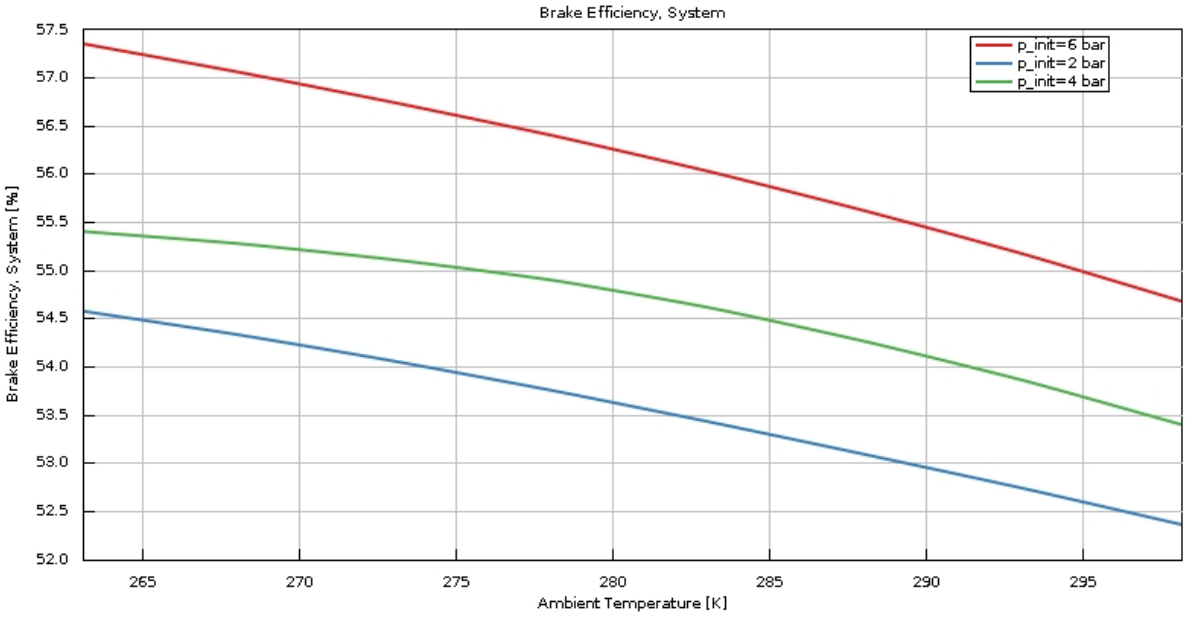

Figure 49. BTE depending on initial pressure and ambient temperature

4.6 Turbo-matching

4.6.1 Initial turbocharger performance

The engine models described in the previous results lack turbo-matching optimization that might tune the turbocharger to best match the specific operating characteristics and performance targets of the engine. The model described in Section 4.4.2 is again analyzed, fixing these additional following parameters:

- Argon content = 95%;
- Lambda = 3.5;
- Ambient temperature = 25 °C.

The compressor performance can be evaluated through different charts. The efficiency map is shown below:

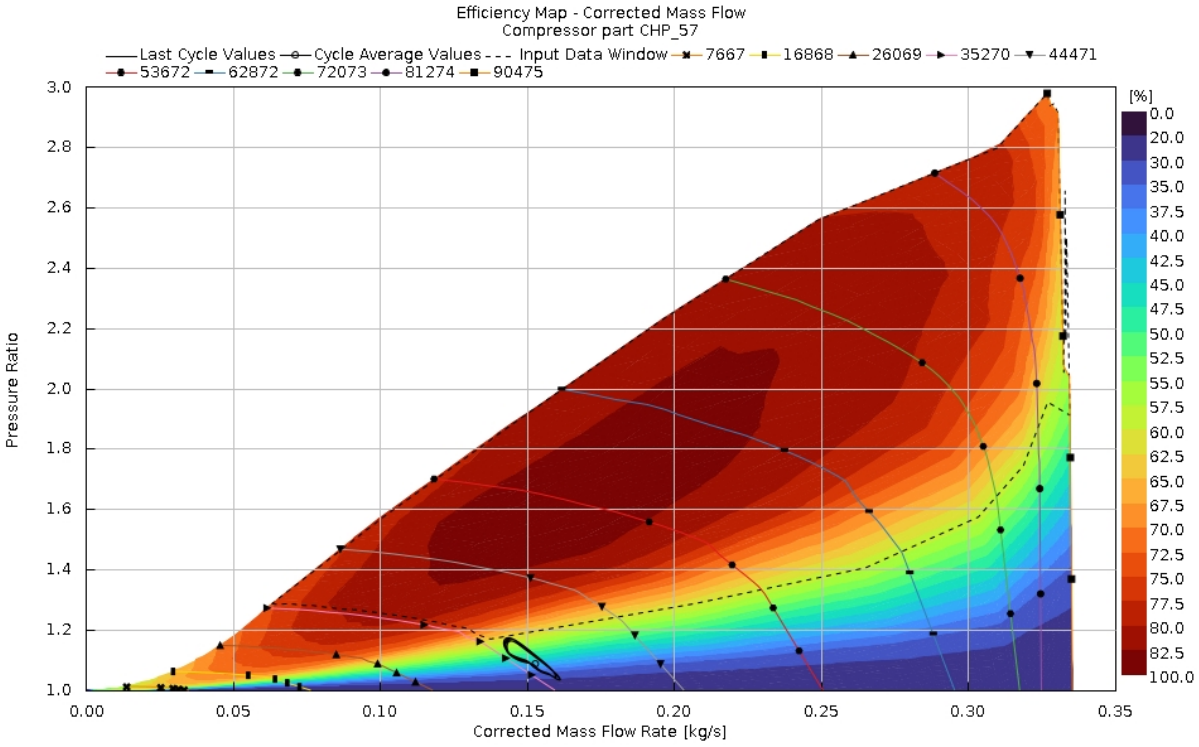

Figure 50. Compressor efficiency map without turbo-matching

4.6.2 Compressor matching

The turbocharger compressor can be tuned to reach higher performance through two main parameters, namely the pressure ratio multiplier and the mass multiplier. The direct consequences of increasing/decreasing those parameters are explained in Section 5.

The engine model implemented in GT-SUITE shown in the last section is kept constant, varying the compressor multipliers.
One can directly evaluate the impact of the pressure ratio multiplier and the mass multiplier on Brake Thermal Efficiency in the following plot.

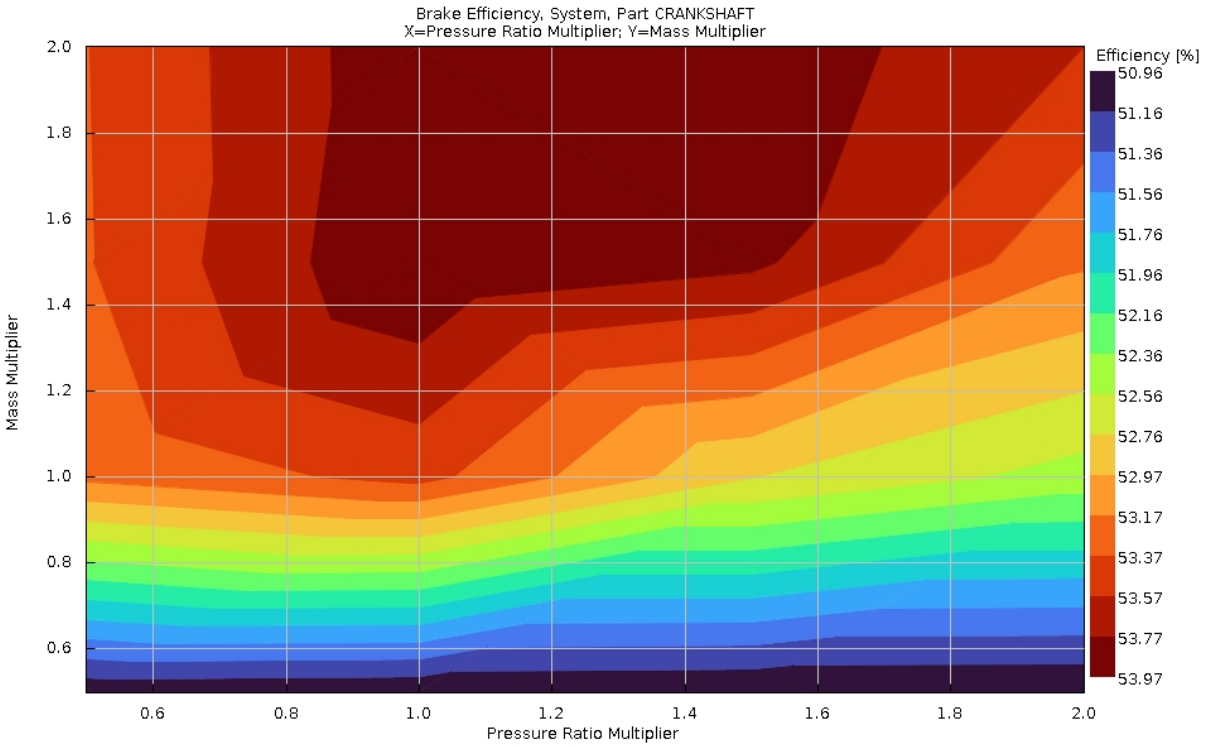

Figure 51. BTE related to CPRM and CMM

Brake Specific Fuel Consumption also depends on the compressor performance, therefore it is meaningful to plot it against the two described parameters:

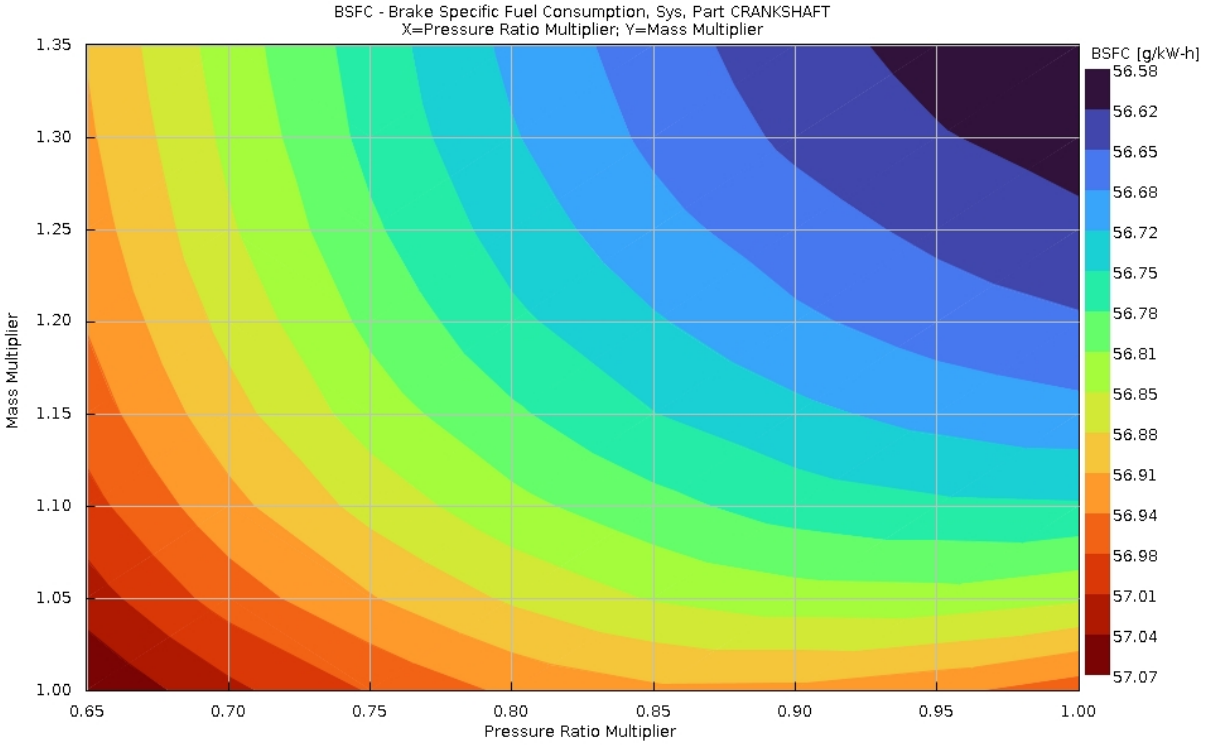

Figure 52. BSFC related to CPRM and CMM

Finally, PMEP can be expressed in relation to the pressure ratio multiplier and the mass multiplier according to:

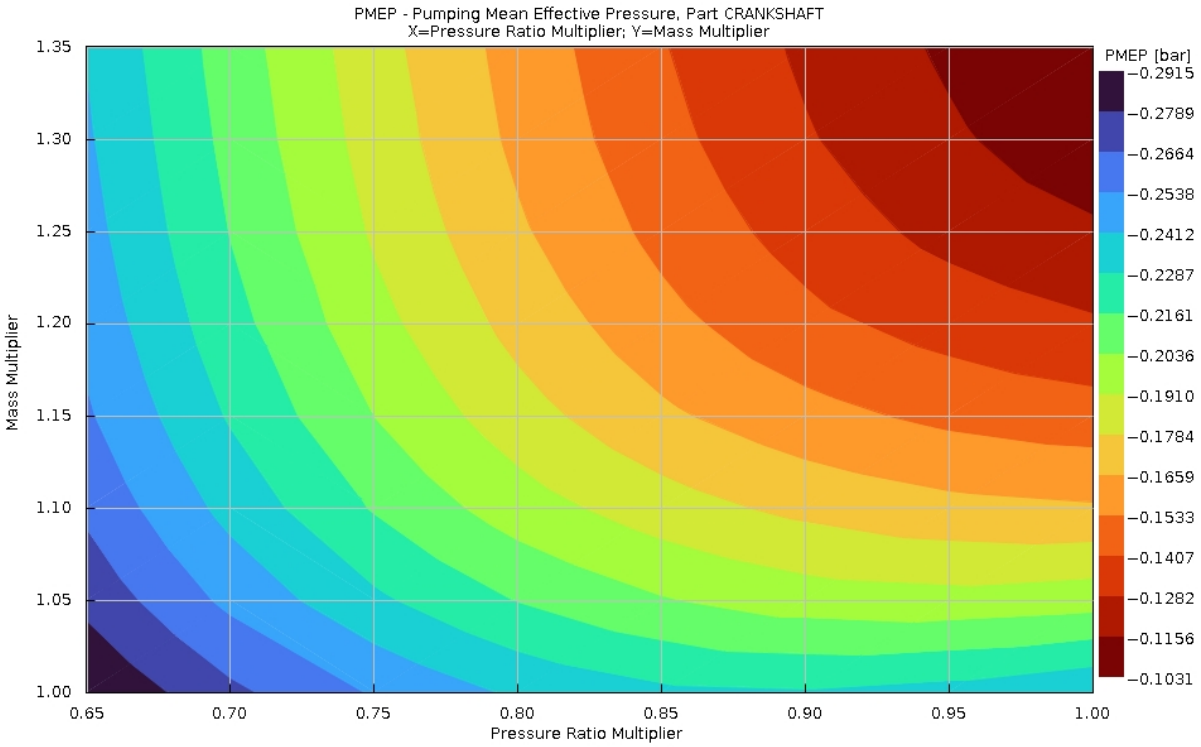

Figure 53. PMEP related to CPRM and CMM

4.6.3 Turbine matching

The same reasoning can be applied to the turbocharger turbine, affected by its efficiency multiplier and mass multiplier. The same model, with fixed compressor multipliers, is simulated to match turbine performance. At first, turbine efficiency is evaluated as follows:

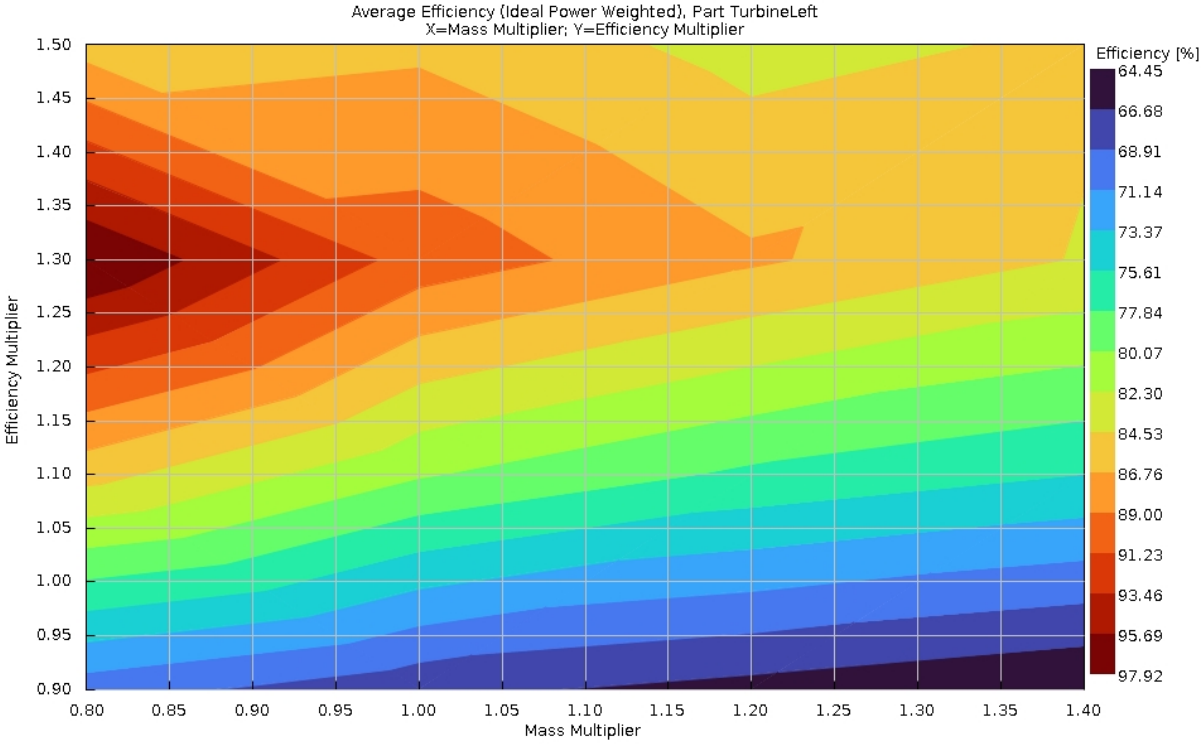

Figure 54. Turbine efficiency related to TEM and TMM

As a second step, BTE is shwon in the following picture.

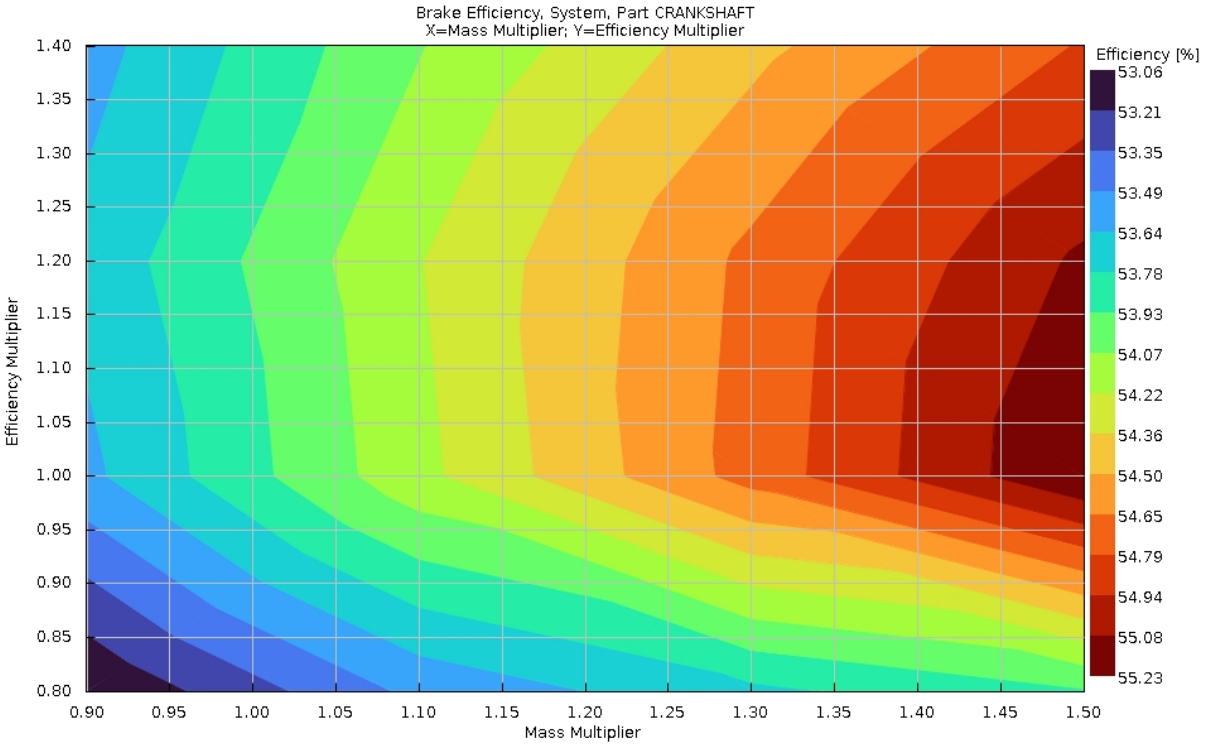

Figure 55. BTE related to TEM and TMM

4.6.4 Turbo-matching influence on engine performance

Compressor and turbine multipliers are finally applied to reach maximum performance; in particular one last engine model is implemented in GT-SUITE, fixing:

- Compressor pressure ratio multiplier = 1;
- Compressor mass multiplier = 1.4;
- Turbine efficiency multiplier = 1.3;
- Turbine mass multiplier = 1.2.

Consequently, the efficiency map for the compressor is shown in the figure 56 (keeping constant conditions compared to figure50).

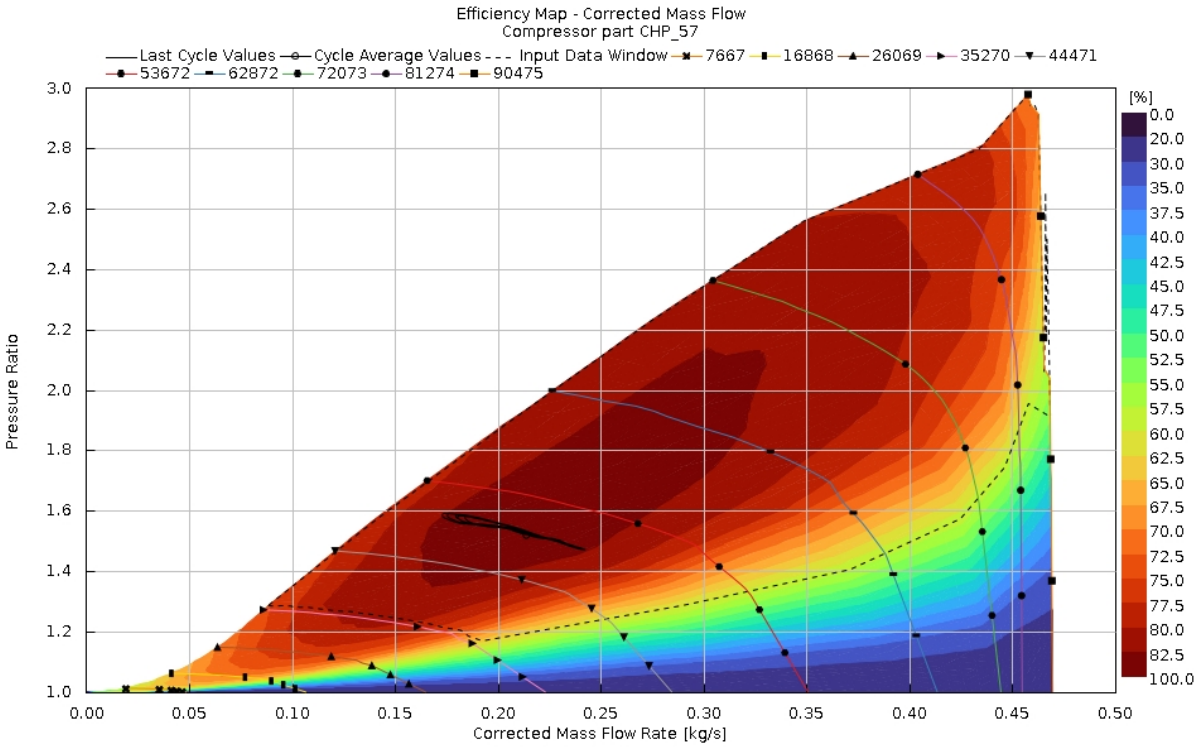

Figure 56. Compressor efficiency map with turbo-matching

Finally, one last model is simulated, with the following initial conditions imposed in GT-SUITE:

- Engine speed = 1200 rpm;
- Load = 75%;
- Initial pressure = 6 bar;
- Argon content = 95%;
- Lambda = 3.5;
- Temperature sweeping from -10 °C to 25 °C.

Turbine efficiency is plotted in the next chart, depending on ambient temperature.

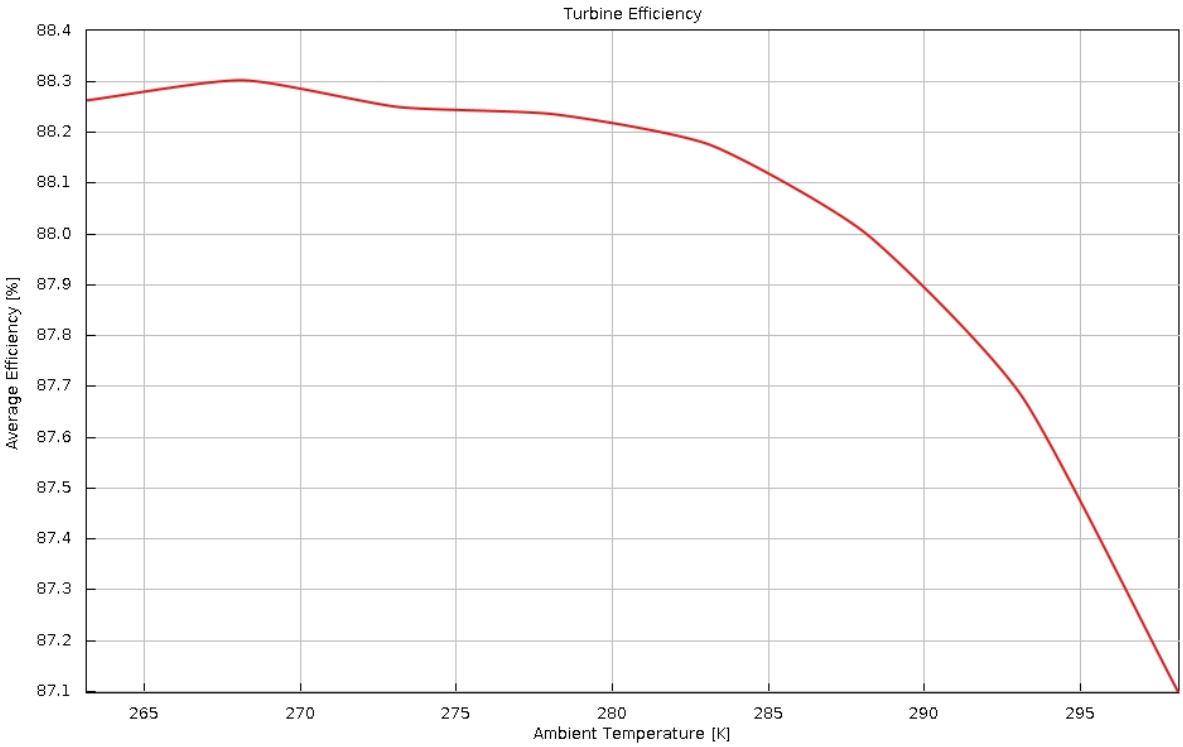

Figure 57. Turbine efficiency in turbo-matched model depending on ambient temperature

Brake Thermal Efficiency strongly increases, as illustrated in figure 58

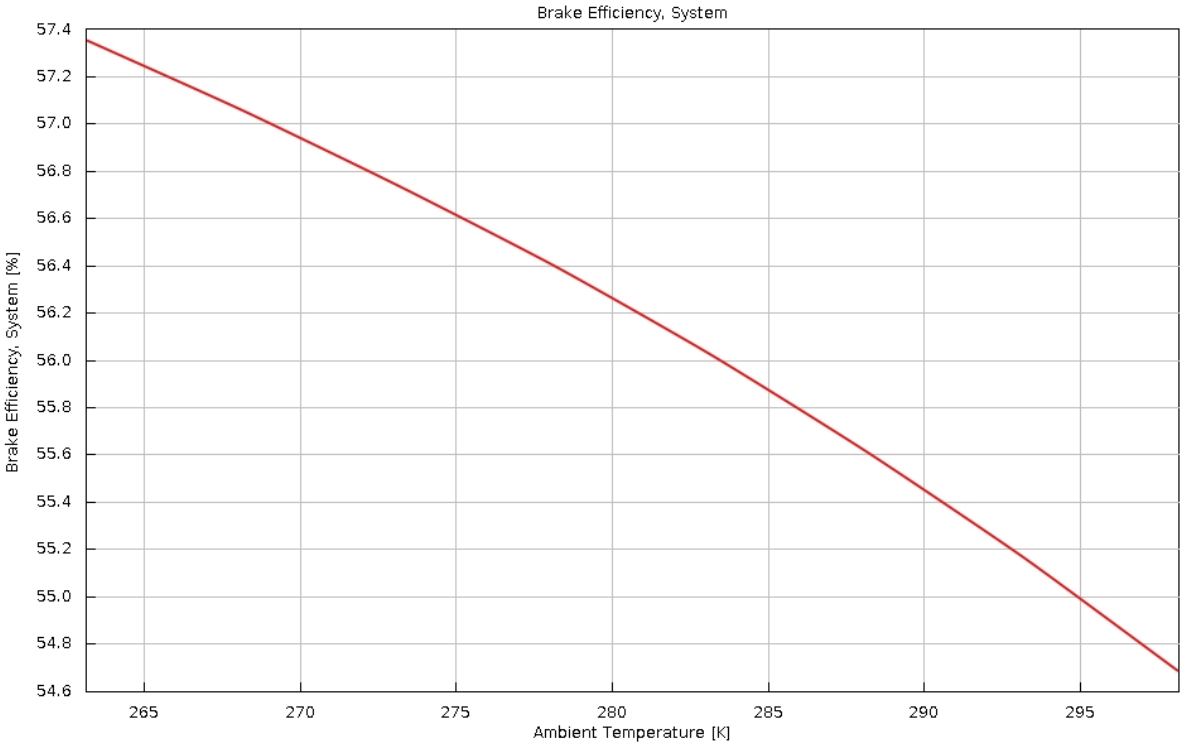

Figure 58. BTE in turbo-matched model depending on ambient temperature

4.6.5 General engine models comparison

One can finally compare the evolving models described in these results by generating a report-file in GT-POST. The following models are taken into consideration:

- **INITIAL MODEL**: referred to as the model without turbocharger, described in Section 3.2.1 (GREEN in the plots).
- **FIRST TC MODEL**: referred to as the first model with a turbocharger, shown in Section 3.2.2 (BLUE in the plots).
- **FIRST TC MODEL + CAC**: referred to as the previous model with the addition of a charge-air cooler (YELLOW in the plots).
- **FIRST TC MODEL + CAC + CM**: referred to as the previous model, additionally operating with compressor matching parameters (ORANGE in the plots).
- **FIRST TC MODEL + CAC + CM + TM**: referred to as the previous model, additionally operating with turbine matching parameters (VIOLET in the plots).

Ambient temperature is swept from -10 °C to 25 °C and initial pressure is optimized in a singular way (as a result of other simulations).
The other conditions are constant in each model, as argon content in the engine is fixed at 97%, engine speed at 1200 rpm, load at 75% and lambda at 3.5.

One can visualize how pumping work differs in the models in figure 59.

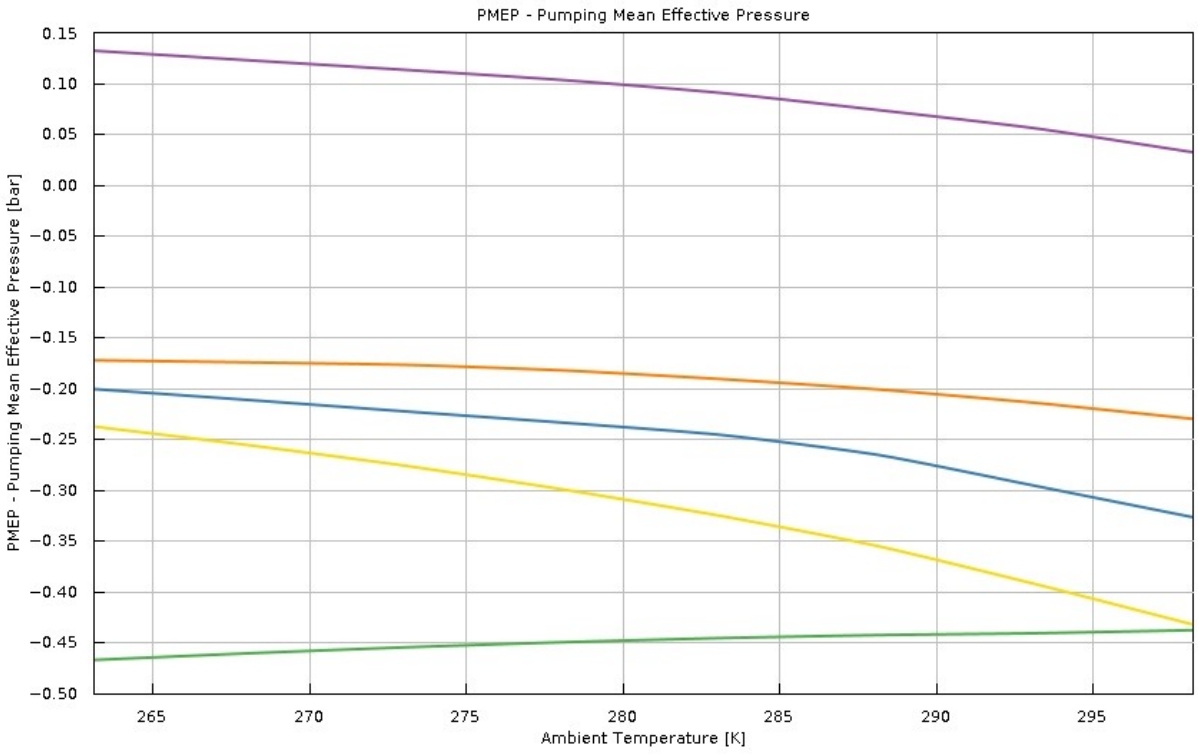

Figure 59. PMEP progressive comparison

Moreover, BSFC is compared in the following plot.

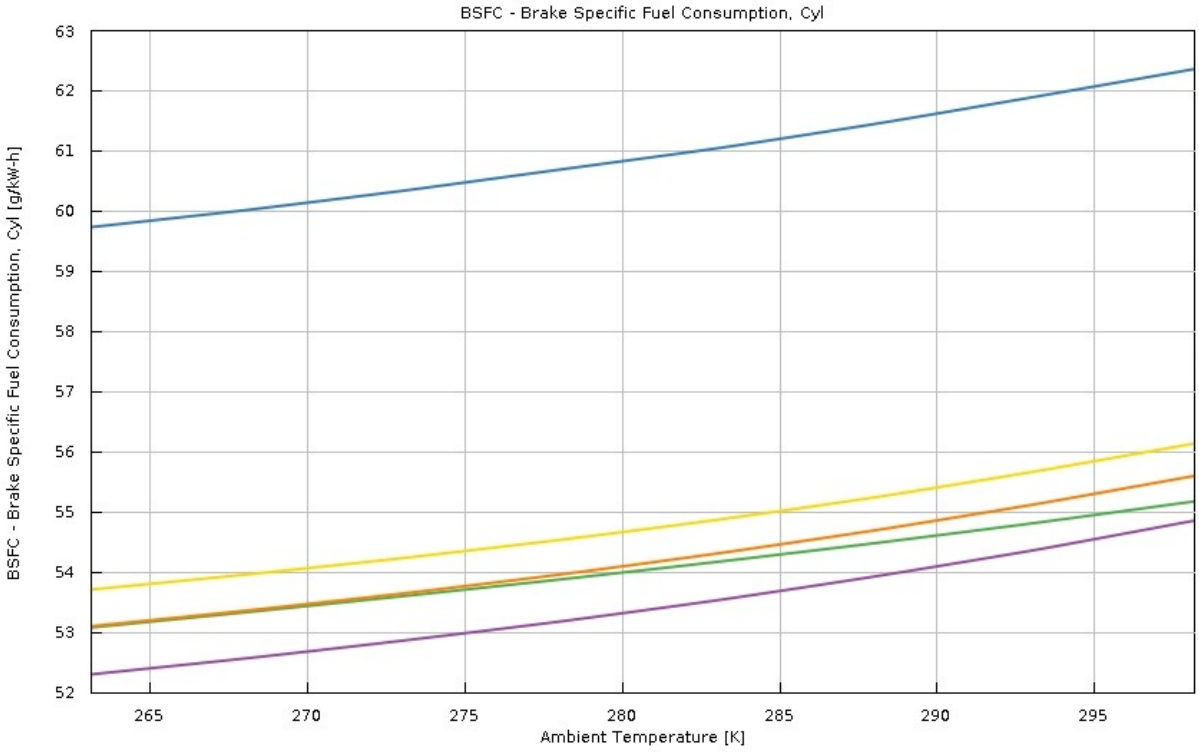

Figure 60. BSFC progressive comparison

Finally, Brake Thermal Efficiency can be appreciated in figure 61.

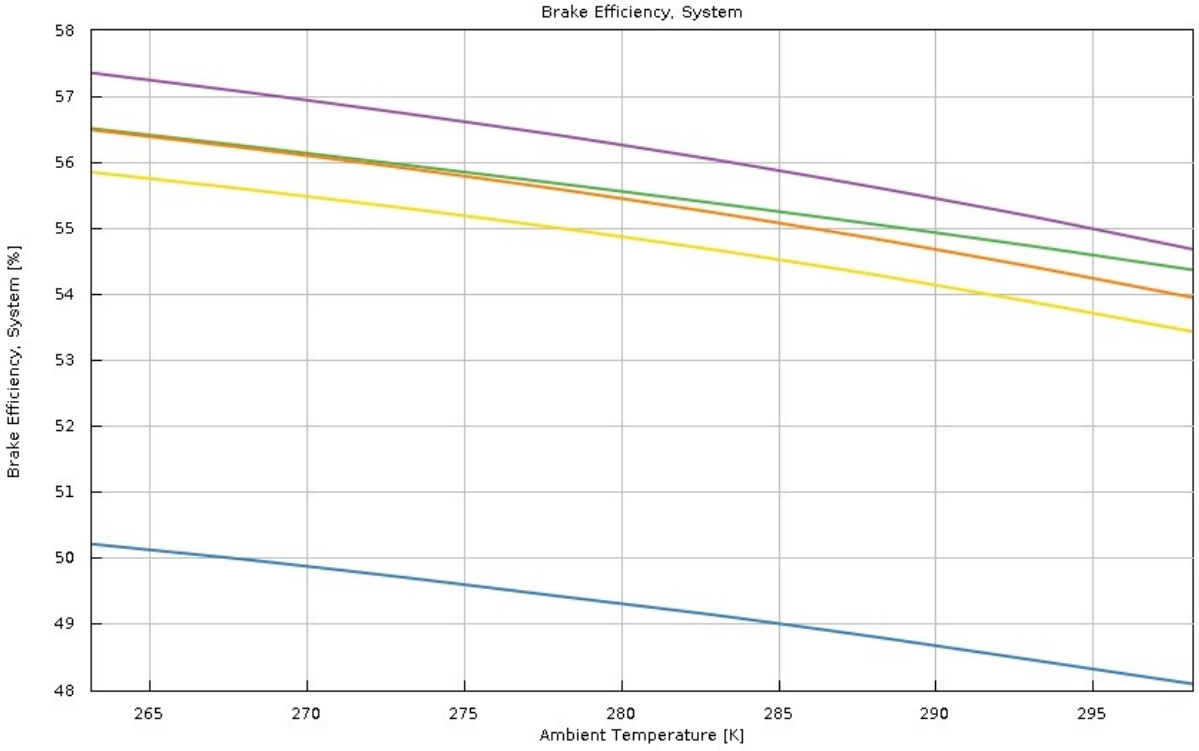

Figure 61. BTE progressive comparison

5 DISCUSSION

5.1 Initial model without Turbocharger

5.1.1 Convergence evaluation

This thesis work aims at evaluating the consequences of the implementation of a turbocharger within a closed-loop Argon-Hydrogen ICE. Multiple simulations have been computed in collaboration with Scania CV AB, and part of those is shown in Chapter 4, while the succession of evolving engine models is explained in Chapter 3.
As a first step, a convergence study is implemented in GT-SUITE to gather information about the effective computing time to converge, as shown in Section 4.1.1.

Figure 10 illustrates the number of iterations needed fro the initial model without turbocharger to reach convergence depending on ambient temperature.
As temperature increases, the number of iterations, and consequently computing time, grows exponentially, due to higher time needed to meet the forth convergence criteria, explained in Section 3.3.2. It is in fact more difficult to reach convergence of the boundary heat flow due to higher exhaust gas temperature.

Same trend is shown in Figure 21, in which the number of iterations to reach convergence is related to load percentage. One can observe that by increasing mechanical stress and/or thermal stress within the engine model, the software requires more time to solve differential equations and fulfill the four criteria.

Further simulations demonstrated that augmenting the engine model complexity, adding a turbocharger or any boosting device, the number of iterations grows more and leads to hours of computing time to reach convergence. As a result, simulation setups must be carefully optimized and justified to prevent excessive use of computational resources. Running these simulations locally would be highly impractical due to their long runtimes and significant computational demands.

5.1.2 Initial model performance

The initial model, described in detail in Section 3.2.1, was evaluated using a Design of Experiments approach to assess its performance under steady-state conditions. In general, each of the following simulations were computed through a DOE study, sweeping on different thermodynamic parameters. Specifically, a preliminary parameter sweep was conducted on torque.

Indicated Efficiency, a measure of how effectively the internal combustion process converts the chemical energy of the fuel into mechanical work on the piston, before accounting for mechanical losses (e.g., friction, pumping), is illustrated in figure 22 where the optimum peak is reached at 1400 Nm, corresponding to 50 % torque for this engine. The initial slope, from 700 Nm to 1400 Nm, is steeper than the slope in the right part of the plot, showing a wide range of high efficiency torque window, at a given engine speed. Mechanical losses are taken into account when plotting Brake Thermal Efficiency, including pumping and friction losses, as well as parasitic losses; BTE is shown in figure 23 where its trend is similar to indicated efficiency in the low-load part. In the high-torque zone (right part of the plot), instead, a plateau is reached between 50% load and 75% load, before slowly decreasing towards full-torque.

It reflects the lower pumping losses when the engine operates at high load, in this specific case. Pumping Mean Effective Pressure is therefore meaningful to plot, in figure 24: in this simulation PMEP is always negative, as the engine is not boosted, therefore exhaust pressure is higher than intake pressure and work is required to move combustion gases in the cylinders. The plot illustrates how PMEP is constant from 25% torque to 50 % torque, coherently reflecting the similar IE and BTE curve slope, while pumping losses decrease after 75% load (less negative PMEP) and consequently BTE is more constant throughout the final part of the graph, compared to the gross efficiency.

A second set of simulations was carried out to assess the influence of ambient temperature on the performance of the closed-loop initial engine model. Since ambient temperature primarily affects the cooling efficiency, it was varied from −10 °C to 35 °C, while all other conditions were held constant and the engine torque was fixed at 75%.

Brake Thermal Efficiency is again plotted in figure 25; it can be clearly observed that it decreases, more or less linearly, when ambient temperature rises. At −10 °C, BTE reaches 55.8%, before decreasing in the right part of the plot. Modern diesel engines typically achieve brake thermal efficiency (BTE) values in the range of 40–45% under steady-state conditions, with some advanced heavy-duty applications exceeding 46% through turbocharging, high-pressure injection, and optimized combustion strategies, therefore one can observe how efficient this technology is, compared to engines relying on carbon fuels. In closed-loop engines, ambient temperature does not directly affect the flow temperature inside the piping system, but it impacts the cooling capacity of the engine. In this thesis work, both the condenser cooler, placed after the exhaust pipes in the initial model and subsequently placed between the turbine and the compressor in the boosted model, and the charge-air-cooler, later implemented after the turbocharger compressor, are strongly affected by external air temperature. The colder the air, the colder the flow inside the engine at the beginning of the cycle; this specific engine model is tuned for Diesel applications, as explained in Section 3.2.5, therefore it is expected to optimally work when the flow temperature at the beginning of the cycle is similar to intake air temperature in normal Diesel open-loop engines.

Brake Specific Fuel Consumption is the last parameter analyzed for this specific simulation in figure 26. It directly depends on how efficient the combustion process is and generally it is inversely related to Brake Thermal Efficiency. Coherently, BSFC is optimized when external air temperature is -10 °C, as the cooling performance is higher and BTE is at its optimal peak. BFSC increasing by 4.5% between -10 °C and 35 °C, almost linearly as BTE decreases, reaching 56.2 g/kWh.

5.2 Engine performance with a pressure-boosting system

5.2.1 Consequences of implementing a turbocharger in the system

The implementation of a turbocharger in the engine model is described in Section 3.2.2, and motivated by the intent of investigating the effect of a pressure-boosting system in a closed-loop ICE.

The first simulation regards a parametric sweep on ambient temperature, keeping load fixed at 100%, engine speed at 1200 rpm, initial pressure at 2 bar and Argon-Oxygen mixture at 87.5% Ar - 12.5% O_2. Figure 27 confirms how ambient temperature affects engine efficiency either in turbocharger applications; in boosted models where the condenser cooler is placed between turbine and compressor, external air temperature firstly impacts the flow temperature at the intake of the compressor, thereafter influencing the general flow temperature in the engine. Turbine is beneficial for different reasons in this case, since it can extract work from exhaust gases and it also lowers flow temperature, decreasing the need of external cooling energy to extract water from the engine.

Figure 28 shows the average turbine efficiency (ideal power weighted) in this simulation: one can state that it is generally lower than typical turbine efficiency in modern applications, highlighting unextracted potential in this specific simulation or engine model. It is relatively constant between -10 °C and 10 °C, while it strongly drops towards 35 °C, reaching 64%, as minimum peak.

A different trend is shown in figure 29, in which compressor average efficiency (again ideal power weighted) increases with external air temperature. The resulting warmer intake conditions generally shift the compressor closer to its optimal operating range, thus enhancing its efficiency under higher ambient temperatures. Depending on the compressor specific operating conditions, lower density flow resulting from higher external ambient temperature, is in this case beneficial to its average efficiency.

5.2.2 One-to-one comparison with the initial model

A direct comparison between the baseline and turbocharged closed-loop models highlights the immediate thermodynamic impact of integrating a pressure-boosting system. Under otherwise comparable conditions, with the load reduced to 50%, the analysis of brake thermal efficiency (BTE) reveals how turbocharging alters the engine's performance profile.

In the turbocharged model, brake thermal efficiency drops by 6% (absolute values), compared to the initial model, with a relatively constant trend which is not impacted by ambient temperature. Figure 30 reflects the huge initial difference in efficiency between the two models, highlighting that turbocharging is not beneficial to this specific simulation.

The same trend is illustrated in Figure 31, in which Brake Specific Fuel Consumption is shown and it results significantly higher in the turbocharged model.

This comparison between the baseline and turbocharged closed-loop engine models in the first simulations demonstrates the direct negative influence of pressure boosting on thermal efficiency. With the load set at 50% and all other conditions held constant, the introduction of the turbocharger results in different thermodynamic properties of the flow inside the engine loop. By analyzing the results in GT-POST, the main difference between the two models is the flow temperature at the beginning of the cycle. The average temperature at the intake is illustrated in

figure 32; the higher intake temperatures—caused by compression and limited intercooling - is totally damaging for the engine performance, especially at low ambient temperature. Compared to the initial model, the intake temperature in the boosted model is about 65 °C higher when air temperature is -10 °C, while it is 45 °C higher at warmer air temperatures.

Similar simulations with different initial conditions show the same results, therefore a turbocharger alone can not be a solution to optimize performance in closed-loop engine. Since the compressor outlet flow re-enters the loop, its thermodynamic conditions are essential and need to be kept in an optmimum range, differently from a typical open-loop appplication.

As explained in Section 3.2.3, a possible solution to this problem is the additional implementation of a heat exchanger after the compressor to restore optimum thermal conditions at the intake of the following cycle. A charge-air cooler is consequently implemented in the engine model, shown in figure 15, and its outcomes are illustrated in the follwing paragraphs.

5.3 Charge-Air Cooler impact in the turbocharged model

5.3.1 Consequences of implementing a Charge-Air Cooler after the compressor

The cycle is modified and completed with a Charge-Air Cooler (CAC) after the turbocharger compressor so that the Argon-Oxygen flow is cooled to temperatures close to the ambient conditions and the engine can perform more efficiently.

The first parametric analysis computed in GT-SUITE for this model regards a sweep on load, ranging from 25% to 100%, keeping constant engine speed at 1200 rpm, compression ratio at 14, ambient temperature at 25 °C, initial pressure at 3.5 bar, and Argon content fixed at 85%. Figure 33 shows an efficiency peak at 75% load under these conditions, reaching 52%. At low load the engine shows lower BTE values, while from 75% to 100% the engine performance stays relatively constant.

Temperature at the end of the cycle is plotted in figure 34 to visualize if the charge-air cooler enables to restore normal thermal conditions. At low load- 25%- the graph shows that, after the second cooler, temperatures are close to the external ones, showing a high cooling capacity; under higher load conditions, temperatures obviously increase, as more heat is generated during the engine cycle, reaching a reasonable maximum value of 318 K at full torque.
This implies that, when starting the following loop, the Argon-Oxygen flow is characterized by thermal properties relatively similar to air properties in an open-loop Diesel ICE, enabling this specific engine model- initially tuned for Diesel applications- to optimally perform.

Following, a very useful view of the flow temperature after the turbocharger is provided in figure 35 (torque is in this case fixed at 700 Nm, corresponding to 25%).
After the compressor and before the charge-air cooler, the average temperature in the pipes is 340 K, coherently with figure 32; the charge-air cooler enables to decrease the flow temperature to 300 K, when external air temperature is 298 K. After being combusted in the cylinders, the exhaust gases exit through two exhaust valves at 515 K and start their path towards the turbine inlet. The flow subsequently re-enters in the turbocharger, in which the turbine cools it extracting mechanical work to drive the compressor; the condensation is therefore facilitated by the turbine work and the condenser cooler requires less energy (external air mass flow) to extract water vapor.

Ideally all oxygen would be extracted, since stoichiometric conditions are imposed in the model, when lambda equals 1, therefore the only element after the turbine and before the oxygen injection at the beginning of the following cycle would be argon (in real conditions there are always traces of oxygen and minor elements). When lambda is higher than 1 (lean combustion) a certain amount of oxygen is left in the flow after the water extraction, therefore in the compressor there will be a different argon-oxygen composition and a minor amount of oxygen will be injected in the following cycle, compared to the case when lambda equals 1. The opposite applies to rich combustion, in which lambda is lower than 1, but that is a condition to avoid since it would lead to a certain unburned amount of hydrogen flowing back in the loop that would distort the mixture composition, altering combustion stability over time.

All these factors influence the behavior of the turbocharger and of the cooling devices, which, in reality, are tuned for a specific flow mixture and are subject to continuous oscillations due to the closed-loop nature of this engine.
This is one of the reasons why closed-loop engines are way more complex than classic open-loop machines.

5.3.2 Comparison with the previous configurations

A direct comparison of the progressive models developed in the previous sections provides valuable insight into the role of turbocharging and thermal management. The evaluation includes the baseline model without boosting, the turbocharged configuration, and the final model incorporating an additional charge-air cooler. All simulations, in this specific section, are performed under full load conditions to clearly assess the incremental impact of each modification on engine performance.

A huge gain in Brake Thermal Efficiency is illustrated in figure 36, showing the positive impact of the charge-air cooler after the compressor, restoring stable thermal conditions in the loop. Compared to the previous model without the CAC, the new engine solution provides a 6.5% gain in BTE in these conditions (external temperature swept from -10 °C to 35 °C, full torque). The turbocharger coupled to the charge-air cooler affects BTE, which reaches values even higher than in the initial model.

One can evaluate Brake Specific Fuel Consumption under these conditions in figure 37: the amount of hydrogen needed to generate 1 KWh is very lower than in the previous model, and it is comparable to the initial model without boosting. The latest model performs better in the range between 12 °C and 35 °C, while it is slightly more consuming at lower temperatures.

5.4 Argon role in a closed-loop engine

5.4.1 Argon impact as working fluid

Argon is one of the main factors that make this engine efficient; its monoatomic nature enables to optimally convert the chemical energy coming from combustion into mechanical work, as explained in section 2.3.4.
In GT-SUITE, argon is considered stable and constant in the engine loops, while in reality a certain amount per cycle is lost and, consequently, refill must be taken into consideration. Argon-oxygen ratio is imposed within the initial conditions by the user in the Case Setup in the software, and stays constant between the oxygen injection and the hydrogen combustion. After combustion, a different phase composition enters the turbine before water vapor is extracted after condensation. As part of the oxygen or all oxygen- depending on lambda- is extracted, a flow with different argon-oxygen ratio approaches the compressor and the charge-air cooler. In the following cycle, the amount of oxygen needed to restore initial conditions is injected and the flow restarts the loop.

Moreover, the argon content in these models is directly related to the oxygen content, therefore it is strongly dependent on lambda. The higher lambda, the higher the amount of oxygen in the engine, implying a higher mass of argon in the flow to keep the argon-oxygen ratio constant at optimum value.

Several simulations have been implemented in GT-SUITE to find the optimum conditions, in which argon fraction, defined as the ratio between argon and (argon + oxygen), is analyzed through a parametric sweep study in which load is fixed at 50%, ambient temperature at 25 °C, initial pressure at 3.5 bar and lambda at 3.

Figure 38 illustrates how Brake Thermal Efficiency varies relatively to argon content in the engine. BTE slightly increases as more argon is present in the engine, augmenting by almost 1%. One can observe that higher argon percentage in the flow would lead to higher γ, keeping oxygen constant, therefore improving theoretical efficiency of the engine.

Figure 39 depicts how temperature in the piping system at the end of the loop decreases as argon mass in the flow increases. Thermal management of the flow is higher, especially in the combustion process, when more argon is present, enable to better convert energy into mechanical work- therefore decreasing heat losses.

A different simulation is computed to determine whether initial pressure, defined in this case as the value of pressure imposed in the engine for the first iteration, can impact argon's capability to ensure a more efficient engine cycle. The same initial conditions are kept all constant, but initial pressure, which is varied between 1 bar and 3.3 bar. Figure 40 states that in every case, keeping initial pressure constant, BTE increases with argon mass. One can, vice versa, deduct from the same image that BTE is higher as initial pressure increases, keeping argon content constant in the engine. Increasing both parameters is therefore beneficial in this specific simulation, the results of which show that an optimum is found when Argon fraction is 95% and initial pressure is 3.5 bar.

5.4.2 Argon impact in the CAC-turbocharged model

To further analyze the influence of mixture composition on turbocharger performance, the same engine model was simulated under varying load and initial pressure conditions. At a fixed

engine speed of 1200 rpm, a compression ratio of 14, and an ambient temperature of 25 °C, the initial pressure was set to 3.5 bar with a constant load of 75%. Under these conditions, changes in the argon–oxygen ratio significantly affect the thermophysical properties of the working fluid, which in turn alter the behavior of both the turbine and compressor.

Notably, the turbine efficiency is impacted by the resulting variations in fluid density and specific heat ratio, as illustrated in Figure 41.
One can notice how turbine efficiency slightly decreases in the left half of the graph, before increasing till reaching a maximum when argon is 75%. In general, efficiency is 4% higher compared to the turbine performance in the initial model without charge-air cooler, shown in picture 28.

Brake efficiency has a similar trend, with very small differences depicted in figure 42; the minimum peak is found when argon is 90% of the intake flow, though it results in a very small difference within this argon range.

The combined influence of mixture composition and combustion strategy is further investigated through a parametric sweep conducted on both the argon fraction and lambda λ, the air–fuel equivalence ratio. This study aims to assess how variations in inert gas dilution and excess oxygen affect the indicated efficiency of the engine. The resulting trends are illustrated in Figure 43.

The lowest efficiency values are observed at low λ (around 2) and low argon fractions (around 85%), where the working fluid contains a higher proportion of water vapor and combustion temperatures are elevated. This leads to greater thermal losses and reduced expansion efficiency. As λ increases, the additional oxygen reduces flame temperature and enhances the thermodynamic properties of the charge. Similarly, a higher argon fraction increases the specific heat ratio (γ) and lowers the molar heat capacity, contributing to more efficient energy conversion during expansion.

These effects combine to yield a broad region of improved performance at high λ and high argon content, with indicated efficiency peaking in the upper-right corner of the map. This trend confirms the advantage of strongly diluted, lean mixtures in closed-loop hydrogen–argon engines, provided that combustion stability can be maintained.

5.5 Initial pressure role in a closed-loop engine

5.5.1 Initial pressure in closed-loop turbocharged enines

The role of initial pressure in a closed-loop turbocharged Argon-Hydrogen ICE is critical, as confirmed by the simulation results discussed in Section 4.5.1.
By definition, the initial pressure is the starting value imposed on the entire engine circuit at the beginning of each simulation run. Unlike in open-loop systems, where intake pressure is constrained by atmospheric conditions, the closed-loop architecture enables arbitrary initial pressure levels— a key degree of freedom when tuning the system's thermodynamic behavior.

One can analyze the consequences of arbitrary imposing different initial pressures by simulating a parametric sweep on load in the engine model, constraining engine speed at 1500 rpm, argon percentage at 85%, ambient temperature at 25 °C and load at 50%.

Figure 44 shows a strong correlation between initial pressure and Brake Thermal Efficiency. The BTE increases significantly as the initial pressure rises from 2 bar to 6 bar, reaching its peak at the upper limit of this sweep. This trend highlights the beneficial effect of higher pre-charging on both combustion quality and flow thermodynamics. A plateau is reached when initial pressure is set at 5.5 bar, corresponding to 49.5% BTE. In general, for each case analyzed in this simulation, maximum cylinder pressure is below the upper threshold imposed by the suppliers.

Figure 45 shows an inverse correlation between initial pressure and turbo-shaft speed, with rotational speed decreasing from approximately 63000 rpm to 54000 rpm as the imposed pressure increases from 2bar to 6 bar. This behavior suggests that higher initial pressure improves the overall flow conditions in the loop, increasing turbine work output and reducing the rotational effort needed to drive the compressor. In other words, the turbocharger operates more efficiently at higher initial pressures, requiring lower shaft speeds to achieve the same compression performance. This result is advantageous from a mechanical design perspective, as it implies reduced mechanical stress and longer component lifespan under high-pressure operating regimes.

Furthermore, a two-parameter sweep has been implemented in GT-SUITE by varying load, and consequently torque, from 25% to 100%, and initial pressure, from 2 bar to 6 bar, keeping the other initial conditions constant.

Figure 46 shows that higher turbine efficiency is reached at low load and low initial pressure. As load increases, the turbine operates better at higher initial pressures; the minimum peak is found at high load and low initial pressure, where turbine efficiency drops at 71%.

Brake Specific Fuel Consumption is depicted in figure 47, also depending on torque and flow pressure in the engine. BSFC is minimized in between 50% load and 85% load when initial pressure is higher than 4 bar, and in general it is relatively stable above 50% load. In the left half of the graph, higher fuel consumption is shown, especially below 30% load. BSFC results constant with initial pressure when load is lower than 50%.

5.5.2 Coupled effect of initial pressure and external air temperature

A similar turbocharged engine model was simulated, this time incorporating a sweep on ambient temperature. This approach allows the evaluation of how the cooling capacity of both the condenser cooler and the charge-air cooler changes with external conditions, thereby increasing the importance of the initial pressure as a control parameter within the closed-loop system.

The simulation was conducted under the following fixed conditions: engine speed of 1200 rpm, compression ratio of 14, an Argon-Oxygen mixture composed of 95% Ar and 5% O_2, load set at 75% and temperature ranged from -10 °C to 25 °C, Three different configurations were analyzed, with the initial pressure varied from 2 bar to 6 bar.

Intake valve opening pressure is shown in figure 48; in this case it is a very important parameter, since it reflects how pressurized argon and oxygen enter the cylinders before combustion begins. A maximum cylinder pressure of 280 bar is imposed by the engine supplier, therefore it is set as the upper threshold inside the cylinders in GT-SUITE. A too high pressure in the intake valve would lead to reach this physical limit, for a given compression ratio, and delayed injection would be implemented in the following engine cycle. One can notice from the mentioned figure that pressure values tend to converge, as the ambient temperature increases, despite the different initial pressure imposed in the model. The biggest pressure difference results at low temperatures, where imposing a 2 bar higher initial pressure leads to 0.3 bar higher intake valve opening pressure. In this simulation the maximum cylinders pressure results 20-30 bar below the upper threshold, avoiding delayed injection phenomena.

Charging argon and oxygen before the injection in the model has a cost. therefore there must be a valid benefit for its implementation to be justified in this engine model. Brake Thermal Efficiency gain is shown in figure 49, in which the model with 6 bar as initial pressure is 3% more efficient, on average, than the model with 2 bar as charging pressure. In the whole temperature range the gain is relatively big, but the biggest advantage is shown in the cold zone of the plot, suggesting that at low flow temperatures, higher density is beneficial for the engine performance. A trade-off between stress and performance must be found in the next phases of this project for this technology to be optimized, considering these information.

5.6 Optimized turbocharged model

5.6.1 Initial turbocharger performance

The results presented in Section 4.2.1 highlight the initial performance of the turbocharger prior to any parametric optimization. The objective was to evaluate the natural operating range of the compressor and turbine maps under the baseline boosted configuration described in Section 15. The imposed conditions for this model include a fixed argon content of 95%, lambda of 3.5, and a temperature sweep from -10 °C to 35 °C,

Figure 50 shows the compressor efficiency map- corresponding to 25 °C as ambient temperature- in terms of corrected mass flow rate and pressure ratio. The recorded operating points fall within a moderately efficient region, but remain significantly distant from the peak of the compressor map. In the current configurations, the efficiency reaches a maximum value of 62% in a relatively narrow window of functioning. The map shows a wide high efficiency zone (dark red in the picture), suggesting the huge potential gain in compressor performance that matching could bring to.

These preliminary findings indicate that the unoptimized turbocharger operates below its ideal potential. Therefore, dedicated parametric tuning is required to better match the compressor and turbine to the flow dynamics of the closed-loop hydrogen–argon cycle.

5.6.2 Compressor matching

To improve the performance of the compressor, a parametric sweep was implemented on two key matching parameters: the compressor pressure ratio multiplier (CPRM) and the compressor mass multiplier (CMM). These tuning factors allow adjustment of the compressor's map to shift operating points toward more favorable regions. By increasing the pressure ratio multiplier, the map is shifted downwards and vice-versa; at the same time, by increasing the mass multiplier the whole working map, as well as the optimum zone, would shift towards left.

The engine model and simulation conditions remain consistent with Section 4.6.2, as argon content is set at 95%, lambda at 3.5, and temperature at 25 °C,

As shown in Figure 51, the Brake Thermal Efficiency increases with CMM, which controls the flow capacity of the compressor, in the midrange and reaches a peak at around 1.4.
A different trend is observed with respect to CPRM: for values of CMM lower than 1, the CPRM does not influence the engine performance, while as CMM becomes greater than 1, the optimum CPRM falls in between 0.8 and 1.6. In particular, 54% BTE is reached in the upper part of the figure, where CMM varies between 1.4 and 2 and CPRM ranges from 0.9 and 1.6.

Fuel consumption results follow a similar pattern: Figure 52 illustrates that BSFC decreases with increasing CPRM and CMM, up to a threshold beyond which efficiency gains are no longer evident. In this case, the amount of fuel saved is relatively low, since in the optimum part of the plot, where CMM equals 1 and CMM is higher than 1.30, BSFC is about 1% lower compared to the un-matched model.

Finally, PMEP results in Figure 53 are coherent with the fuel consumption outocmes. The optimum zone, where PMEP is maximized (less negative in this case) is found at CPRM equal to 1 and CMM higher than 1.25; in general, the higher both the multipliers, the higher PMEP, reducing pumping losses in the engine.

The optimal trade-off, which was subsequently adopted in the final simulations, corresponds to a compressor pressure ratio multiplier (CPRM) of 1.0 and a compressor mass multiplier (CMM) of 1.4.

5.6.3 Turbine matching

Following the same logic, turbine matching was carried out by tuning the turbine efficiency multiplier (TEM) and turbine mass multiplier (TMM), keeping the compressor matching parameters constant and equal to 1.

The impact of turbine matching on Turbine efficiency is reflected in Figure 54. In this case, a clear optimum is shown for TMM values lower than 1 and TEM close to 1.3. The lower part of the plot, below an imaginary straight line correspondent to TEM equal to 1, is totally to avoid due to a dramatic efficiency drop (blue zone in the plot).

The influence of these multipliers on brake thermal efficiency is shown in Figure 55. As expected, increasing the mass multiplier leads to improved efficiency, due to better utilization of the available exhaust enthalpy. Keeping the efficiency multiplier constant, the gain brought by the higher mass in the turbine is translated to +2% in turbine efficiency, reaching a 55% peak. Looking at the efficiency multiplier, the optimum range lies between 0.90 and 1.3, regardless of the mass entering the turbine.

The best trade-off, subsequently implemented in the following simulations, is found at TEM = 1.3 and TMM = 1.2.

5.6.4 Turbo-matching influence on engine performance

After identifying optimal values for both the compressor and turbine multipliers, a final simulation was conducted using the following parameters: CPRM = 1.0, CMM = 1.4, TEM = 1.3, and TMM = 1.2. All other conditions were kept consistent with the baseline.

Figures 56 illustrates how compressor efficiency can significantly improve compared to the unoptimized case. The figure, referred to the single case with external temperature set at 25 °C, demonstrates how efficient the compressor can be, reaching 95%. For each of the other cases simulated, in which temperature sweeping from -10 °C to 35 °C, the compressor map is very similar, working within the optimum range (dark red in the middle of the plot).
This result is particularly significant as it highlights the wide operating range of the analyzed turbocharged engine, in which substantial variations in the working fluid temperature—and consequently its density—are effectively managed through appropriate turbo-matching.

Finally, a last engine model was simulated in GT-SUITE under the following initial conditions: an engine speed of 1200rpm, a load of 75%, an initial pressure of 6bar, an argon content of 97.5%, and a lambda value of 3.5. The ambient temperature was swept from −10°C to 25°C to assess performance under varying thermal boundary conditions.

Turbine efficiency, as shown in Figure 57, remains relatively stable over a wide ambient temperature range. It reaches generally high values, around 88%, especially under colder ambient conditions. Considering the average values of turbine efficiency provided by previous engine models, always lower than 70% (see figure 28 and figure 41), one can notice how convenient it is to operate on matching parameters for a turbocharger.

Figure 58 confirms a substantial gain in BTE, particularly at moderate ambient conditions. The highest peak is once again shown at -10 °C, where efficiency gets to 57%. Over a sweep of 35 temperature degrees, a 2.8% difference in efficiency variation in efficiency is observed, following an almost linear decreasing trend. This demonstrates the effectiveness of turbo-matching in closed-loop systems, where pressure ratios and thermodynamic conditions deviate significantly from traditional open-loop ICEs.

5.6.5 General comparison

The final comparison presented in Section 4.6.5 evaluates the evolution of engine performance from the baseline model to the fully optimized configuration. Key indicators such as PMEP, BSFC, valve opening pressure, and BTE are plotted over a temperature sweep. Five different engine models are compared through a parametric study on external temperature, in which engine speed, load, lambda and argon content are fixed, while initial pressure is set to its optimized value based on specific simulations.

Figure 59 shows a progressive evolution in Pumping Mean Effective Pressure, particularly between the baseline and turbo-matched models, confirming reduced gas exchange losses due to optimized pressure ratios.
At the beginning, pumping work is negative due to the absence of a boosting system, therefore a certain energy is required to push the flow towards the exhaust. As the model evolves, pumping losses are less negative due to a lower pressure gradient between inlet and outlet ports. When both the compressor and the turbine are tuned and optimized for this specific application, PMEP becomes positive, regardless of ambient temperature, indicating a beneficial pressure gradient in the cylinder. In general, higher ambient temperatures correspond to lower pumping pressure, coherently with the results in the previous sections.

Similarly, Figure 60 highlights a significant drop in hydrogen consumption, relatively constant throughout the wide temperature sweep. Brake Specific Fuel Consumption is reduced by almost 2% in the final matched model, compared to the initial model without turbocharger. Higher hydrogen reduction is shown at low ambient temperature, while under warmer conditions the curves tend to converge. The highest fuel consumption is measured for the initial turbocharged model, without a charge air cooler, indicating once again how far the flow properties are from the optimal conditions in that model. Moreover, the amount of hydrogen injected per cycle is directly related to both oxygen and argon needed in the cycle, as lambda and Ar-O2 ratio are fixed, therefore a lower hydrogen consumption implies a lower amount of oxygen injected per cycle, argon mass present in the loop, as well as a reduced refill frequency.

Brake Thermal Efficiency, as shown in Figure 61, validates the optimization process carried out by the progressive evolution of the models. The worst scenario is depicted in the first turbocharged model (without additional cooling), while as a charge-air cooler is included in the model BTE strongly increases. In these specific conditions, matching the compressor parameters leads to reaching efficiency values of the initial model without a turbocharger. The final model, tuned for both the turbine and the compressor, shows a consistently higher Brake Thermal Efficiency across the full temperature range, validating the turbo-matching strategy as a key optimization step for this engine architecture.

5.6.6 Environmental impact of a Argon-Hydrogen closed-loop ICE

One of the key innovations introduced by this engine concept is the complete elimination of carbon emissions during the engine cycle. In this system, argon and oxygen replace ambient air as the working fluid, while pure hydrogen is used as the sole fuel, thereby excluding any carbon-based components. Hydrogen and oxygen are cyclically injected in the model before the combustion phase and subsequently released as water vapor (all hydrogen is extracted, and consequently, a corresponding stoichiometric amount of oxygen), while argon is ideally retained within the system. As a result, both carbon and nitrogen species are ideally absent from the combustion process. The only potential source of carbon contamination arises from oil consumption within the engine, inherent to its mechanical operation.

Despite significant advancements in internal combustion engine technology, conventional ICEs remain a major contributor to global greenhouse gas emissions and urban air pollution. The widespread reliance on fossil fuels leads to the release of carbon dioxide (CO_2), nitrogen oxides (NO_x), particulate matter (PM), and unburned hydrocarbons (UHC), all of which have adverse effects on both environmental and human health. As regulatory frameworks (EPA2027 as the latest) tighten and public awareness of climate change grows, the sustainability of traditional ICEs is increasingly called into question.
In this context, the development of alternative combustion strategies, such as the Argon-Hydrogen closed-loop ICE explored in this study, represents a promising pathway to drastically reduce or even eliminate harmful emissions while retaining the performance and operational flexibility of ICEs.

Brake Specific Fuel Consumption is a key aspect explored in this thesis work, as figure 31, figure 37, figure 47, figure 52 and figure 60 demonstrate. Several simulations regarding argon-oxygen ratio and lambda have been carried out to try to save fuel, under a wide range of operating conditions. At the end, a fuel consumption reduction of 2% is obtained in the optimized model, compared to the initial model without turbocharger.

Looking ahead, various strategies will need to be developed to further minimize hydrogen consumption, thereby reducing the frequency of tank refueling and enhancing the overall efficiency of the system.

6 CONCLUSIONS

6.1 General conclusions and future work

6.1.1 Conclusions

This thesis has explored the simulation-driven optimization of a high-pressure direct injection Argon-Hydrogen internal combustion engine operating in a closed-loop configuration. Starting from a base model inspired by a conventional diesel engine, several enhancements were introduced, including turbocharging, charge-air cooling, and turbo-matching, in order to evaluate performance gains under various thermodynamic and operating conditions.

An initial convergence study revealed a high number of iterations and significant computational time required to achieve steady-state convergence. As a result, subsequent simulations were carefully planned and optimized to ensure efficient use of computational resources. The baseline model, configured without any boosting system, was established as a benchmark to evaluate the effectiveness of later modifications. Early results demonstrate that even this initial configuration exhibits remarkably high efficiency when compared to conventional modern internal combustion engines.

A fixed-geometry turbocharger was integrated into the system with the aim of recovering thermal energy from the exhaust gases. The initial results indicate a reduction in Brake Thermal Efficiency and an increase in Brake Specific Fuel Consumption. This performance drop is primarily attributed to a significant rise in the working fluid temperature, approximately 80°C higher after the compressor compared to the baseline model. Overall, the results validate that a turbocharger cannot be implemented in a closed-loop Argon-Hydrogen engine without considering adequate thermal management. The implementation of a fixed-geometry turbocharger in the present model was intentionally chosen as a foundational step in integrating boosting within the closed-loop Argon-Hydrogen engine. This configuration offers a simplified starting point for simulation setup and result interpretation, making it particularly suitable for early-stage development. However, as the project progresses, future simulations should evaluate alternative configurations, including variable geometry turbochargers and electrically assisted systems, to more accurately reflect the dynamic operating conditions and unlock additional efficiency gains.

To address thermal issues, a charge-air cooler was integrated into the model downstream of the compressor, allowing the argon-oxygen mixture to be cooled before re-entering the loop, thereby restoring optimal intake temperatures. The integration of a Charge-Air Cooler after the turbocharger compressor significantly improves the thermodynamic behavior of the engine cycle. Results indicate that the CAC is effective in restoring intake temperatures to values close to ambient air, particularly under low-load operation. At higher loads, although intake temperatures increase due to greater heat generation, the CAC still maintains effective temperature control. This enhanced thermal management leads to a notable increase in Brake Thermal Efficiency, suggesting that thermal equilibrium at the start of each engine cycle, achieved via proper charge cooling, is essential to optimize combustion in the closed-loop hydrogen-argon engine. Remarkably, the optimized CAC model even surpasses the baseline configuration in efficiency for most of the tested temperature range.

The analyses conducted in Section 4.4.1 clearly confirm that argon enables more efficient conversion of combustion energy into mechanical work by increasing the specific heat ratio γ and minimizing vibrational or rotational energy losses.

Argon improves the thermal stability of the system, and flow temperature at the end of the cycle decreases as argon content increases, indicating reduced thermal losses and more effective heat retention. Turbine and compressor efficiencies respond to fluid density and heat capacity, both of which depend on the inert gas composition. While absolute gains are modest, the simulations confirm that thermodynamic tuning of the argon-oxygen mixture is critical for maintaining system balance and enabling effective turbocharger matching. Moreover, a parametric sweep combining lambda and argon fraction shows that indicated efficiency peaks at high dilution and lean conditions, reinforcing the value of strongly diluted hydrogen combustion in achieving high-efficiency operation, provided that combustion stability is maintained.

Initial pressure is a critical parameter for optimizing the performance of a closed-loop engine. Unlike open-loop configurations, the closed-loop system allows the initial pressure to be freely imposed, offering an additional degree of freedom in tuning engine behavior. Brake Thermal Efficiency increases substantially with higher initial pressures. When both load and initial pressure are varied simultaneously, turbine efficiency reaches its highest values at high load and high initial pressure, confirming that pressurizing the system improves fuel economy across a wide operating range. The combined effect of ambient temperature and initial pressure further emphasizes the need for a balanced approach. Higher ambient temperatures reduce the effectiveness of cooling systems, thereby increasing pumping losses and decreasing intake density; nonetheless, a higher initial pressure compensates for these thermal penalties. These insights confirm that selecting the initial pressure is not merely a boundary condition choice, but a strategic design parameter that must be optimized in conjunction with other system variables to achieve high efficiency and stable operation in closed-loop hydrogen ICEs.

The results discussed in Section 4.6 confirm the effectiveness of applying a turbo-matching strategy in the development of a high-efficiency closed-loop Argon-Hydrogen engine. Compressor matching showed that increasing the compressor mass multiplier to 1.4 has a significant effect on Brake Thermal Efficiency, allowing to operate closer to its high-efficiency region without overstressing the shaft. Meanwhile, turbine tuning revealed that an efficiency multiplier of 1.3 and a mass multiplier of 1.2 produced the best trade-off between turbine efficiency and system stability. When these optimized parameters were combined, the resulting turbo-matched model demonstrated a clear performance improvement over all previous configurations. Compressor and turbine efficiencies approach 95% and 88%, respectively, and remain stable across a wide ambient temperature range. Additionally, positive PMEP indicates beneficial gas dynamics within the cylinder. Most importantly, BTE reaches its highest peak (57%) at low ambient temperature, remaining consistently higher than all other model configurations across the full test range, and BSFC is reduced by approximately 2% compared to the initial model. These gains validate turbo-matching as a critical optimization step in closed-loop ICE systems.

From an environmental perspective, the closed-loop Argon-Hydrogen concept eliminates direct CO_2 emissions during combustion, positioning this technology as a near-zero-emission alternative to conventional ICEs. The only source of carbon contamination originates from minimal oil consumption, highlighting the potential for fully decarbonized propulsion systems in heavy-duty applications.

6.1.2 Future work

Following this pre-development phase, future work will focus on refining and calibrating the entire engine model for hydrogen-specific applications. With additional resources and expertise

expected to be involved, particular emphasis will be placed on adapting combustion, heat transfer, and boosting subsystems to better reflect the behavior of hydrogen as a fuel in a closed-loop configuration. Further studies will investigate alternative turbocharging strategies, including variable geometry and electrically assisted turbochargers, to enhance flexibility across operating conditions and transient cycles.

Once the simulation framework has reached a satisfactory level of maturity, real engine validation will represent the next critical step. Experimental testing in engine test cells will provide essential data for model correlation, ensuring predictive accuracy under dynamic conditions. This phase will also help identify any practical challenges related to control strategies, thermal management, or emissions. Ultimately, the goal is to integrate the hydrogen–argon engine into a heavy-duty truck platform, bridging the gap between concept validation and real-world deployment.

7 REFERENCES

[1] SAE Technical Paper. *Intake and Exhaust Valve Timing Control on a Heavy-Duty, Direct-Injection Natural Gas Engine*. 2015. URL: https://www.sae.org/publications/technical-papers/content/2015-01-0864/ (visited on 05/30/2025).

[2] TU/e Eindhoven University. *Argon Power Cycle*. 2019. URL: https://www.tue.nl/en/research/research-groups/power-flow/projects/argon-power-cycle (visited on 05/30/2025).

[3] Seth Svensson and Glen Martin. *Improved Method for Studying MCCI Flame Interactions with an Engine Combustion Chamber*. 2021. URL: https://www.sae.org/publications/technical-papers/content/2021-01-0507/ (visited on 05/30/2025).

[4] Scania CV AB. *Argon Matrix in a Closed-Loop Hydrogen Internal Combustion Engine*. 2024.

[5] R. Kuroki et al. *Study of High Efficiency Zero-Emission Argon Circulated Hydrogen Engine*. 2010. URL: https://www.sae.org/publications/technical-papers/content/2010-01-0581/ (visited on 05/30/2025).

[6] Miguel Sierra Aznar. *Numerical and Experimental Investigation of the Argon Power Cycle for Power Generation Efficiency Improvement and Emissions Reduction*. 2018. URL: https://escholarship.org/uc/item/4q20v9rd (visited on 05/30/2025).

[7] J.P. Holman. *Thermodynamics, 3rd edition*. 1980.

[8] John B. Heywood. *Internal Combustion Engine Fundamentals*. 2018. URL: https://www.iust.ac.ir/files/mech/ayatgh_c5664/files/internal_combustion_engines_heywood.pdf (visited on 05/30/2025).

[9] David A. Crolla, ed. *Automotive Engineering: Powertrain, Chassis System and Vehicle Body*. Amsterdam: Butterworth-Heinemann, 2009. ISBN: 9781856175777. URL: https://www.amazon.com/Automotive-Engineering-Powertrain-Chassis-Vehicle/dp/1856175774 (visited on 05/30/2025).

[10] Mohd Radzi Abu Mansor and Masahiro Shioji. *Investigation of the Combustion Process of Hydrogen Jets under Argon-Circulated Hydrogen-Engine Conditions*. 2016. URL: https://www.sciencedirect.com/science/article/abs/pii/S0010218016301961 (visited on 05/30/2025).

[11] A. Kusztelan et al. *A Review of Novel Turbocharger Concepts for Enhancements in Energy Efficiency*. 2011. URL: https://iasks.org/articles/ijtee-v02-i2-pp-75-82.pdf (visited on 05/30/2025).

[12] BorgWarner Turbo Systems. *Turbocharging Technologies for Modern Engines*. Technical publication. 2021. URL: https://www.borgwarner.com/newsroom/press-releases/2021/03/01/turbocharging-technologies-for-modern-engines (visited on 05/30/2025).

[13] Adam J. Feneley, Apostolos Pesiridis, and Amin Mahmoudzadeh Andwari. *Variable Geometry Turbocharger Technologies for Exhaust Energy Recovery and Boosting. A Review*. 2011. URL: https://www.sciencedirect.com/science/article/pii/S1364032116311807 (visited on 05/30/2025).

[14] GT-POWER, Gamma Technologies. *Flow Theory Material*. 2010. URL: https://www.gtisoft.com/gt-power/ (visited on 05/30/2025).

APPENDIX A: SUPPLEMENTARY INFORMATION

A.0.1 Analytical model to solve turbocharger equations

In GT-SUITE, the thermodynamic behavior of key components such as compressors, turbines, and heat exchangers is governed by well-established conservation laws and empirical map-based models.

For compressors and turbines, GT interpolates performance maps that define corrected mass flow, pressure ratio, and isentropic efficiency. These maps are used in conjunction with the conservation of energy to calculate the output conditions. The isentropic outlet temperature is first determined from the pressure ratio, and the actual outlet temperature is corrected using the interpolated isentropic efficiency. Power exchanged across the turbomachinery is then evaluated through enthalpy differences. [14]

For a turbine, the output power is calculated as:

$$\dot{W}_{\text{turbine}} = \dot{m} \cdot c_p \cdot (T_{\text{in}} - T_{\text{out}})$$

and for a compressor:

$$\dot{W}_{\text{comp}} = \dot{m} \cdot c_p \cdot (T_{\text{out}} - T_{\text{in}})$$

Before a turbocharged engine model can be simulated in GT-SUITE, the performance maps of both the turbine and compressor must be specified. These maps are typically supplied by turbocharger manufacturers and may be input directly into the CompressorMap and TurbineMap reference objects or read from SAE-standardized text files. These maps include data in the form of several speed lines, each consisting of pressure ratio, mass flow rate, and isentropic efficiency.

For compressors, the data point with the lowest mass flow for each speed line is assumed to lie on the surge line. For turbines, each speed line must include the peak efficiency point, with data points provided on either side of the peak to enable interpolation and extrapolation.

GT-SUITE performs several preprocessing steps before map data can be used in a simulation:

- Correction of data to reference inlet pressure and temperature.
- Interpolation to fill gaps in sparse or irregular datasets.
- Extrapolation to extend maps beyond measured boundaries for wide-range operability.

Corrected values are computed using:

$$\dot{m}_{\text{corr}} = \frac{\dot{m}\sqrt{T_{\text{in}}}}{P_{\text{in}}}, \quad N_{\text{corr}} = \frac{N}{\sqrt{T_{\text{in}}}}$$

where $\dot{m}$ is the mass flow rate, T_{in} is the inlet total temperature, P_{in} is the inlet total pressure, and N is the shaft speed.

Turbine data may be either corrected or reduced. When reduced, the effects of inlet pressure and temperature are removed, enabling easier comparison across different operating conditions. GT-SUITE supports both corrected and reduced data formats.

A.0.2 Analytical Model for Heat Exchanger Equations

Heat exchangers such as charge-air coolers and condensers are modeled using the effectiveness–NTU method. The NTU is defined as:

$$\mathrm{NTU} = \frac{UA}{C_{\min}}$$

where:

- U is the overall heat transfer coefficient [W/m^{2}K],
- A is the heat transfer surface area [m^2],
- $C_{\min}$ is the minimum heat capacity rate between the hot and cold streams [W/K].

In GT-SUITE, the value of UA can either be directly specified by the user or calculated internally using empirical correlations based on geometry, flow conditions, and fluid properties. The rate of heat transfer is then expressed as:

$$\dot{Q} = \varepsilon \cdot C_{\min} \cdot (T_{\mathrm{h,in}} - T_{\mathrm{c,in}})$$

Here, ε represents the effectiveness of the heat exchanger. The outlet temperatures are derived from standard energy balance equations. GT allows these computations to be influenced by user-defined UA values or by estimating heat transfer coefficients via built-in correlations. Together, these methods provide an accurate estimation of real component performance within the simulation framework.

Effectiveness is defined as:

$$\varepsilon = \frac{\dot{Q}}{\dot{Q}_{\max}}$$

where $\dot{Q}_{\max}$ is the theoretical maximum heat transfer possible between the fluids:

$$\dot{Q}_{\max} = C_{\min}(T_{\mathrm{h,in}} - T_{\mathrm{c,in}})$$

The variable C represents the heat capacity rate, equivalent to the product between the mass flow rate and the specific heat capacity.
Thus, knowing all the needed parameters, the effectiveness can be computed for both the parallel and the counter flow configurations. Then, it can be shown that the effectiveness of the heat exchanger is related to NTU, by an equation dependent on the system configuration and the ratio of the heat capacity rates of the two fluids (C_r). In the present case, the exact relationships for the parallel and the counter flow configurations are respectively shown in the following equations.

$$\varepsilon = \frac{1 - e^{-\mathrm{NTU}(1+C_r)}}{1 + C_r}$$

$$\varepsilon = \frac{1 - e^{-\mathrm{NTU}(1-C_r)}}{1 - C_r e^{-\mathrm{NTU}(1-C_r)}}$$